MURRAY BASIN

CLUSTER REPORT

CLIMATE
CHANGE
IN AUSTRALIA

PROJECTIONS

FOR AUSTRALIA'S NRM REGIONS

CSIRO

Australian Government

Department of the Environment

Bureau of Meteorology

−20° −10° 0° 10° 20° 30° 40° 50°

MURRAY BASIN

CLUSTER REPORT

CLIMATE CHANGE

IN AUSTRALIA

PROJECTIONS

FOR AUSTRALIA´S NRM REGIONS

−20°   −10°   0°   10°   20°   30°   40°   50°

TABLE OF CONTENTS

−20°   −10°   0°   10°   20°   30°   40°   50°

PREFACE

Australia's changing climate represents a significant challenge to individuals, communities, governments, businesses and the environment. Australia has already experienced increasing temperatures, shifting rainfall patterns and rising oceans.

The Intergovernmental Panel on Climate Change (IPCC) *Fifth Assessment Report* (IPCC, 2013) rigorously assessed the current state and future of the global climate system. The report concluded that:

- greenhouse gas emissions have markedly increased as a result of human activities
- human influence has been detected in warming of the atmosphere and the ocean, in changes in the global water cycle, in reductions in snow and ice, in global mean sea level rise, and in changes in some climate extremes
- it is extremely likely that human influence has been the dominant cause of the observed warming since the mid-20th century
- continued emissions of greenhouse gases will cause further warming and changes in all components of the climate system.

In recognition of the impact of climate change on the management of Australia's natural resources, the Australian Government developed the Regional Natural Resource Management Planning for Climate Change Fund. This fund has enabled significant research into the impact of the future climate on Australia's natural resources, as well as adaptation opportunities for protecting and managing our land, soil, water, plants and animals.

Australia has 54 natural resource management (NRM) regions, which are defined by catchments and bioregions. Many activities of organisations and ecosystem services within the NRM regions are vulnerable to impacts of climate change.

For this report, these NRM regions are grouped into 'clusters', which largely correspond to the broad-scale climate and biophysical regions of Australia (Figure A). The clusters are diverse in their history, population, resource base, geography and climate. Therefore, each cluster has a unique set of priorities for responding to climate change.

CSIRO and the Australian Bureau of Meteorology have prepared tailored climate change projection reports for each NRM cluster. These projections provide guidance on the changes in climate that need to be considered in planning.
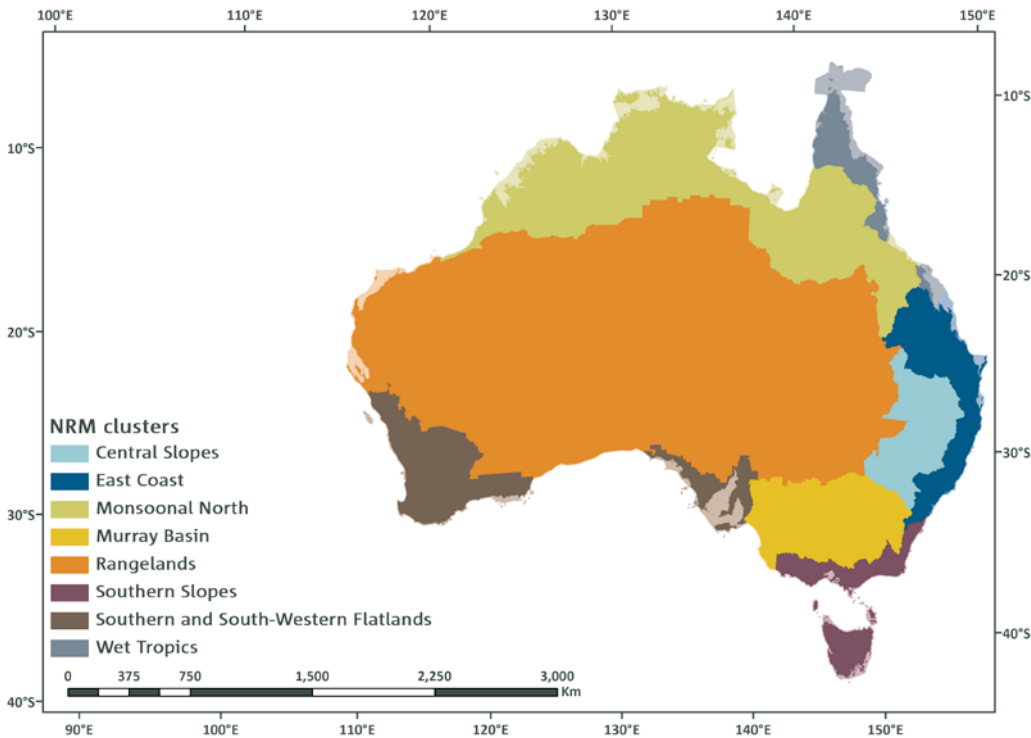

FIGURE A: THE EIGHT NATURAL RESOURCE MANAGEMENT (NRM) CLUSTERS

This is the regional projections report for the Murray Basin cluster. This document provides projections in a straightforward and concise format with information about the cluster as a whole, as well as additional information at finer scales where appropriate.

This cluster report is part of a suite of products. These include a brochure for each cluster that provides the key projection statements in a brief format. There is also the Australian climate change projections Technical Report, which describes the underlying scientific basis for the climate change projections. Box 1 describes all supporting products.

This report provides the most up to date, comprehensive and robust information available for this part of Australia, and draws on both international and national data resources and published peer-reviewed literature.

The projections in this report are based on the outputs of sophisticated global climate models (GCMs). GCMs are based on the laws of physics, and have been developed over many years in numerous centres around the world. These models are rigorously tested for their ability to reproduce past climate. The projections in this report primarily use output from the ensemble of model simulations brought together for the Coupled Model Inter-comparison Project phase 5 (CMIP5) (Taylor *et al.*, 2012), where phase 5 is the most recent comparison of model simulations addressing, amongst other things, projections of future climates. In this report, outputs from GCMs in the CMIP5 archive are complemented by regional climate modelling and statistical downscaling.

BOX 1: CLIMATE CHANGE IN AUSTRALIA – PRODUCTS

This report is part of a suite of Climate Change in Australia (CCIA) products prepared with support from the Australian Government's Regional Natural Resource Management Planning for Climate Change Fund. These products provide information on climate change projections and their application.

CLUSTER BROCHURES

Purpose: key regional messages for everyone

A set of brochures that summarise key climate change projections for each of the eight clusters. The brochures are a useful tool for community engagement.

CLUSTER REPORTS

Purpose: regional detail for planners and decision-makers

The cluster reports are to assist regional decision-makers in understanding the important messages deduced from climate change projection modelling. The cluster reports present a range of emissions scenarios across multiple variables and years. They also include relevant sub-cluster level information in cases where distinct messages are evident in the projections.

TECHNICAL REPORT

Purpose: technical information for researchers and decision-makers

A comprehensive report outlining the key climate change projection messages for Australia across a range of variables. The report underpins all information found in other products. It contains an extensive set of figures

and descriptions on recent Australian climate trends, global climate change science, climate model evaluation processes, modelling methodologies and downscaling approaches. The report includes a chapter describing how to use climate change data in risk assessment and adaptation planning.

WEB PORTAL

URL: www.climatechangeinaustralia.gov.au

Purpose: one stop shop for products, data and learning

The CCIA website is for Australians to find comprehensive information about the future climate. This includes some information on the impacts of climate change that communities, including the natural resource management sector, can use as a basis for future adaptation planning. Users can interactively explore a range of variables and their changes to the end of the 21st century. A 'Climate Campus' educational section is also available. This explains the science of climate change and how climate change projections are created.

Information about climate observations can be found on the Bureau of Meteorology website (www.bom.gov.au/climate). Observations of past climate are used as a baseline for climate projections, and also in evaluating model performance.

EXECUTIVE SUMMARY

INTRODUCTION

This report presents projections of future climate for Murray Basin based on our current understanding of the climate system, historical trends and model simulations of the climate response to changing greenhouse gas and aerosol emissions. The simulated climate response is that of the CMIP5 climate model archive, which also underpins the science of the *Fifth Assessment Report* of the Intergovernmental Panel on Climate Change (IPCC, 2013).

The global climate model (GCM) simulations presented here represent the full range of emission scenarios, as defined by the Representative Concentration Pathways (RCPs) used by the IPCC, with a particular focus on RCP4.5 and RCP8.5. The former represents a pathway consistent with low-level emissions, which stabilise the carbon dioxide concentration at about 540 ppm by the end of the 21st century. The latter is representative of a high-emission scenario, for which the carbon dioxide concentration reaches about 940 ppm by the end of the 21st century.

Projections are generally given for two 20-year time periods: the near future 2020–2039 (herein referred to as 2030) and late in the century 2080–2099 (herein referred to as 2090). The spread of model results are presented as the range between the 10th and 90th percentile in the CMIP5 ensemble output. For each time period, the model spread can be attributed to three sources of uncertainty: the range of future emissions, the climate response of the models, and natural variability. Climate projections do not make a forecast of the exact sequence of natural variability, so they are not 'predictions'. They do however show a plausible range of climate system responses to a given emission scenario and also show the range of natural variability for a given climate. Greenhouse gas concentrations are similar amongst different RCPs for the near future, and for some variables, such as rainfall, the largest range in that period stems from natural variability. Later in the century, the differences between RCPs are more pronounced, and climate responses may be larger than natural variability.

For each variable, the projected change is accompanied by a confidence rating. This rating follows the method used by the IPCC in the *Fifth Assessment Report*, whereby the confidence in a projected change is assessed based on the type, amount, quality and consistency of evidence (which can be process understanding, theory, model output, or expert judgment) and the degree of agreement amongst the different lines of evidence (IPCC, 2013). The confidence ratings used here are set as *low, medium, high* or *very high*.

HIGHER TEMPERATURES

Temperatures in the cluster have increased since national records began in 1910, especially since 1960. Over 1910–2013, mean surface air temperature has increased by 0.8 °C using a linear trend.

Continued substantial warming for the Murray Basin cluster for mean, maximum and minimum temperature is projected with *very high confidence*, taking into consideration the robust understanding of the driving mechanisms of warming and the strong agreement on direction and magnitude of change amongst GCMs and downscaling results.

For the near future (2030), the mean warming is projected to be around 0.6 to 1.3 °C above the climate of 1986–2005, with only minor difference between RCPs. For late in the 21st century (2090), it is 1.3 to 2.4 °C for RCP4.5 and 2.7 to 4.5 °C for RCP8.5.

HOTTER AND MORE FREQUENT HOT DAYS. LESS FROST

A substantial increase in the temperature reached on the hottest days, the frequency of hot days and the duration of warm spells are projected with *very high confidence,* based on model results and physical understanding. Correspondingly, a decrease in the frequency of frost days is projected with *high confidence*.

A change in diurnal range (the difference between daily minimum and maximum temperature) is projected during the cool part of the year (April to October) where daily maximum could warm up to 1 °C more than daily minimum by 2090 following the RCP8.5 high emission scenario. The difference relates primarily to the projected cool season rainfall decline and the strong relationship between rainfall and the diurnal temperature range.

LESS RAINFALL IN THE COOL SEASON, NO RAINFALL CHANGES IN THE WARM SEASON

The Murray Basin cluster experienced prolonged periods of extensive drying in the early 20th century and again by the end of the century. In the latter, drying occurred primarily during the cool season. Overall, there is no long term trend in annual rainfall throughout the 20th century.

In the near term (2030), there is *high confidence* that natural climate variability will remain the major driver of rainfall differences from the climate of 1986–2005 (annual-mean changes of -10 to +5 %, winter-mean changes of -15 to +10 %, and summer-mean changes of -15 to +15 %).

Late in the century (2090) under both RCP4.5 and RCP8.5, there is *high confidence* that cool season rainfall will continue to decline and there is *medium confidence* that rainfall will remain unchanged in the warm season (Nov-Mar). As well as GCM results and downscaling results, this assessment takes into account physical understanding of the relationship between atmospheric circulation and rainfall across the Murray Basin cluster, model representation of this, and projected changes in circulation. By 2090, the changes from the GCMs in winter span around -20 to +5 % under RCP4.5 and -40 to +5 % under RCP8.5, and those in summer span -15 to +10 % under RCP4.5 and -15 to +25 % under RCP8.5. There is *medium confidence* in the magnitudes of change.

Snowfall and maximum snow depth have declined significantly since 1960 and are projected to continue to decline for all RCPs with *high confidence*, particularly under RCP8.5.

INCREASED INTENSITY OF HEAVY RAINFALL EVENTS, MORE TIME IN DROUGHT

Understanding of physical processes coupled with high model agreement gives *high confidence* that the intensity of heavy rainfall events will increase. There is *low confidence* in the magnitude of change, and therefore the time when any change may be evident against natural variability, cannot be reliably projected.

There is *medium confidence* that the time spent in meteorological drought, and the frequency of extreme drought, will increase over the course of century under RCP8.5.

POSSIBLE DECREASE IN WINTER WIND SPEEDS

Small changes are projected for mean surface wind speeds with *high confidence* under all RCPs by 2030. Decreases in winter wind speeds are projected for 2090 with medium confidence based on model results and physical understanding (*i.e.* a southward movement of storm tracks and a strengthening of the sub-tropical ridge). Small or inconsistent changes are present in the other seasons.

INCREASES IN SOLAR RADIATION AND DECREASES IN HUMIDITY IN WINTER AND SPRING

Small changes are projected for solar radiation and relative humidity by 2030. By 2090, there is *high confidence* in increased winter and spring radiation (related to decreases in cloudiness associated with reduced rainfall), *medium confidence* in decreases in relative humidity in summer and autumn, and *high confidence* in decreases in winter and spring.

INCREASED EVAPORATION RATES, AND REDUCED SOIL MOISTURE. CHANGES TO RUNOFF ARE LESS CLEAR

Projections for potential evapotranspiration indicate increases in all seasons, with largest absolute rates projected with *high confidence* in summer by 2090. However, despite high model agreement there is only *medium confidence* in the magnitude of the projected change due to shortcomings in the simulations of observed historical changes.

Soil moisture projections suggest overall seasonal decreases by 2090 (*medium confidence*). These changes in soil moisture are strongly influenced by those in rainfall, but tend to be more negative due to the increase in potential evapotranspiration. For similar reasons, runoff is projected to decrease, but only with *low confidence*. More detailed hydrological modelling is needed to assess changes to runoff.

HARSHER FIRE-WEATHER CLIMATE IN THE FUTURE

There is *high confidence* that climate change will result in a harsher fire-weather climate in the future. However, there is only *low confidence* in the magnitude of the projected change to fire weather, as this depends on the rainfall projection and its seasonal variation. The enhanced summer rainfall projected in some scenarios could moderate the number of severe fire weather days.

HIGHER SEA LEVELS AND MORE FREQUENT SEA LEVEL EXTREMES

Relative sea level has risen around Australia at an average rate of 1.4 mm/year between 1966 and 2009, and 1.6 mm/year after the influence of the El Niño Southern Oscillation (ENSO) on sea level is removed.

There is *very high confidence* that sea level will continue to rise during the 21st century. By 2030, the projected range of sea level rise for the cluster coastline is 0.07 to 0.18 m above the 1986–2005 level, with only minor differences between emission scenarios. As the century progresses, projections are sensitive to emissions pathways. By 2090, the intermediate emissions case (RCP4.5) gives a rise of 0.28 to 0.64 m and the high emissions case (RCP8.5) gives a rise of 0.39 to 0.84 m. These ranges of sea level rise are considered *likely* (at least 66 % probability). However, if a collapse in the marine based sectors of the Antarctic ice sheet were initiated, these projections could be several tenths of a metre higher by late in the century.

Taking into account the nature of extreme sea levels along the Murray Basin coastline and the uncertainty in the sea level rise projections, an indicative extreme sea level 'allowance' is provided. The allowance represents the minimum distance required to raise an asset to maintain current frequency of breaches under projected sea level rise. In 2030, the vertical allowances along the cluster coastline are in the range of 12 to 13 cm for all RCPs, and by 2090, 48 to 54 cm for RCP4.5 and 66 to 74 cm for RCP8.5.

WARMER AND MORE ACIDIC OCEANS IN THE FUTURE

Sea surface temperature (SST) has increased significantly across the globe over recent decades and is projected to rise with *very high confidence*. Across the coastal waters of the Murray Basin cluster region in 2090, warming is projected in the range of 1.5 to 3.4 °C for RCP8.5.

About 30 % of the anthropogenic carbon dioxide emitted into the atmosphere over the past 200 years has been absorbed by the oceans. This has led to a 0.1 pH fall in the ocean's surface water pH (a 26 % rise in acidity). Continued acidification will compromise the ability of calcifying marine organisms such as corals, oysters and some plankton to form their shells or skeletons. There is *very high confidence* that around Australia the ocean will become more acidic and also *high confidence* that the rate of ocean acidification will be proportional to carbon dioxide emissions. By 2030, pH is projected to fall by up to an additional 0.08 units in the coastal waters of the cluster. By 2090, pH is projected to fall up to 0.15 under RCP4.5 and up to 0.33 under RCP8.5. These values would represent an additional 40 % and 110 % in acidity respectively.

MAKING USE OF THESE PROJECTIONS FOR CLIMATE ADAPTATION PLANNING

These regional projections provide the best available science to support impact assessment and adaptation planning in the Murray Basin cluster. This report provides some guidance on how to use these projections, including the Australian Climate Futures web tool, available from the Climate Change in Australia website. The web tool allows users to investigate the range of climate model outcomes for their region across timescales and RCPs of interest, and to select and use data from models that represent a particular change of interest (*e.g.* warmer and drier conditions).

1   THE MURRAY BASIN CLUSTER

This report describes climate change projections for the Murray Basin cluster, which comprises 12 NRM regions across the Australian Capital Territory (ACT) and three states: New South Wales (NSW), Victoria (VIC) and South Australia (SA). It extends from the flatlands of inland NSW to south-east South Australia along the southern and eastern boundaries of the Great Dividing Range and includes Australia's highest mountain (Mt Kosciusko at 2228 m).

The coastal strip from the lower lake of the Murray River to the South Australia-Victoria border is this cluster's only coastline. The western boundary in SA follows the lower part of the Flinders ranges. The largest population centre within the cluster is Canberra, though several important regional centres are also found within the cluster (Figure 1.1).

A range of climate change impacts and adaptation challenges have been identified by the NRM organisations across this cluster. Broad acre cropping and intensive agriculture, invasive species and biodiversity management, water security, alpine tourism and coastal inundation are priorities for the cluster's natural resource management and planning community.
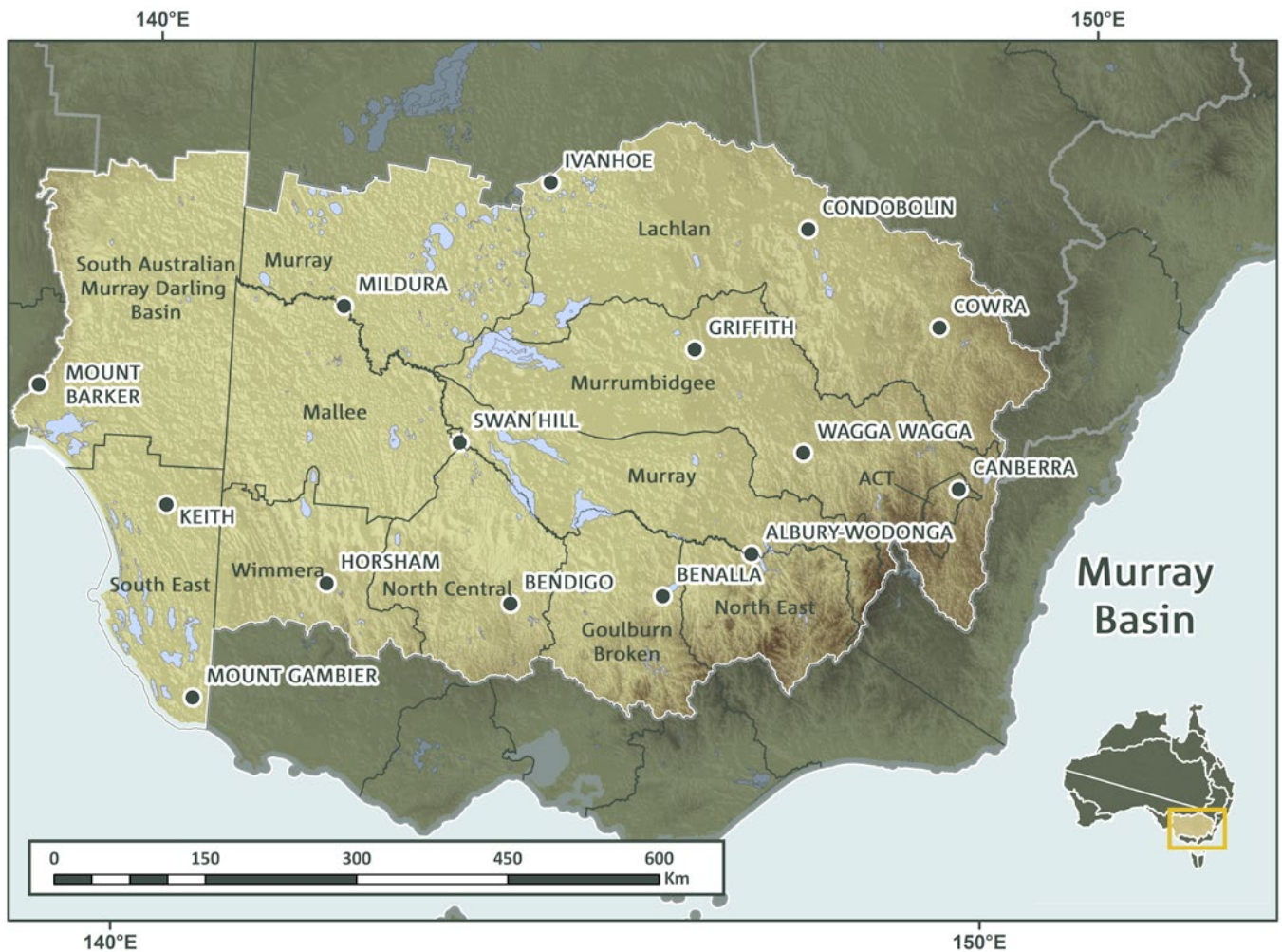

FIGURE 1.1: THE MURRAY BASIN CLUSTER AND MAIN LOCALITIES WITH RESPECT TO THE AUSTRALIAN CONTINENT.

2   CLIMATE OF MURRAY BASIN

In this Section, the climate of Murray Basin is presented for the reference period 1986–2005 (Box 3.1 presents the observational data sets used in this report). The Murray Basin cluster is relatively dry and temperate (Figure 2.1). In terms of climate types, the cluster includes warm and dry grassland in the north-west, temperate with hot summers in the east, warm summers in the south and mild summers at higher elevation[1]. Generally, summers are warm and winters are mild, with a small temperature gradient between the warm inland of NSW (mean annual temperature 18 °C) and further south and east. However, regions at high altitudes in the Great Dividing Range can have annual mean temperatures as low as 5 °C.
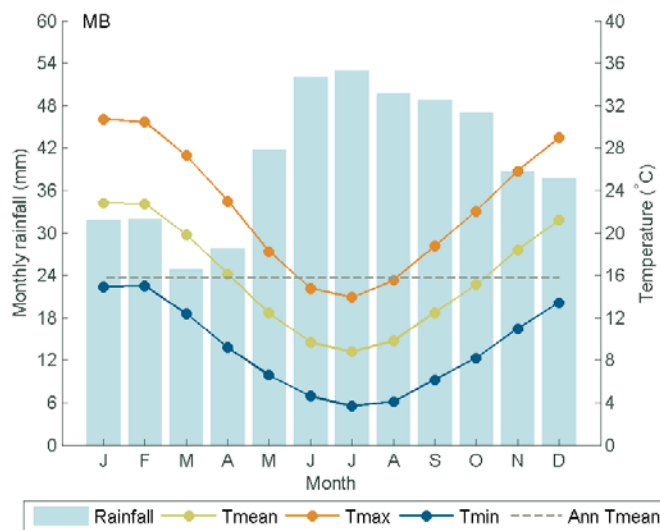
FIGURE 2.1: MONTHLY RAINFALL (BLUE BARS) AND TEMPERATURE CHARACTERISTICS FOR THE MURRAY BASIN CLUSTER (1986-2005). TMEAN IS MONTHLY MEAN TEMPERATURE (GREEN LINE), TMAX IS MONTHLY MEAN MAXIMUM TEMPERATURE (ORANGE LINE), TMIN IS MONTHLY MEAN MINIMUM TEMPERATURE (BLUE LINE), AND ANN TMEAN IS THE ANNUAL AVERAGE OF MEAN TEMPERATURE (GREY LINE) (16 °C). TEMPERATURE AND RAINFALL DATA ARE FROM AWAP.

Maps of daily mean temperature (Figure 2.2) show the spatial variability in temperature throughout the year (summer and winter are shown), dominated by a north south gradient that is stronger in summer. On all the maps, the effect of topography (lower temperature at higher elevation) can be seen in the south-east corner of the cluster. The highest temperatures are experienced in January, with an average daily maximum temperature reaching 33 to 36 °C for the upper northern part of the Murray Basin and remaining temperate along the Great Dividing range in the south. Lowest temperatures

occur most commonly in July with average minimum temperatures of 0 to 3 °C in the elevated areas in the south-east. Milder conditions are found along the coast, with cooler temperatures in summer and warmer temperatures winter.

The annual cycle of rainfall averaged across the cluster shows the dominance of the cool season rainfall (Figure 2.1). In this report, the 'cool season' is defined as the period for which the monthly long-term temperature average is equal or below the annual average. Temperature for the month April is equal to the annual mean; depending on dataset it can be estimated as slightly lower or higher than the annual average. In the Murray Basin cluster the cool season is April to October. The 'warm season' correspondingly is November to March (Figure 2.1). This approach differs from other approaches where to use a fixed arbitrary length is used (e.g. 6 months).

Spatial variability for rainfall is very large (Figure 2.3), varying by a factor of 10 between the north west, where rainfall is close to the threshold that defines desert conditions (annual totals less than 250 mm) to the elevated areas where rainfall is in excess of 2000 mm.

The Murray Basin cluster is located under the descending arm of the Hadley Cell, which is a part of the global meridional circulation, the main mechanism by which the planet transfers extra heat received at the Equator to the Poles. The descending arm of the Hadley Cell is dominated by high pressure systems, resulting in relatively dry air and little rainfall. This band of high pressure is called the sub-tropical ridge (STR). The STR is weaker and located further south in summer and stronger but further north in winter (Drosdowsky, 2005). The rainfall observed over the Murray Basin cluster is associated with low pressure weather systems observed in between high pressure systems that are associated with either mid-latitude storm tracks (predominantly south of the STR) or cut-off lows (predominantly north of the STR).

1   http://www.bom.gov.au/iwk/climate_zones/map_2.shtml
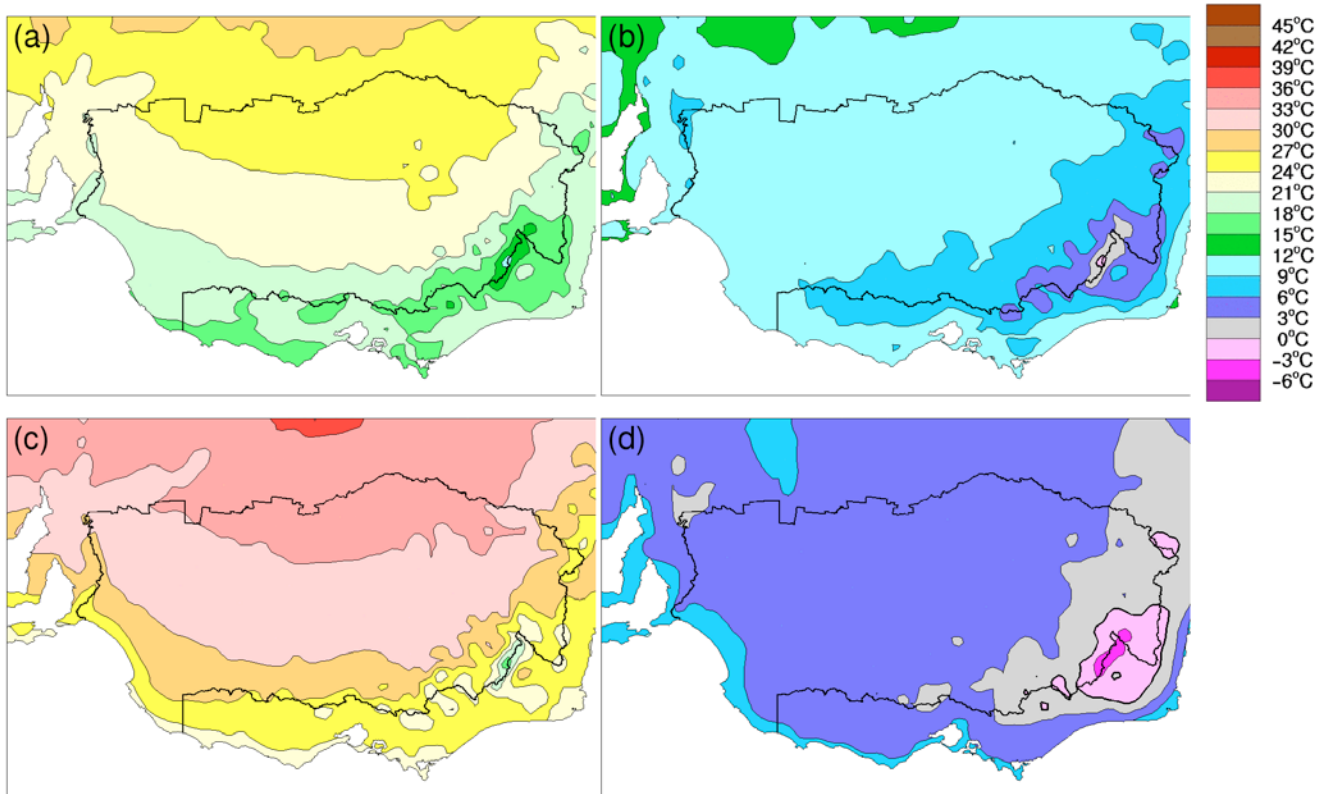
FIGURE 2.2: MAPS OF (A) AVERAGE SUMMER DAILY MEAN TEMPERATURE, (B) AVERAGE WINTER DAILY MEAN TEMPERATURE, (C) AVERAGE JANUARY MAXIMUM DAILY TEMPERATURE AND (D) AVERAGE JULY MINIMUM DAILY TEMPERATURE FOR THE PERIOD 1986–2005.
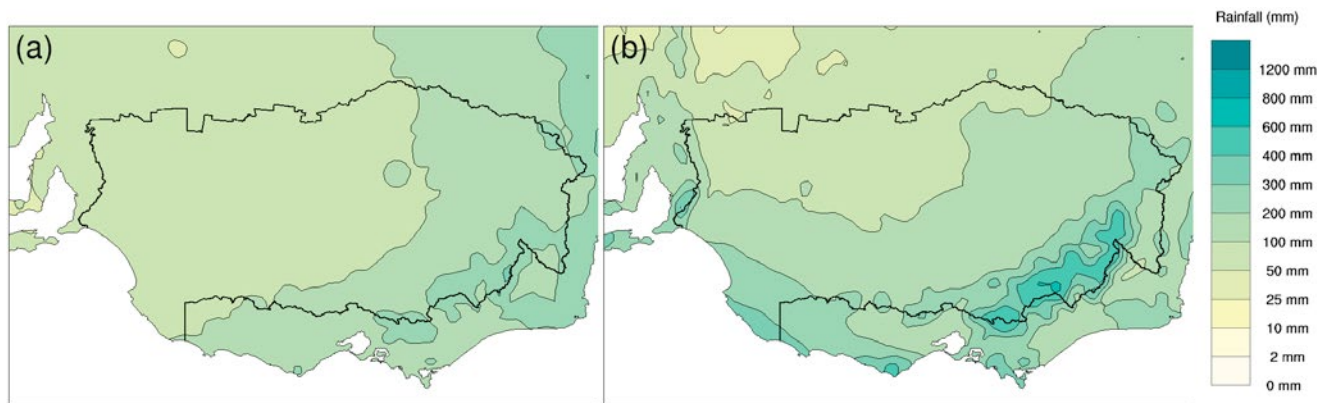
FIGURE 2.3: MAP OF AVERAGE RAINFALL FOR THE WARM SEASON (NOVEMBER TO MARCH) (A) AND COOL SEASON (APRIL TO OCTOBER) (B) IN 1986–2005.

Climate anomalies such as droughts and floods are a common feature of inland Australia and the Murray Basin cluster. Their occurrences are explained by influences of well known large-scale natural modes of variability of the climate system. These modes and their relevance to the Australian climate are described in detail in Chapter 4 of the Technical Report.

However, these modes explain at best a quarter of the year to year variability and thus a large part of the variability is simply due to the randomness of weather systems. Year to year standard deviations of monthly total rainfall are consistently between 20 and 25 mm per month (Figure 2.4). They tend to be lower for spring months, when modes such as the El Niño Southern Oscillation (ENSO) and the Indian Ocean Dipole (IOD) have the largest impact on Australian climate (see Section 4.1.1 in the Technical Report for details). The marked annual cycle in the variability means that cool season rainfall is more reliable than warm season rainfall.

For periods extending to decades and beyond, long-term trends (when evident) need to be assessed in the context of year to year variability. In the absence of clear evidence of observed changes in the naturally occurring modes of variability (*e.g.* ENSO and IOD), it is instructive to assess observed changes in the atmospheric circulation relevant to regional rainfall (see Box 2.1 on the meridional circulation and its impact on the climate of the Murray Basin cluster).

This large-scale picture is important when considering the projections provided by the GCMs, whose primary skill lies in reproducing this general circulation. The main ingredients of the extra-tropical climate affecting the Murray Basin cluster will remain a continuous alternation of high and low pressures or weather patterns.
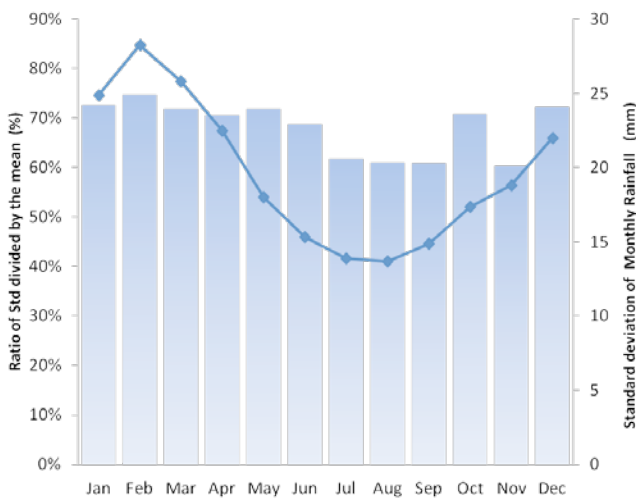
FIGURE 2.4: ANNUAL CYCLE OF THE STANDARD DEVIATION (STD) OF MONTHLY RAINFALL (BLUE BARS, LEFT Y-AXIS) AND DIVIDED BY THE MEAN MONTHLY RAINFALL EXPRESSED IN PERCENTAGE TERMS (RIGHT Y-AXIS).

BOX 2.1: OBSERVED CHANGES IN MERIDIONAL CIRCULATION AND THEIR RELEVANCE TO THE MURRAY BASIN
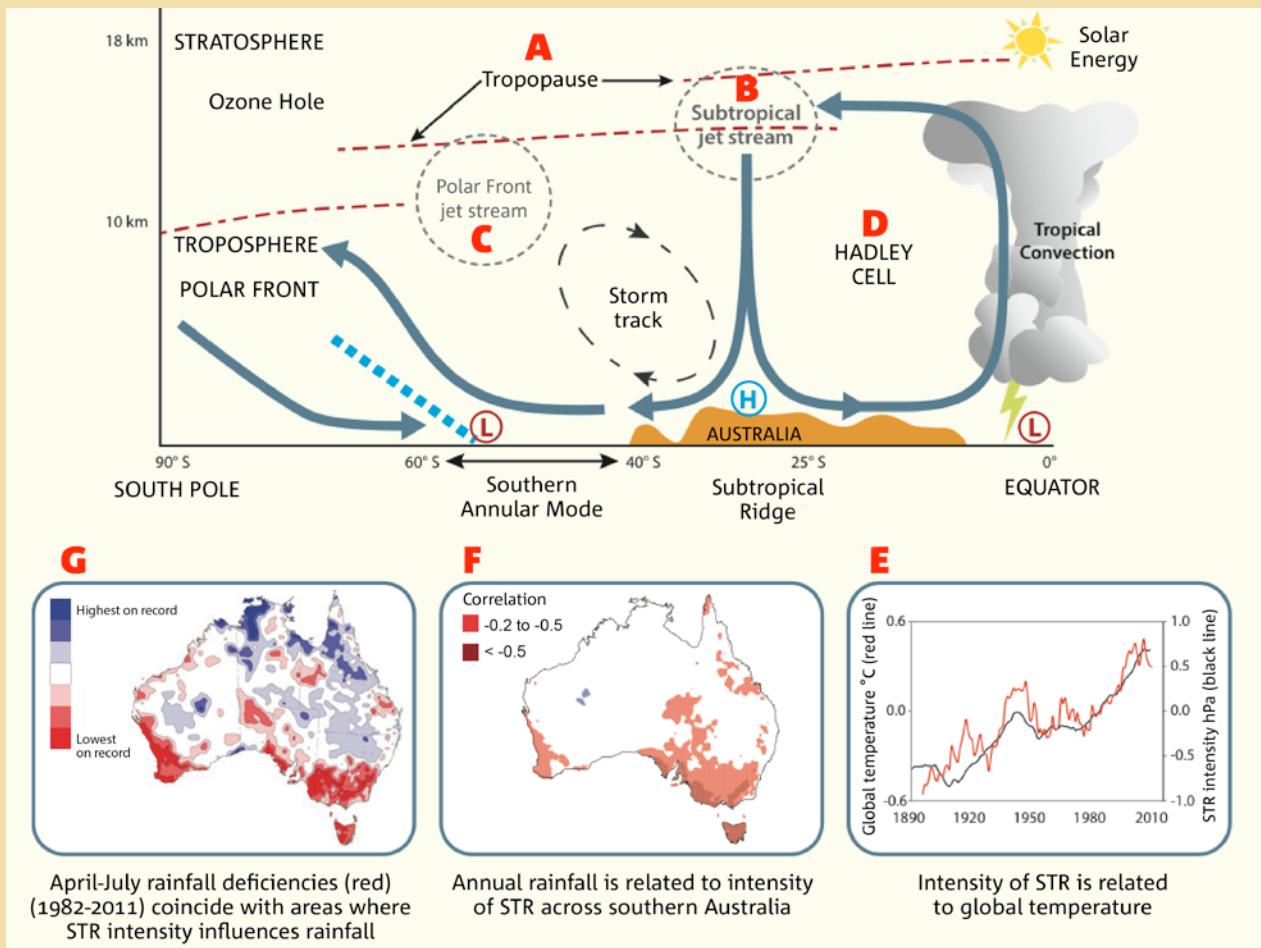
Adapted from: CSIRO (2012)

The figure above uses a north-south cross-section through the atmosphere in eastern Australian longitudes to illustrate the atmospheric circulation in this plane ('the meridional circulation') and how changes in this may affect regional climate. The mean meridional circulation transfers excess energy received at the Equator toward the Pole. The following changes have been observed in key components of this process:

The tropics have expanded in recent decades. The edge of the tropical tropopause (A) has trended poleward during the last 30 years (Lucas *et al.*, 2014). The sub-tropical jet (B) has been observed to decrease in intensity while the polar front jet (C) has increased in intensity (Frederiksen and Frederiksen, 2011). The descending arm of the Hadley Cell (D) has trended poleward during the last 30 years (Nguyen *et al.*, 2013).

All these large-scale changes indicate a poleward extension of the Mean Meridional Circulation (Lucas *et al.*, 2014). This extension affects the climate observed across the Murray Basin cluster through changes to the sub-tropical ridge intensity. An intensification of the sub-tropical ridge was observed during the last 120 years and that intensification has occurred in conjunction with the global warming of the planet (E) (Timbal and Drosdowsky, 2013). Annual rainfall in much of southern Australia has a significant negative relationship with the intensity of the sub-tropical ridge (F), in particular across the Murray Basin cluster and for cool season rainfall (Timbal and Drosdowsky, 2013). The spatial extent of the drying in the early part of the cool season (April to July) during the last 30 years (G) coincides with the areas where the sub-tropical ridge influences rainfall, in particular across the Murray Basin cluster.

3   SIMULATING REGIONAL CLIMATE

Researchers use climate models to examine future global and regional climate change. These models have a foundation in well-established physical principles and are closely related to the models used successfully in weather forecasting. Climate modelling groups from around the world produce their own simulations of the future climate, which may be analysed and compared to assess climate change in any region. For this report, projections are based on historical and future climate simulations from the CMIP5 model archive that holds the most recent simulations, as submitted by approximately 20 modelling groups (Taylor *et al.*, 2012). The number of models used in these projections varies by RCP and variable depending on availability *e.g.* for monthly temperature and rainfall, data are available for 39 models for RCP8.5 but only 28 models for RCP2.6 (see Chapter 3 in the Technical Report).

The skill of a climate model is assessed by comparing model simulations of the current climate with observational data sets (see Box 3.1 for details on the observed data used for model evaluation for the Murray Basin cluster). Accurate simulation of key aspects of the regional climate provides a basis for placing some confidence in the model's projections. However, models are not perfect representations of the real world. Some differences in model output relative to the observations are to be expected. The measure of model skill can also vary depending on the scoring measure used and regions being assessed.

BOX 3.1: COMPARING MODELS AND OBSERVATIONS: EVALUATION PERIOD, DATA SETS, AND SPATIAL RESOLUTION

Model skill is assessed by running simulations over historical time periods and comparing simulations with observed climate data. Projections presented here are assessed using the 1986–2005 baseline period, which conforms to the *Fifth Assessment Report* (IPCC, 2013). The period is also the baseline for projected changes, as presented in bar plots and tabled values in the Appendix. An exception is the time series projection plots, which use a baseline of 1950–2005, as explained in Section 6.2.2 of the Technical Report.

Several data sets are used to evaluate model simulations of the current climate. For assessment of rainfall and temperature, the observed data are derived from the Australian Water Availability Project (AWAP) (Jones *et al.*, 2009) and from the Australian Climate Observations Reference Network – Surface Air Temperature (ACORN-SAT), a data set developed for the study of long-term changes in monthly and seasonal climate (Fawcett *et al.*, 2012). For mean sea level pressure derived indices the HadSLP2 dataset is used (Allan and Ansell, 2006).

The spatial resolution of climate model data (around 200 km between the edges of grid cells) is much coarser than observations. The Murray Basin cluster is 459,000 km^2 and the GCMs from the CMIP5 dataset have a reasonable number of grids cells covering this cluster: at least 2-10 full grid cells (for most models) and several more partially covering the clusters: 5 to 23 for 29 models, with 2 high resolution models having more than 35 grid cells. This means that simulation of past and future climates should be interpreted as representative of a region which could include areas of adjacent clusters.
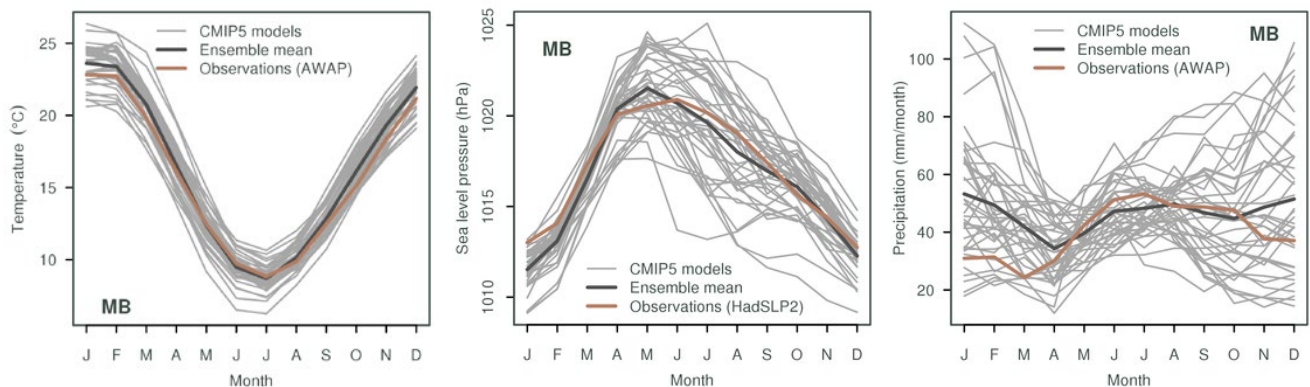
FIGURE 3.1: THE ANNUAL CYCLE OF TEMPERATURE (LEFT PANEL), SEA LEVEL PRESSURE (MIDDLE PANEL) AND RAINFALL (RIGHT PANEL) IN THE MURRAY BASIN CLUSTER SIMULATED BY CMIP5 MODELS (GREY LINES) WITH MODEL ENSEMBLE MEAN (BLACK LINE) AND OBSERVED CLIMATOLOGY (BASED ON AWAP FOR TEMPERATURE AND RAINFALL, AND ON HADSLP2 FOR MEAN SEA LEVEL PRESSURE) FOR THE BASELINE PERIOD 1986–2005 (BROWN LINE).

All GCMs considered for this report are competent in reproducing the mean cluster annual cycle of temperature (left panel in Figure 3.1) with little scatter amongst models (usually within 2 °C of observations for any month). The strong similarities between simulated and observed seasonal patterns, and the knowledge that regional temperatures are related to the general circulation of the atmosphere, together indicate that the models do a reasonable job of simulating the current atmosphere and stand a good chance of simulating realistic future projections.

The ability of CMIP5 models to capture the general circulation for this cluster is seen in the reproduction of the annual cycle of mean sea level pressure (MSLP). The seasonal movement of the sub-tropical ridge is reasonably simulated (middle panel in Figure 3.1), although the scatter amongst models is large. Individual models have errors up to 6 hPa, which is substantial in comparison to an annual cycle of 10 hPa, but this is a systematic bias (a systematic shift all year around) and the critical movement of the annual cycle is well captured. This is important, as the movement of the STR is an essential driver of the regional rainfall. During the cool season, STR movement explains a large amount of the interannual variability of rainfall. It was also shown to explain 70 to 80 % of the observed rainfall deficit during the Millennium Drought across large parts of South-Eastern Australia (Timbal *et al.*, 2010) (see Box 2.1 for details).

For rainfall, climate models show a very large scatter around the observations (right panel in Figure 3.1). The largest errors are found for the warm season rainfall, while errors for the cool season, particularly for the early part of the season, are less. Some CMIP5 models have a poor representation of the annual cycle with a summer maximum in rainfall. These models contribute to bias the ensemble mean toward a wetter than observed warm season rainfall, although the ensemble mean remains close to the observations for most of the cool season rainfall.

In addition to the CMIP5 model results, downscaling can be used to derive finer spatial information in the regional projections, thus potentially capturing processes occurring on a finer scale. While downscaling can provide added value on finer scale processes, it increases the uncertainty in the projections since there is no single best downscaling method, but a range of methods that are more or less appropriate depending on the application. It is advisable to consider more than one technique, as different downscaling techniques have different strengths and weaknesses.

For the regional projections we consider downscaled projections from two techniques: outputs from a dynamical downscaling model, the Conformal Cubic Atmospheric Model (CCAM) (McGregor and Dix, 2008) using six CMIP5 GCMs as input; and the Bureau of Meteorology analogue-based statistical downscaling model with 22 CMIP5 GCMs as input for rainfall and 21 CMIP5 GCMs as input for temperature (Timbal and McAvaney, 2001). Where relevant, projections from these methods are compared to those from GCMs (the primary source of climate change projections in this report). The downscaled results are only emphasised if there are strong reasons for giving the downscaled data more credibility than the GCM data (see Section 6.3 in the Technical Report for further details on downscaling).

4   THE CHANGING CLIMATE OF THE MURRAY BASIN

This Section presents projections of climate change to the end of the 21st century for a range of climate variables (including average and extreme conditions) of relevance to the Murray Basin cluster. Where there are relevant observational data available, the report shows historical trends.

As outlined in the *Fifth Assessment Report* (IPCC, 2013), greenhouse gases, such as carbon dioxide, have a warming effect on global climate. These gases absorb heat that would otherwise be lost to space, and re-radiate it back into the atmosphere and to the Earth's surface. The IPCC concluded that it was *extremely likely* that more than half of the observed increase in global average surface air temperature from 1951–2010 has been caused by the anthropogenic increase in greenhouse gas emissions and other anthropogenic forcings. Further increases in greenhouse gas concentrations resulting primarily from burning fossil fuel will lead to further warming, as well as other physical and chemical changes in the atmosphere, ocean and land surface.

The CMIP5 simulations give the climate response to a set of greenhouse gas, aerosol and land-use scenarios that are consistent with socio-economic assumptions of how the future may evolve. These scenarios are known as the Representative Concentration Pathways (RCPs) (Moss *et al.*, 2010; van Vuuren *et al.*, 2011). Box 4.1 presents a brief introduction to the RCPs.

In its *Fifth Assessment Report* (IPCC, 2013), the IPCC concluded that global mean surface air temperatures for 2081–2100 relative to 1986–2005 are likely to be in the following ranges: 0.3 to 1.7 °C warmer for RCP2.6 (representing low emissions); 1.1 to 2.6 °C and 1.4 to 3.1 °C warmer for RCP4.5 and RCP6.0 respectively (representing intermediate emissions); and 2.6 to 4.8 °C warmer for RCP8.5 (representing high emissions).

The projections for the climate of the Murray Basin cluster consider model ranges of change, as simulated by the CMIP5 ensemble. However, the projections should be viewed in the context of the confidence ratings that are provided, which consider a broader range of evidence than just the model outputs. The projected change is assessed for two 20-year time periods: a near future 2020–2039 (herein referred to as 2030) and a period late in the 21st century, 2080–2099 (herein referred to as 2090) following RCPs 2.6, 4.5 and 8.5 (Box 4.1)[2].

The spread of model results is presented in graphical form (Box 4.2) and provided as tabulated percentiles in Table 1 (10th, 50th and 90th) and Table 3 (5th, 50th and 95th, for sea level rise) in the Appendix. CMIP5 results for additional time periods between 2030 and 2090 are provided through the Climate Change in Australia website (Box 1).

Unless otherwise stated, users of these projections should consider the ranges of projected change, as indicated by the different plots and tabulated values, as applicable to each location within the cluster.

---

2   For sea level rise and sea allowance, the future averaging periods are 2020–2040 and 2080–2100. In the report, these are referred to as 2030 and 2090 respectively.

BOX 4.1: REPRESENTATIVE CONCENTRATION PATHWAYS (RCPs)

The climate projections presented in this report are based on climate model simulations following a set of greenhouse gas, aerosol and land-use scenarios that are consistent with socio-economic assumptions of how the future may evolve. The well mixed concentrations of greenhouse gases and aerosols in the atmosphere are affected by emissions as well as absorption through land and ocean sinks.

There are four Representative Concentration Pathways (RCPs) underpinned by different emissions. They represent a plausible range of radiative forcing (in W/m²) during the 21st century relative to pre-industrial levels. Radiative forcing is a measure of the energy absorbed and retained in the lower atmosphere. The RCPs are:

- RCP8.5: high radiative forcing (high emissions)
- RCP4.5 and 6.0: intermediate radiative forcing (intermediate emissions)
- RCP2.6: low radiative forcing (low emissions).

RCP8.5, represents a future with little curbing of emissions, with carbon dioxide concentrations reaching 940 ppm by 2100. The higher of the two intermediate concentration pathways (RCP6.0) assumes implementation of some mitigation strategies, with carbon dioxide reaching 670 ppm by 2100. RCP4.5 describes somewhat higher emissions than RCP6.0 in the early part of the century, with emissions peaking earlier then declining, and stabilisation of the carbon dioxide concentration at about 540 ppm by 2100. RCP2.6 describes emissions that peak around 2020 and then rapidly decline, with the carbon dioxide concentration at about 420 ppm by 2100. It is likely that later in the century active removal of carbon dioxide from the atmosphere would be required for this scenario to be achieved. For further details on all RCPs refer to Section 3.2 and Figure 3.2.2 in the Technical Report.

The previous generation of climate model experiments that underpins the science of the IPCC's *Fourth Assessment Report* used a different set of scenarios. These are described in the IPCC's Special Report on Emissions Scenarios (SRES) (Nakićenović and Swart, 2000). The RCPs and SRES scenarios do not correspond directly to each other, though carbon dioxide concentrations under RCP4.5 and RCP8.5 are similar to those of SRES scenarios B1 and A1FI respectively.

In the Technical and Cluster Reports, RCP6.0 is not included due to a smaller sample of model simulations available compared to the other RCPs. Remaining RCPs are included in most graphical and tabulated material of the Cluster Reports, with the text focusing foremost on results following RCP4.5 and RCP8.5.

4.1   RANGES OF PROJECTED CLIMATE CHANGE AND CONFIDENCE IN PROJECTIONS

Quantitative projections of future climate change in the Murray Basin cluster are presented as ranges of change. This allows for differences in how future climate may evolve due to three factors that are not known precisely – greenhouse gas and aerosol emissions, the climate response and natural variability:

- Future emissions cannot be known precisely and are dealt with here by examining several different RCPs described in Box 4.1. There is no 'correct' scenario, so the choice of how many and which scenarios to examine is dependent on the decision-making context.

- The response of the climate system to emissions is well known in some respects, but less well known in others. The thermodynamic response (direct warming) of the atmosphere to greenhouse gases is well understood, although the global climate sensitivity varies. However, changes to atmospheric circulation in a warmer climate are one of the biggest uncertainties regarding the climate response. The range between different climate models (and downscaled models) gives some indication of the possible responses. However, the range of model results is not a systematic or quantitative assessment of the full range of possibilities, and models have some known regional biases that affect confidence.

- Natural variability (or natural 'internal variability' within the climate system) can dominate over the 'forced' climate change in some instances, particularly over shorter time frames and smaller geographic areas. The precise evolution of climate due to natural variability (*e.g.* the sequence of wet years and dry years) cannot be predicted (IPCC, 2013, see Chapter 11). However, the projections presented here allow for a range of outcomes due to natural variability, based on the different evolutions of natural climatic variability contained within each of the climate model simulations.

The relative importance of each of these factors differs for each variable, different timeframes and spatial scale. For some variables with large natural variability, such as rainfall, the predominant reason for differing projections in the early period is likely to be dominated by natural variability rather than differences in emission scenarios (the influence of which becomes relatively more important as greenhouse gas concentrations increase). In addition, unpredictable events, such as large volcanic eruptions, and processes not included in models, could influence climate over the century. See the *Fifth Assessment Report* (IPCC, 2013) Chapter 11 for further discussion of these issues.

The projections presented here are accompanied by a confidence rating that follow the system used by the IPCC in the *Fifth Assessment Report* (Mastrandrea *et al.*, 2010), whereby the confidence in a projected change is assessed based on the type, amount, quality and consistency of evidence (which can be process understanding, theory, model output, or expert judgment) and the extent of agreement amongst the different lines of evidence. Hence, this confidence rating does not equate precisely to probabilistic confidence. The levels of confidence used here are set as *low, medium, high* or *very high*. Note that although confidence may be high in the direction of change, in some cases confidence in magnitude of change may be *medium* or *low* (*e.g.* due to some known model deficiency). When confidence is low only qualitative assessments are given. More information on the method used to assess confidence in the projections is provided in Section 6.4 of the Technical Report.

BOX 4.2: UNDERSTANDING PROJECTION PLOTS
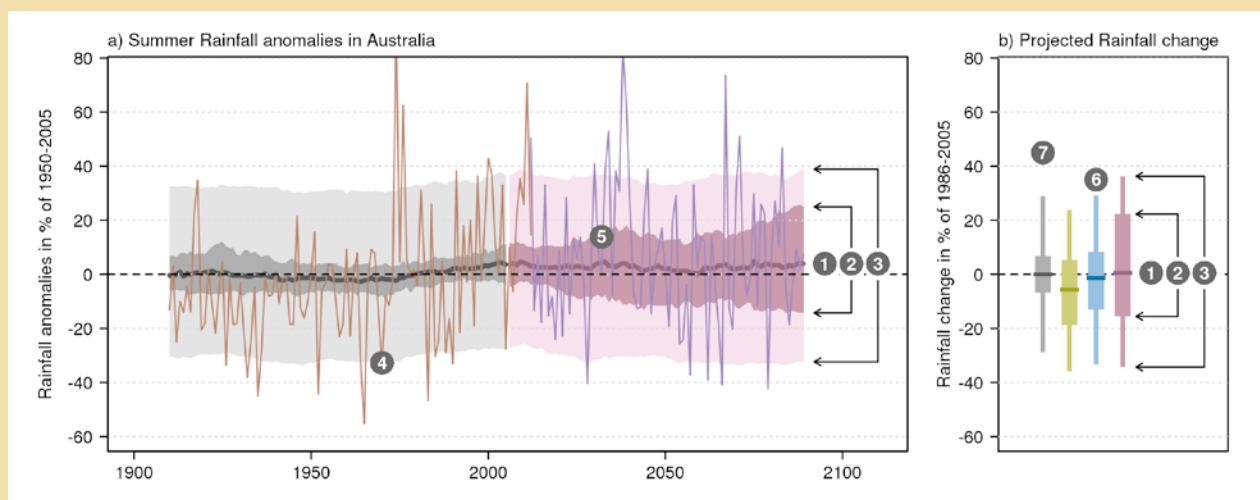
Projections based on climate model results are illustrated using time series (a) and bar plots (b). The model data are expressed as anomalies from a reference climate. For the time series (a), anomalies are calculated as relative to 1950–2005, and for the bar plots (b) anomalies are calculated as the change between 1986–2005 and 2080–2099 (referred to elsewhere as '2090'). The graphs can be summarised as follows:

1. The middle (bold) line in both (a) and (b) is the median value of the model simulations (20-year moving average); half the model results fall above and half below this line.

2. The bars in (b) and dark shaded areas in (a) show the range (10th to 90th percentile) of model simulations of 20-year average climate.

3. Line segments in (b) and light shaded areas in (a) represent the projected range (10th to 90th percentile) of individual years taking into account year to year variability in addition to the long-term response (20-year moving average).

In the time series (a), where available, an observed time series (4) is overlaid to enable comparison between observed variability and simulated model spread. A time series of the future climate from one model is shown to illustrate what a possible future may look like (5). ACCESS1-0 was used for RCP4.5 and 8.5, and BCC-CSM-1 was used for RCP2.6, as ACCESS1-0 was not available.

In both (a) and (b), different RCPs are shown in different colours (6). Throughout this document, green is used for RCP2.6, blue for RCP4.5 and purple for RCP8.5, with grey bars used in bar plots (b) to illustrate the expected range of change due to natural internal climate variability alone (7).

4.2   TEMPERATURE

Surface air temperatures in the cluster have been increasing since national records began in 1910, especially since 1960 (Figure 4.2.1, Figure 4.2.2). By 2013, mean temperature has risen by 0.8 °C using a linear trend. For the same period, daytime maximum temperatures have risen by 0.7 °C while overnight minimum temperatures have increased by 1.0 °C using a linear trend (Figure 4.2.4).
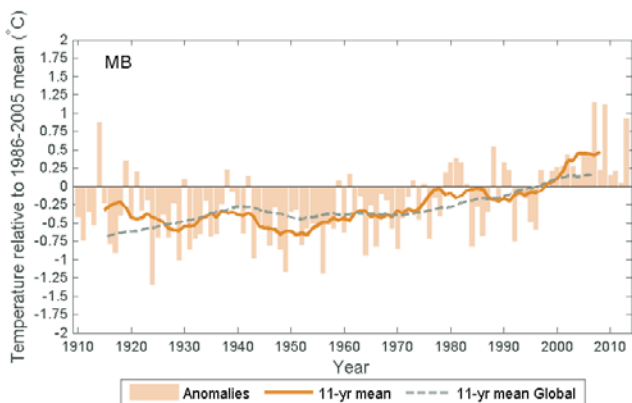
FIGURE 4.2.1: OBSERVED ANNUAL MEAN TEMPERATURE ANOMALIES (°C) FOR 1910–2013 COMPARED TO THE BASELINE 1986–2005 FOR MURRAY BASIN. CLUSTER AVERAGE DATA ARE FROM ACORN-SAT AND GLOBAL DATA ARE FROM HADCRUT3V (BROHAN *ET AL.*, 2006).

The warming across the cluster is broadly in keeping with global temperature changes. However it displays marked differences on decadal time-scales, and even more so on a year to year basis. This is an important reminder that while the warming observed across the cluster is primarily driven by global warming, year to year and even decadal anomalies are also driven by regional factors, some linked to the more variable rainfall trends (see Section 4.4 for details). The warming is fairly uniform across the cluster with lower warming in South Australia and higher warming in the east of the basin.
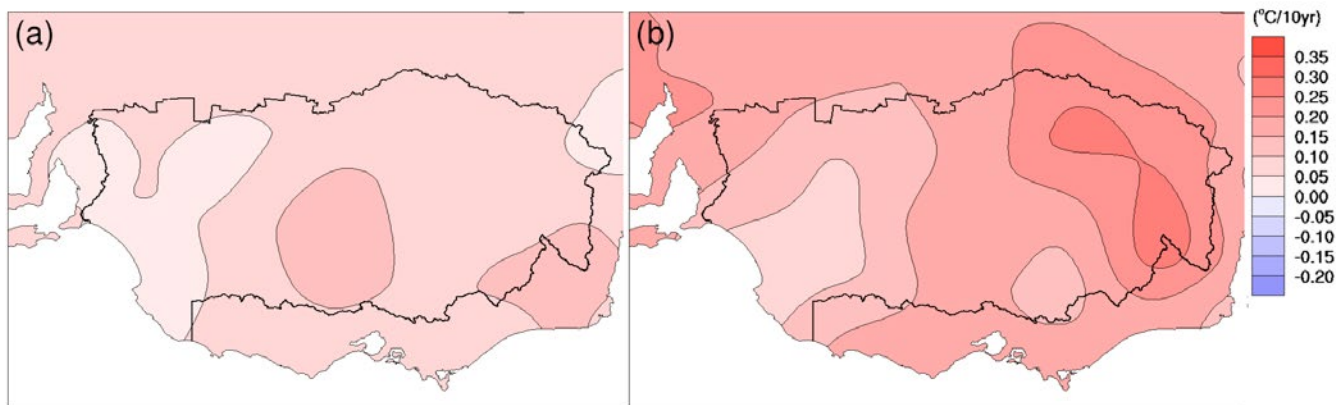
FIGURE 4.2.2: MAPS OF TREND IN MEAN TEMPERATURE (°C/10YEARS) FOR (A) 1910–2013 AND (B) 1960–2013 (ACORN-SAT).
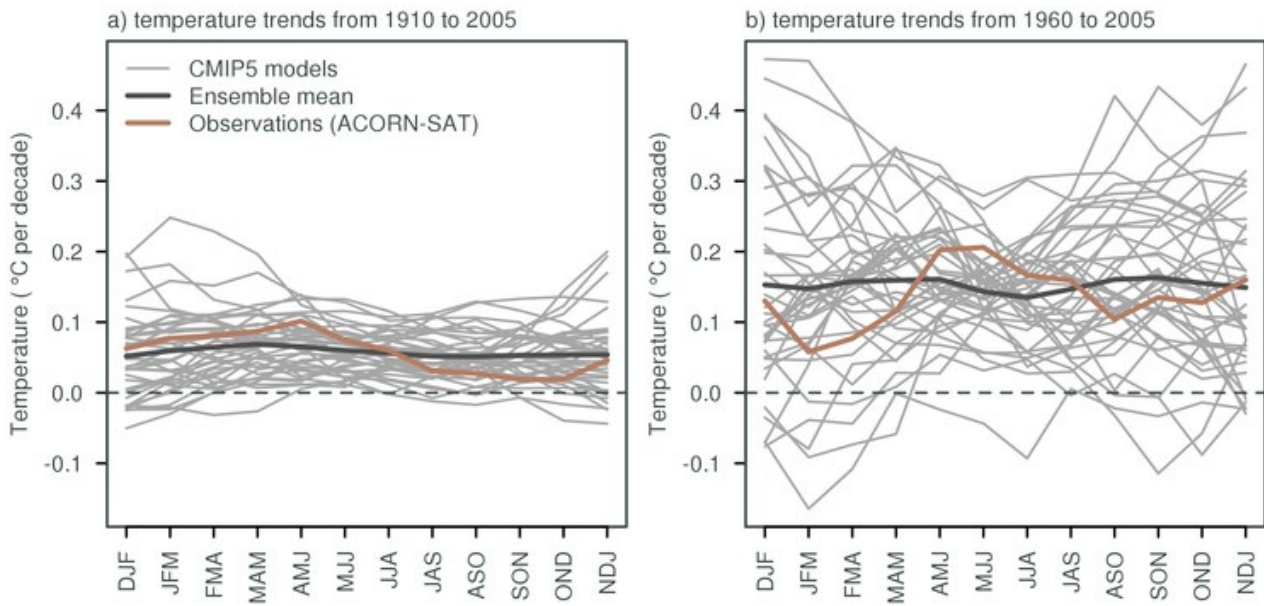
FIGURE 4.2.3: SIMULATED (GREY) AND OBSERVED (BROWN) MONTHLY TRENDS IN TEMPERATURE FROM 1910–2005 (A) AND 1960–2005 (B). THE SOLID BLACK LINE IN BOTH PANELS DENOTES THE MULTI-MODEL ENSEMBLE MEAN TREND. DATA ARE FROM ACORN-SAT.

While the observed warming is fairly similar all year around for the mean and daily minimum and maximum temperature over the last 30 years, the daily minimum temperature during the cool season has shown little warming (Figure 4.2.4). This explains why large parts of the Murray Basin cluster have not experienced a reduction of frost occurrences. Instead the cluster has seen more damaging frost due to overall warming, which causes an earlier start in the year of the growing cycle and thus exposure of plants to cooler temperatures earlier in the season. The difference in temperature trends between daily maximum and minimum temperatures during the cool season, leading to an increase in the diurnal temperature range, is consistent with the observed rainfall trends during the last 30 years; with reduced rainfall in the cool season and hence stronger radiative cooling during the night (see Section 4.4 for details).

The modelled increase in the mean temperature (averaged for the cluster) over the 20th century shows similar rates to observed temperatures (Figure 4.2.5). Daily maximum and minimum temperatures are roughly consistent with

the mean warming. For the 21st century, stronger warming rates are found for the higher emission scenarios (see right-hand plots in Figure 4.2.5), as enhanced radiative forcing is directly linked to atmospheric warming. Model spread increases with time due to variation in model sensitivity to forcing. The graphs show sustained warming under RCP8.5, which by 2090 reaches a median of 4.2 °C for maximum temperature during the warm season and 3.9 °C during the cool season. The corresponding increases for minimum temperature are 3.9 °C and 3.2 °C. In Table 1 in the Appendix, numbers are provided for four standard seasons for RCP2.6, RCP4.5 and RCP8.5 for 20-year periods centred on 2030 and 2090. Overall, for 2030, the mean warming is around 0.6 to 1.3 °C, with only minor difference between RCPs, and for 2090 it is 1.3 to 2.4 °C for RCP4.5 and 2.7 to 4.5 °C for RCP8.5.

When comparing the projected warming to the spread of inter-annual variability estimated by the climate models (grey bars in Figure 4.2.5), projected warming is well outside the spread of natural variability apart for RCP2.6, and therefore highly significant.
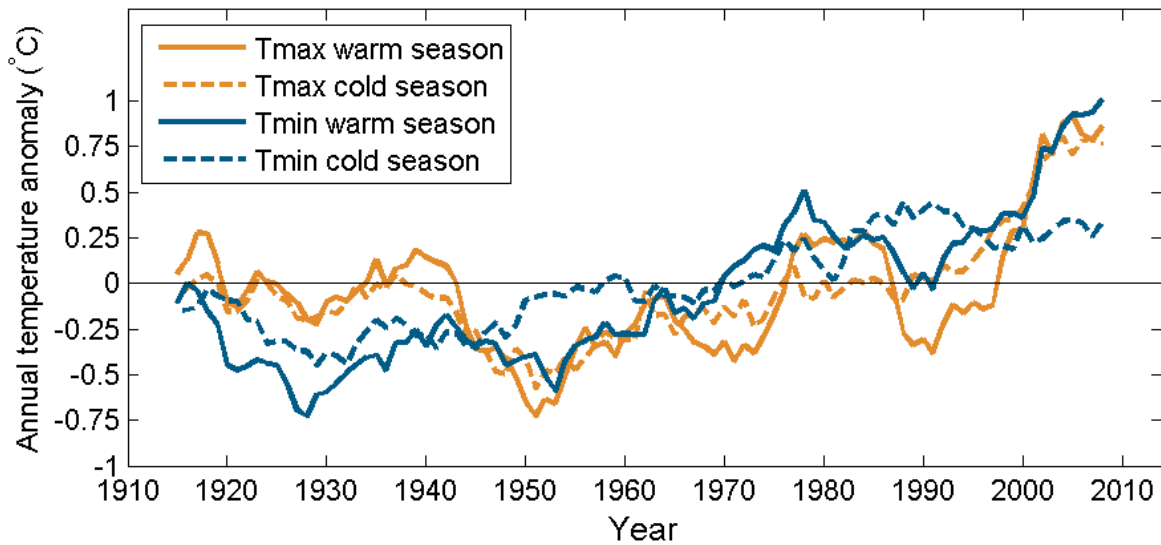
FIGURE 4.2.4: 11-YEAR RUNNING MEAN OF MURRAY BASIN CLUSTER DAILY MINIMUM (BLUE LINE) AND OBSERVED ANNUAL MEAN OF DAILY MAXIMUM (ORANGE LINE) AIR TEMPERATURE PRESENTED AS ANOMALIES RELATIVE TO THE 1910–2013 AVERAGE (°C) (ACORN-SAT); SOLID LINES SHOW THE COOL SEASON (APRIL TO OCTOBER) AND DASHED LINES SHOW THE WARM SEASON (NOVEMBER TO MARCH).

If fitting a linear trend to the full temperature record for the Cluster (measurements starting in 1910 for ACORN-SAT), the rate of increase is somewhat higher for minimum temperature relative to maximum temperature in the cool and warm seasons. However, for a more recent time period (the past 30 years), minimum temperature increases at a much slower rate compared to maximum temperature during the cool season (Figure 4.2.4), which is consistent with the future rainfall projection presented in Section 4.4.
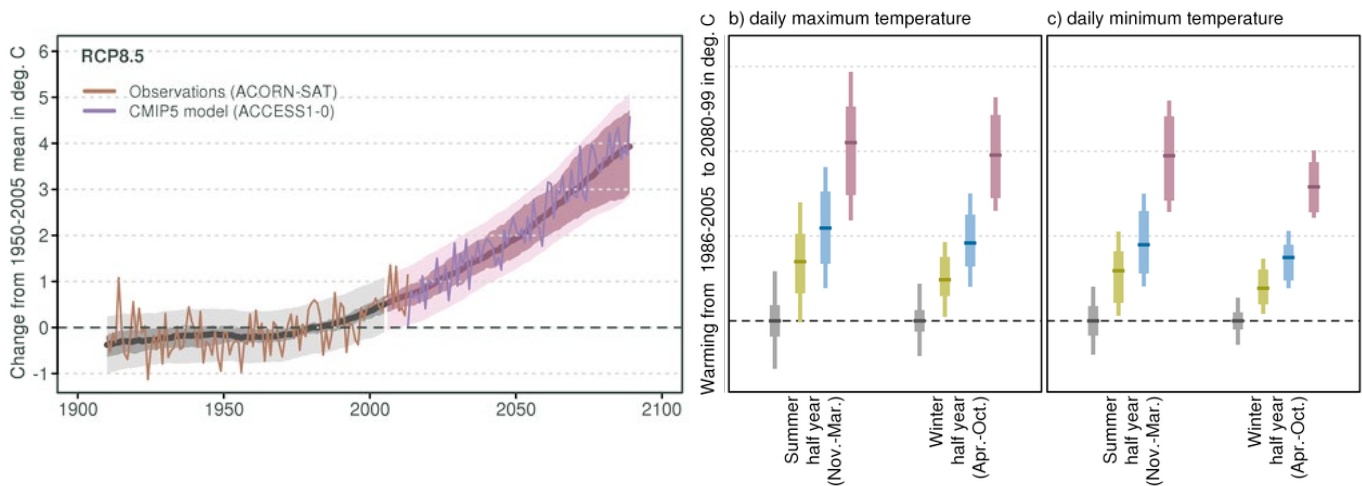
FIGURE 4.2.5: TIME SERIES (A) FOR MURRAY BASIN ANNUAL AVERAGE SURFACE AIR TEMPERATURE (°C) FOR 1910–2090, AS SIMULATED IN CMIP5 RELATIVE TO THE 1950–2005 MEAN FOR RCP8.5 (A). THE CENTRAL LINE IS THE MEDIAN VALUE, AND THE SHADING IS THE 10TH AND 90TH PERCENTILE RANGE OF 20-YEAR MEANS (INNER) AND SINGLE YEAR VALUES (OUTER). THE GREY SHADING INDICATES THE PERIOD OF THE HISTORICAL SIMULATION, WHILE THE FUTURE SCENARIO (RCP8.5) IS SHOWN WITH COLOUR-CODED SHADING (IN PURPLE). ACORN-SAT OBSERVATIONS AND PROJECTED VALUES FROM A TYPICAL MODEL ARE SHOWN. BAR PLOTS IN (B) AND (C) SHOW THE PROJECTED RANGES FOR DAILY MAXIMUM AND MINIMUM TEMPERATURE FOR 2080–99 WITH RESPECT TO 1986–2005 FOR NATURAL CLIMATE VARIABILITY ONLY (GREY), RCP2.6 (GREEN), RCP4.5 (BLUE) AND RCP8.5 (PURPLE). TIME SERIES AND BAR PLOTS ARE EXPLAINED IN BOX 4.2.

Included in the left graph of Figure 4.2.5 is an example of a model simulation. The model simulation is included to illustrate that individual model runs produce temporal variability similar to that of observed temperature, *i.e.* models do not simulate a sequentially steady increase in temperature from one year to another, as in an observed time series. The projected model data show individual years that are warmer or cooler than preceding years. When comparing the trajectory of warming to the spread of natural variability, the warming signal due to increased emissions appears to emerge from the natural variability around the 2050s for most RCPs. Here, 'emergence' means when the range of temperatures in the future moves beyond that of the envelope of current climate.

The projected warming across the Murray Basin cluster has a small south-west to north-east gradient (Section 7.1.1 in the Technical Report presents maps illustrating this point). It is also worth noting that over the last 40 years, the observed warming, while spatially quite homogeneous, displayed a similar south-west to north-east gradient (Figure 4.2.1). In comparison with the previous generation of climate models (CMIP3), the CMIP5 models are showing very similar spatial patterns and a slightly lower warming trend (see Technical Report for details).

Here we illustrate what the mean annual temperature might become by 2090 following the high emission scenario across the south-east of Australia (Figure 4.2.6), for median warming. The area that currently has a mean temperature below 15 °C is reduced to the south-east corner of the cluster at the highest elevations. The statistical downscaling of the models (right graph in Figure 4.2.6) suggests that the cool areas in the Alps could reduce further than in the GCM simulations.

Overall, the two maps of the future mean temperature over the Murray Basin cluster are fairly consistent. However, compared to the results obtained directly from climate models, those obtained by downscaling show a stronger increase at the foothills of the Great Dividing Range (*i.e.* the 20 °C contour comes closer to the high elevation terrain on the northern flank of the Range), and there are small differences along the coast (the most notable ones are along the Eastern coast outside the Murray Basin cluster). These maps illustrate the potential benefit in terms of spatial details of using downscaled climate change projections when available and when suitable to the particular application (see section 6.3 in the Technical Report for a discussion on downscaling methods, their abilities and limitations).

Taking into consideration the strong agreement on direction and magnitude of change amongst GCMs and downscaling results and the robust understanding of the driving mechanisms of warming and its seasonal variation, there is *very high confidence* in substantial increase for daily mean, maximum and minimum temperature for the Murray Basin cluster.
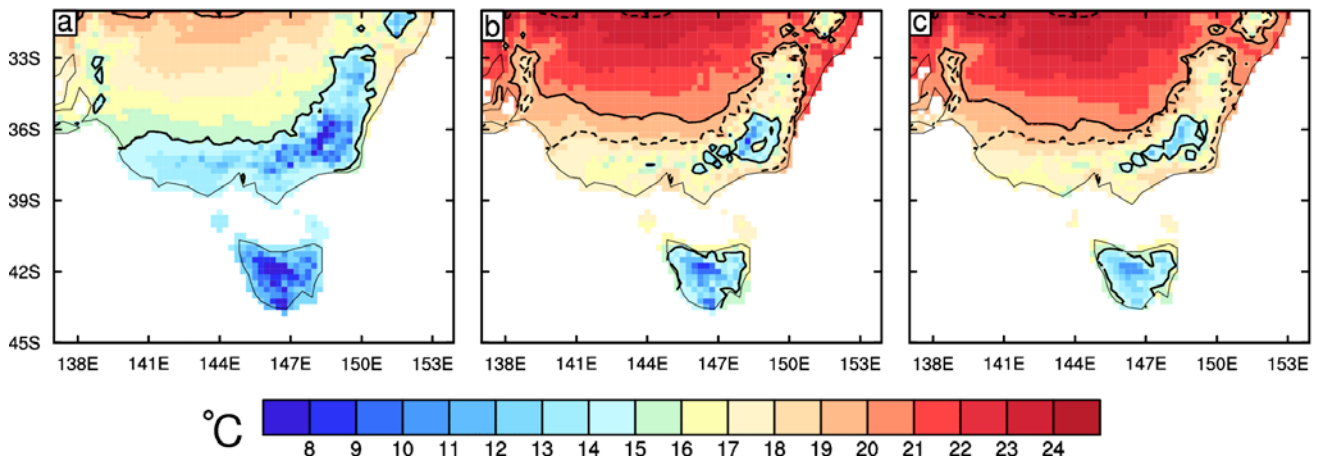
FIGURE 4.2.6: ANNUAL MEAN SURFACE AIR TEMPERATURE (°C), FOR THE PRESENT CLIMATE (A), AND FOR 2090 USING GCM PROJECTED WARMING (B) OR FOR THE STATISTICAL DOWNSCALING OF THESE MODELS (C). THE PRESENT CLIMATE IS BASED ON THE AWAP DATA SET FOR 1986–2005 (A 0.25 DEGREE GRID). THE FUTURE CASE IS USING THE MEDIAN CHANGE AT 2090, UNDER RCP8.5 (UNDER A GLOBAL WARMING OF 3.7 °C CASE). THE RIGHT PANEL SHOWS THE DOWNSCALED MEDIAN CHANGE BY 2090 OF THE 22 GCMS FOR WHICH THE STATISTICAL DOWNSCALING WAS PERFORMED. THESE RESULTS WERE PRODUCED ON 0.05 DEGREE GRID, BUT WERE AVERAGED ON A 0.25 DEGREE GRID. FOR CLARITY, THE 15 AND 20 °C CONTOURS ARE SHOWN WITH SOLID BLACK LINES. IN (B) AND (C) THE SAME CONTOURS FROM THE ORIGINAL CLIMATE ARE PLOTTED AS DOTTED LINES.

4.2.1 EXTREMES

Changes to temperature extremes often lead to greater impacts than changes to the mean climate. To assess these, researchers examine CMIP5 projected changes to measures such as the warmest day in the year, warm spell duration and frost risk days (see definitions below).
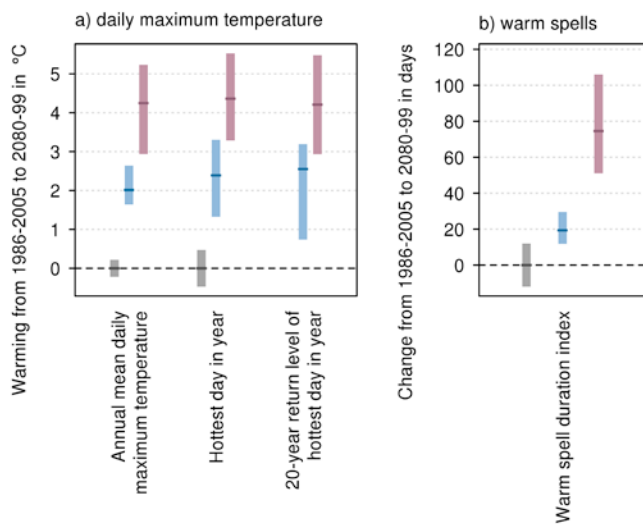
FIGURE 4.2.7: PROJECTED CHANGES IN SURFACE AIR TEMPERATURE EXTREMES BY 2090 IN (A) MEAN DAILY MAXIMUM TEMPERATURE, HOTTEST DAY OF THE YEAR AND THE 20-YEAR RETURN VALUE OF THE HOTTEST DAY OF THE YEAR (°C); AND (B) CHANGE IN THE NUMBER OF DAYS IN WARM SPELLS FOR MURRAY BASIN (SEE TEXT FOR DEFINITION OF VARIABLES). RESULTS ARE SHOWN FOR RCP4.5 (BLUE) AND RCP8.5 (PURPLE) RELATIVE TO THE 1986–2005 MEAN. NATURAL CLIMATE VARIABILITY IS REPRESENTED BY THE GREY BAR. BAR PLOTS ARE EXPLAINED IN BOX 4.2.

The annual maximum of the daily maximum temperature represents the hottest day within a year. By 2090, this value is expected to rise about 2.4 °C (median value) following RCP4.5 and 4.5 °C following RCP8.5 (Figure 4.2.7), the hottest day in the 20-years (20-year return value, equal to a 5 % chance of occurrence within any one year) is also projected to increase by a similar amount. Furthermore it also supports the application of the projected changes for selected time slices and RCPs to the historical daily record at selected sites approach to obtain a local estimate of the change in frequency of hot days. This is illustrated in Box 4.3 for Canberra where it can be seen that the number of days above 35 °C by 2090 more than doubles under the RCP4.5 and median warming, and the number of days over 40 °C more than triples.

To better define changes in extreme hot temperatures, in addition to the hottest day in the year, several metrics can be used to quantify the magnitude, frequency and duration of maximum/minimum values or rare events. To better

approximate future behaviour of heatwaves (and cold spells), relevant extremes can be thought of as extended lengths of cold/warm spells, defined as the annual count of days for events with at least six consecutive days with minimum/maximum below/above the 10th/90th percentile, as estimated from a baseline climate. As an example the 90th percentile for daily temperature maximum in Canberra is 29.8 °C based on Bureau of Meteorology historical data for March 1939 to June 2014. The GCM projections indicate a marked increase in the warm spell duration index through the century, starting from values near zero. There are very large increases projected for RCP8.5 by 2090 (Figure 4.2.7): median warming gives an increase in warm spells of 75 days compared to 1986–2005.

Strong model agreement and understanding of physical mechanisms of warming lead to *high confidence* in the substantial increase in the heat related extremes.

4.2.2 FROST DAYS

Changes in the frequency of surface frost are of potential importance to agriculture, energy and other sectors, and to the environment. Assessing frost occurrence directly from global model output is not reliable, in part because of varying biases in land surface temperatures. For this cluster, we were able to examine statistical downscaling of the 22

CMIP5 models. This technique has the ability to describe local temperature with minimal bias and hence it is possible to analyse the number of days with minimum temperature below 2 °C as a proxy for the risk of frost occurrences. Average numbers of frost occurrences across the Murray Basin cluster are projected to decrease in all seasons (Figure 4.2.8).
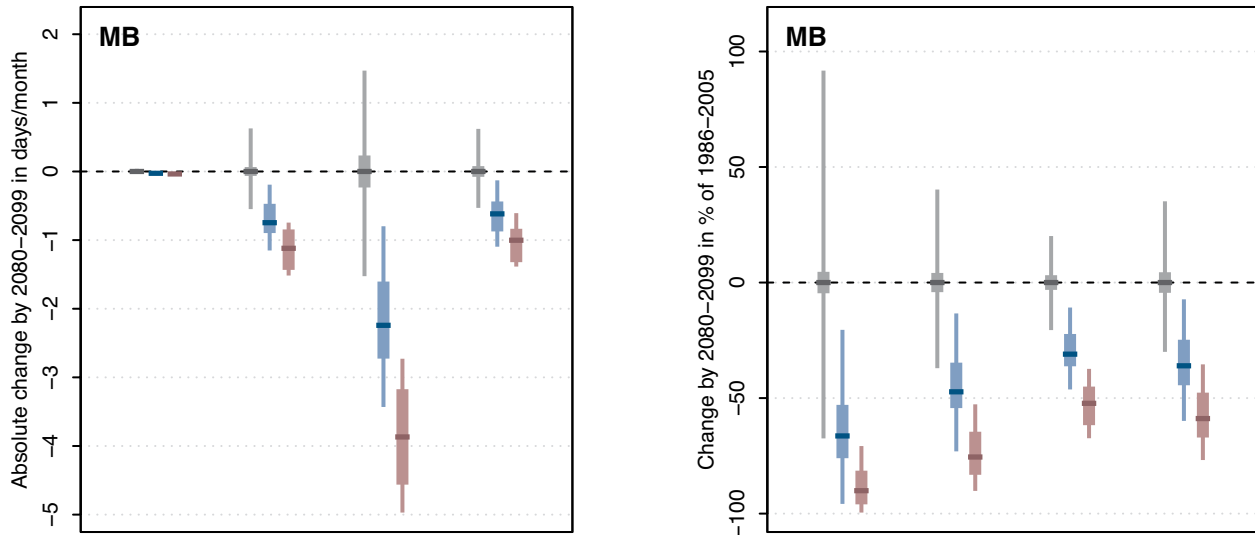
FIGURE 4.2.8: SEASONAL PROJECTED CHANGE IN FROST OCCURRENCES FOR 2080−99 IN RELATION TO THE PERIOD 1986−2005 AVERAGED ACROSS THE MURRAY BASIN CLUSTER IN ABSOLUTE (DAYS, LEFT GRAPH) OR RELATIVE (PERCENTAGE OF THE CURRENT CLIMATE, RIGHT GRAPH) TERMS. THE BARS AND HORIZONTAL TICKS DENOTE 10TH, 50TH AND 90TH PERCENTILE OF THE STATISTICALLY DOWNSCALED CMIP5 RESULTS. THE SCENARIOS FROM LEFT TO RIGHT ARE: NATURAL VARIABILITY ONLY (GREY), RCP4.5 (BLUE) AND RCP8.5 (PURPLE).

BOX 4.3: HOW WILL THE FREQUENCY OF HOT DAYS AND FROST RISK DAYS CHANGE IN CANBERRA?

To illustrate what the CMIP5 projected warming implies for changes to the occurrence of hot days and frost days in Canberra, a simple downscaling example was conducted.

The type of downscaling used here is commonly referred to as Change Factor Approach (see Section 6.3.1. in the Technical Report), whereby a change (calculated from the simulated model change) is applied to an observed time series. In doing so, it is possible to estimate the frequency of extreme days under different emission scenarios.

In Table B4.3, days with maximum temperatures above 35 and 40 °C, and frost risk days (minimum temperature less than 2 °C) are provided for a 30-year period (1981–2010), and for downscaled data.

TABLE B4.3: CURRENT AVERAGE ANNUAL NUMBER OF DAYS (FOR THE 30-YEAR PERIOD 1981–2010) ABOVE 35 AND 40 °C AND BELOW 2 °C (FROSTS) FOR CANBERRA AIRPORT (ACT) BASED ON ACORN-SAT. ESTIMATES FOR THE FUTURE ARE DOWNSCALED 30-YEAR PERIODS, CALCULATED USING CHANGE FACTORSTHE MEDIAN CMIP5 WARMING FOR 2030 AND 2090. FOR 2030, ONLY RCP4.5 IS SHOWN, AS THESE RESULTS ARE SIMILAR TO THOSE FOR RCP2.6, AND RCP8.5. THE MEDIAN PROJECTION ACROSS THE MODELS IS SHOWN, AND WITHIN BRACKETS THE 10TH AND 90TH PERCENTILE CMIP5 WARMING FOR THESE PERIODS), APPLIED TO THE 30-YEAR ACORN-SAT STATION SERIES. NUMBERS ARE TAKEN FROM TABLE 7.1.2 AND TABLE 7.1.3 IN THE TECHNICAL REPORT.

THRESHOLD	CURRENT	2030 RCP4.5	2090 RCP4.5	2090 RCP8.5
Over 35 °C	7.1	12 (9.4 to 14)	17 (13 to 23)	29 (22 to 39)
Over 40 °C	0.3	0.6 (0.4 to 0.8)	1.4 (0.8 to 2.8)	4.8 (2.3 to 7.5)
Below 2 °C	91	81 (87 to 76)	68 (75 to 61)	43 (52 to 35)

There is a strong reduction in frost, dependent on the emission scenarios, but passing outside the range of natural variability by 2090 in the case of RCP8.5. In absolute terms, the largest reduction of frost occurrences is seen in winter, but in percentage terms it is largest in summer (frost in that season is only encountered in the small Alpine region within the cluster). It is interesting to note that spring frosts decline less rapidly than autumn ones, which combined with advanced plant phenology due to generally warmer conditions, indicates that risks associated with late frost occurrences may not necessarily decline. This is a complex area which requires careful modelling based on individual plant phenology.

To give an indication to changes in frost occurrence at a representative site, Box 4.3 also illustrates the change in frost days at Canberra using the simple approach of applying the mean warming to the historical minimum temperature record (as was done for hot days). This approach does not allow for the effect of any changes in variability (unlike the approach described above) but gives broadly comparable results (also see Section 7.1 in the Technical Report).

In summary, strong model agreement and understanding of physical mechanisms of warming lead to *high confidence* in a projected substantial decrease in the frequency of frost.

4.3   MEAN SEA LEVEL PRESSURE

As discussed in Box 1, changes in mean sea level pressure (MSLP) are important as they relate to rainfall change in the Murray Basin cluster, in particular during the cool season when the intensity of the sub-tropical ridge (STR) has the main influence on rainfall. Analysis of the CMIP5 simulations confirms that most climate models project an increase in the intensity of the STR, dependent on the magnitude of the projected warming. Using CMIP3 models, Kent *et al.* (2013) found that the mean intensification is 0.24 hPa/°C. In addition to intensification, climate models indicate a shift poleward of the STR, which will also reduce cluster rainfall. The intensification and poleward shift of the STR is consistent with the observed trend in the last 30 years and the observed broadening of the Mean Meridional Circulation (MMC) (see Box 2.1). Projections indicate a consensus amongst models toward a further broadening of the MMC (IPCC, 2013).

The annual mean MSLP projections for the Murray Basin cluster for RCP8.5 show an increase reaching 1 hPa by 2090 (left plot in Figure 4.3.1). The annual mean is made up of a small increase during the warm season and a large increase during the cool season (right graph in Figure 4.3.1), which is the time of the year where the relationship between the STR intensity and rainfall in the Murray Basin is important. For 2090, there is *high confidence* about the direction of the
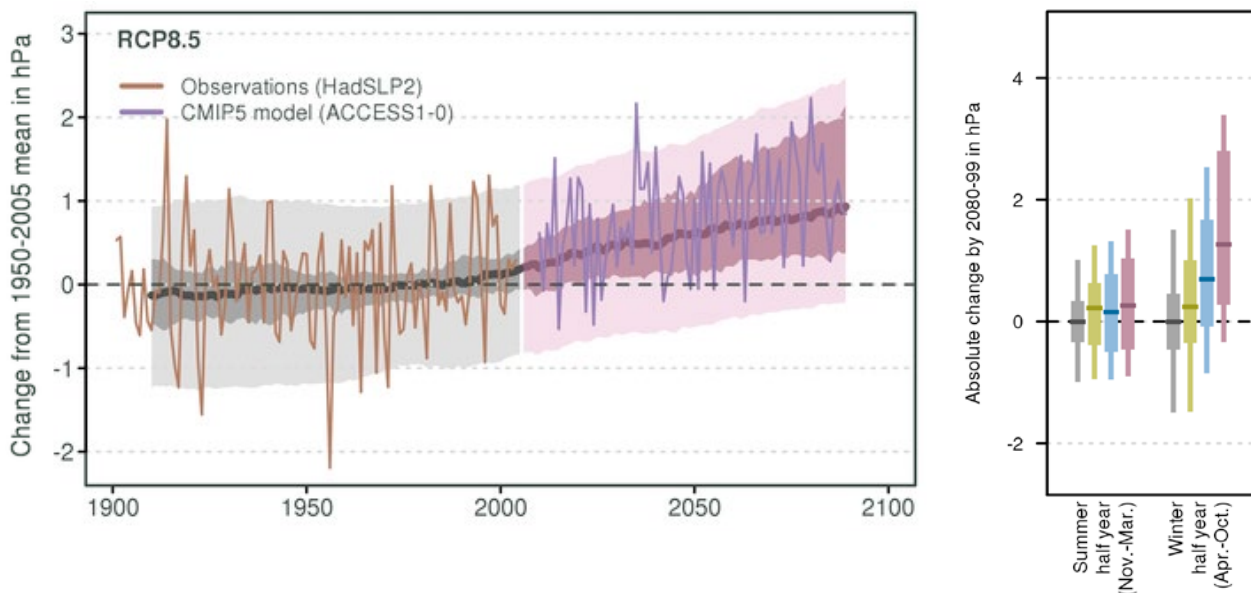
FIGURE 4.3.1: TIME SERIES FOR SOUTHERN AUSTRALIA (INCLUDES THE AREA OF THE MURRAY BASIN, THE SOUTHERN AND SOUTH WESTERN FLATLANDS AND THE SOUTHERN SLOPES CLUSTERS) ANNUAL AVERAGE MSLP (HPA), AS SIMULATED IN CMIP5 MODELS RELATIVE TO THE 1950–2005 MEAN FOR RCP8.5 (LEFT). THE CENTRAL LINE IS THE MEDIAN VALUE, AND THE SHADING IS THE 10TH AND 90TH PERCENTILE RANGE OF 20-YEAR MEANS (INNER) AND SINGLE YEAR VALUES (OUTER). THE GREY SHADING INDICATES THE PERIOD OF THE HISTORICAL SIMULATION, WHILE THE FUTURE SCENARIO IS SHOWN WITH COLOUR-CODED SHADING (PURPLE). HADSLP2 OBSERVATIONS ARE SHOWN IN BROWN AND PROJECTED VALUES FROM A TYPICAL MODEL ARE SHOWN INTO THE FUTURE IN GREY. BAR PLOTS (RIGHT) SHOW SEASONAL CHANGES (HPA) FOR SOUTHERN AUSTRALIA FOR 2080–99 WITH RESPECT TO 1986–2005 FOR NATURAL CLIMATE VARIABILITY ONLY (GREY), RCP2.6 (GREEN), RCP4.5 (BLUE) AND RCP8.5 (PURPLE). TIME SERIES AND BAR PLOTS ARE EXPLAINED IN BOX 4.2.

change, but the increase is gradual during the 21st century and its magnitude depends on the emission scenario.

In addition, in the Appendix tables, projections are provided for 2030 and 2090 relative to the 1986–2005 period showing the 10th, 50th and 90th percentile change, as projected by the CMIP5 model archive for RCP2.6, RCP4.5 and RCP8.5 scenarios.

Based on the observed relationship between STR intensity and rainfall, we expect these MSLP projections to translate into rainfall trends (*i.e.* drying in the cool season). However, a very uneven ability across climate models to reproduce the observed STR-rainfall relationship was noted for CMIP3 models (Kent *et al.*, 2013).

4.4   RAINFALL

The Murray Basin cluster has experienced some remarkable rainfall variability in the last 15 years, including the record breaking Millennium drought affecting most of the Murray-Darling Basin (Leblanc *et al.*, 2012) included in the Murray Basin cluster. The Millennium drought ended with two of the wettest years on record for Australia in 2010–11 (Beard *et al.*, 2011, Bureau of Meteorology, 2012). For 2010–11, the 2-year average was 690 mm per year and was the third wettest 2-year period (after 1973–74 and 1955–56) on record. However, while the Millennium drought was dominated by

autumn and early winter rainfall declines (primarily within the cool season), the very wet La Niña driven 2010–11 period was predominantly delivered as warm season rainfall. This has contributed to a marked ongoing decrease in the difference between cool and warm season rainfall.
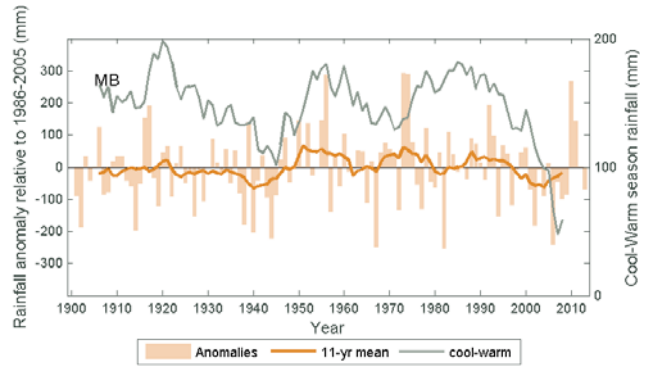
FIGURE 4.4.1: MURRAY BASIN CLUSTER AVERAGE OF THE OBSERVED ANNUAL RAINFALL ANOMALIES (ORANGE BARS: DIFFERENCES IN MM FOR 1901–2013 COMPARED TO THE BASELINE 1986–2005) SINCE 1901 INCLUDING THE 11-YEAR RUNNING MEAN (BOLD ORANGE LINE), AND THE 11-YEAR RUNNING MEAN OF THE DIFFERENCE BETWEEN THE APRIL-OCTOBER (COOL) AND NOVEMBER-MARCH (WARM) RAINFALL (GREY LINE). DATA ARE FROM AWAP.
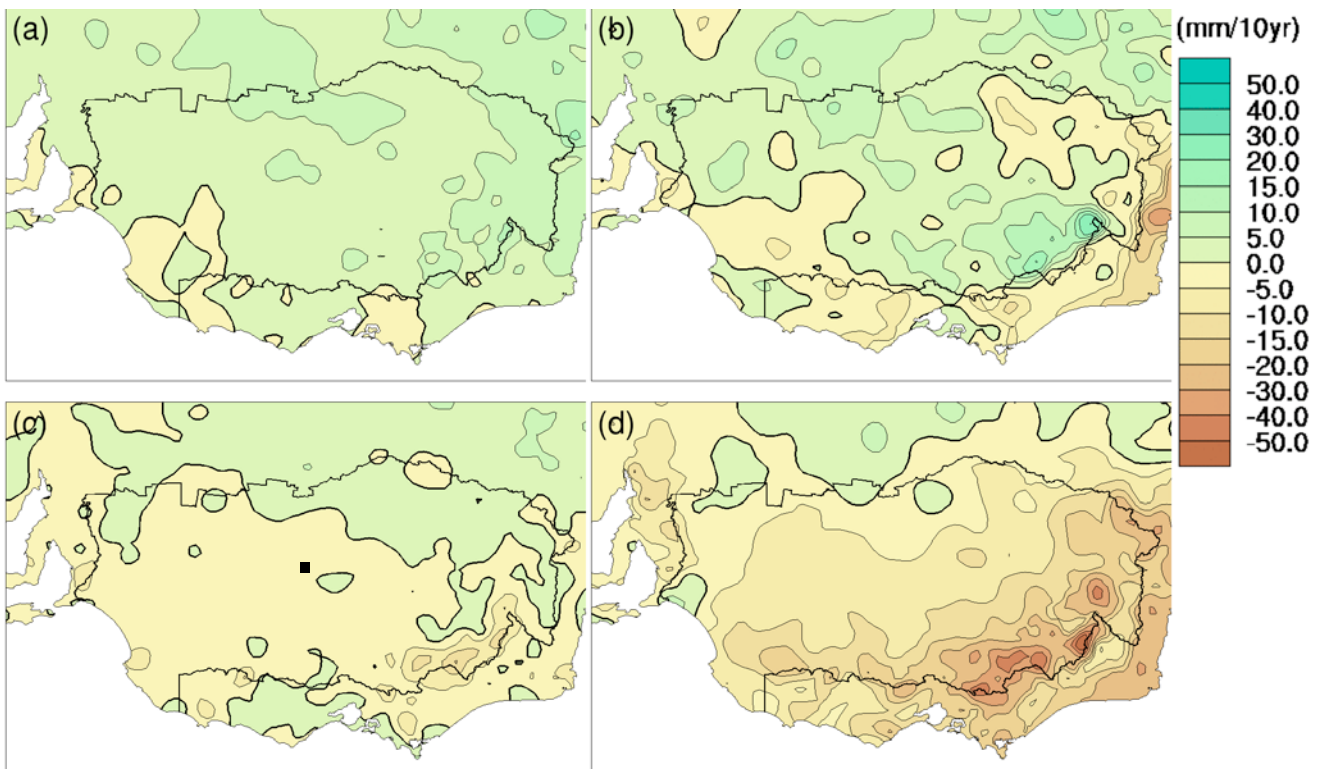
FIGURE 4.4.2: SEASONAL MAPS OF RAINFALL TRENDS (MM/DECADE) FOR WARM SEASON (A) 1901–2013 AND (B) 1960–2013, COOL SEASON (C) 1901–2013 AND (D) 2060–2013.

The spatial extent of the rainfall decline since 1960 covers the entire Murray Basin cluster in autumn (the season where the decline has been the strongest) and a large part of the cluster in winter and spring (Figure 4.4.2). In contrast, most of the cluster has experienced increasing summer rainfall. Using the cool and warm seasons described in this report, their respective trends are mostly opposing each other across much of the Murray Basin cluster (not so outside the cluster on the Eastern Seaboard). The largest trends in both seasons are observed over the complex orography in the south-eastern part of the cluster with a sharp contrast between the two seasons.

The observed rainfall decline has strong similarity with the STR intensification (see Box 2.1), both in terms of spatial area affected, including the Murray Basin cluster (CSIRO, 2012) as well as the magnitude. Timbal and Drosdowsky (2013) reported that about 70 % of the rainfall deficit during the cool season over the Millennium drought was consistent with the expected rainfall response to the observed strengthening of the STR for an area covering the south-west of Eastern Australia and hence a large section of the Murray Basin cluster.

The CMIP5 models do capture an expansion of the MMC, in particular the Hadley Cell and the strengthening of the STR (Nguyen *et al.*, 2014), albeit with a reduced intensity compared to the reanalyses and observations. However the same GCMs are not able to reproduce the observed rainfall trends. There is a large range of responses across models, but the ensemble mean shows no tendency toward drying during the cool season and a weak tendency toward wetter conditions for the warm season (not shown).

Annual mean rainfall projections are shown for 2090 under RCP8.5 (left panel in Figure 4.4.3) and for the warm and cool seasons for three emissions scenarios (right panel in Figure 4.4.3). Tabulated results for various emission scenarios, 2030 and 2090 and for the four traditional seasons are given in Appendix Table 1.

By 2030, the changes are not strongly different to those due to natural variability under any RCP. Model spread is large and increases with time due to variation in model sensitivity to forcing. Hence the very weak long-term trend will be hard to identify from the very large natural variability, which will continue during the 21st century. In the Appendix, numbers are provided using the four traditional calendar seasons for three RCPs and for 2030 and 2090. In 2030, changes under all RCPs are around -10 to +5 % annually, and around -15 to +10 % in winter, and -15 to +15 % in summer. By 2090 the changes in winter span -20 to +5 % under RCP4.5 and -40 to +5 % under RCP8.5, and those in summer span -15 to +10 % under RCP4.5 and -15 to +25 % under RCP8.5.
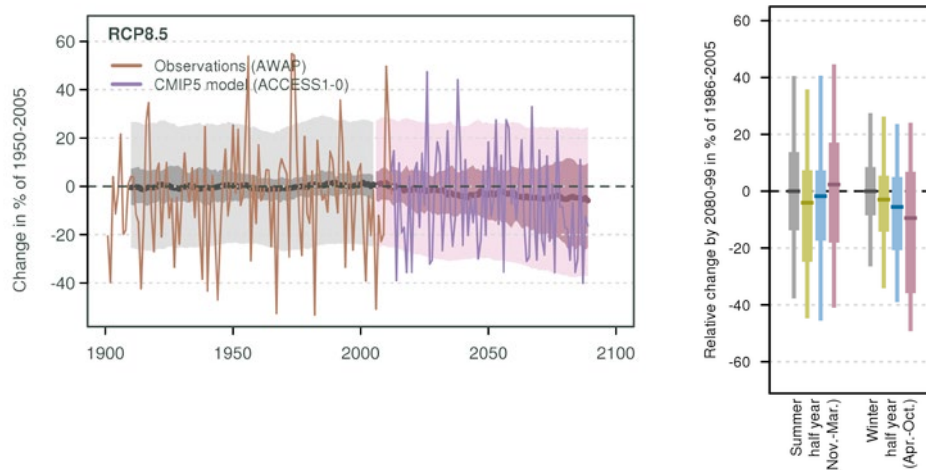
FIGURE 4.4.3: TIME SERIES FOR MURRAY BASIN ANNUAL AVERAGE RAINFALL FOR 1910–2090, AS SIMULATED IN CMIP5 RELATIVE TO THE 1950–2005 MEAN FOR RCP8.5 (LEFT). THE CENTRAL LINE IS THE MEDIAN VALUE, AND THE SHADING IS THE 10TH AND 90TH PERCENTILE RANGE OF 20-YEAR MEANS (INNER) AND SINGLE YEAR VALUES (OUTER). THE GREY SHADING INDICATES THE PERIOD OF THE HISTORICAL SIMULATION, WHILE THE FUTURE SCENARIO IS SHOWN WITH COLOUR-CODED SHADING (PURPLE). AWAP OBSERVATIONS ARE SHOWN IN BROWN (BEGINNING 1901) AND PROJECTED VALUES FROM A TYPICAL MODEL ARE SHOWN (PURPLE LINE). BAR PLOTS (RIGHT) SHOW SEASONAL CHANGES (%) FOR MURRAY BASIN FOR 2080–99 WITH RESPECT TO 1986–2005 FOR NATURAL CLIMATE VARIABILITY ONLY (GREY), RCP2.6 (GREEN), RCP4.5 (BLUE) AND RCP8.5 (PURPLE). TIME SERIES AND BAR PLOTS ARE EXPLAINED IN BOX 4.2.

It is worth noting that the severity of the observed rainfall decline during the cool season over the last 30 years (not shown) stands out as exceptional. In comparison to the envelope of the climate model simulations of the 20th century, it represents a very extreme case, albeit one that falls within the modelled range of natural variability. In comparison with the future projections, it is on par with the most extreme modelled projections by 2090 using RCP8.5. It is worth remembering that while climate models do reproduce the observed changes driving the observed cool season decline (meridional circulation and STR changes), they do so with a much reduced magnitude. Hence, it is possible that climate models are not as sensitive as the real climate system to the overall change in circulation impacting the Murray Basin cluster. For this reason, a large reduction in cool season rainfall, while at the extreme of the modelling results, should not be discarded for planning purposes.

Downscaling shows overall agreement with the thrust of the CMIP5 model projections (Figure 4.4.4). Some differences emerge due to the smaller sample of GCMs considered by each downscaling method. The weak warm season rainfall increase is enhanced with the dynamical downscaling, but not so by the statistical downscaling approach. For the cool seasons, both downscaling methods agree on a future reduction of the rainfall and enhance the magnitude of the decline, although this is partly driven by sub-sampling the CMIP5 suite of models. Furthermore, current trends in the cool season have a strong signature in relation to the orography (Figure 4.4.2), which is a characteristic that GCMs cannot capture, but downscaling might. Section 3 in this report and Section 6.3 in the Technical Report present further details on downscaling methods.
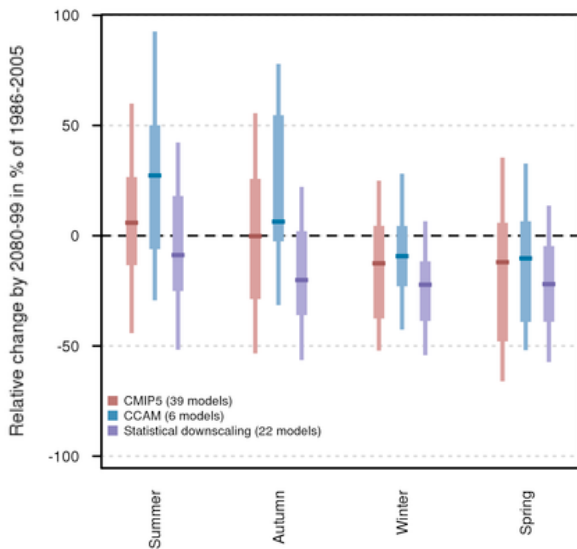
In summary, considering (1) the physical understanding of the relationship between the Mean Meridional Circulation, the sub-tropical ridge and rainfall across the Murray Basin cluster; (2) the projections of MSLP increase and STR strengthening (see previous section), (3) the difficulties that the models have in adequately capturing the observed relationship between STR and rainfall, and (4) the results from downscaling, there is *high confidence* that cool season rainfall will decline in the future. The magnitude of this decline is, however, very uncertain. For the warm season, there is *medium confidence* that future rainfall will remain unchanged. There is also *high confidence* that natural variability will remain large relative to any anthropogenic changes, at least for the near future (2030).

4.4.1   HEAVY RAINFALL EVENTS

Extremes of rainfall can be defined in many different ways, although always focusing on aspects of frequency, duration and magnitude. This report focuses on indices of extremes that capture characteristics of heavy rainfall, such as the largest annual 1-day totals and the proportion of total rainfall attributed to heavy rainfall. In a warming climate, rainfall extremes are expected to increase in magnitude mainly due to a warmer atmosphere being able to hold more moisture (Sherwood *et al.*, 2010). However, this can be enhanced or suppressed in any single region by changes to the circulation.

FIGURE 4.4.5: PROJECTED CHANGES IN MURRAY BASIN MEAN RAINFALL, MAGNITUDE OF ANNUAL MAXIMUM 1-DAY RAINFALL AND MAGNITUDE OF THE 20-YEAR MAXIMUM RETURN VALUE FOR THE 1-DAY RAINFALL FOR 2090 (SEE TEXT FOR DEFINITION OF VARIABLES). RELATIVE RAINFALL ANOMALIES ARE GIVEN IN PERCENTAGE WITH RESPECT TO THE 1986–2005 MEAN FOR THE RCP4.5 (BLUE) AND RCP8.5 (PURPLE) SCENARIOS.). NATURAL CLIMATE VARIABILITY IS REPRESENTED BY THE GREY BAR. BAR PLOTS ARE EXPLAINED IN BOX 4.2.
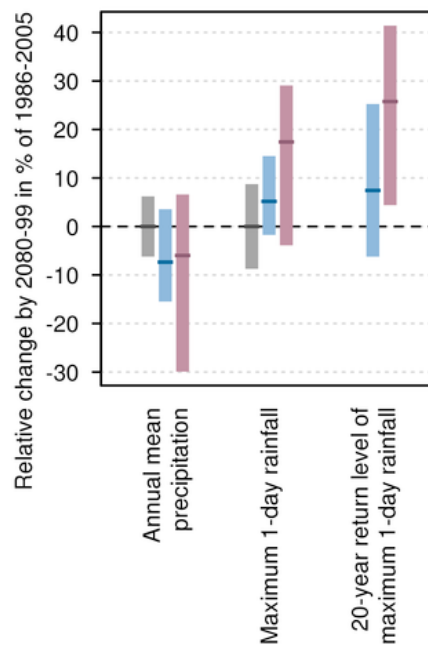
FIGURE 4.4.4: PROJECTED RELATIVE CHANGE IN MURRAY BASIN SEASONAL RAINFALL FOR 2090 WITH RESPECT TO 1986–2005 FOLLOWING RCP8.5. BARS SHOW RESULTS ACCORDING TO USING CMIP5 GCMS AND TWO DOWNSCALING METHODS (CCAM AND SDM). RAINFALL ANOMALIES ARE GIVEN IN PERCENT WITH RESPECT TO 1986–2005 UNDER RCP8.5. BAR PLOTS ARE EXPLAINED IN BOX 4.2.

For the Murray Basin cluster, the CMIP5 models simulate an increase in extreme rainfall. Figure 4.4.5 shows the projected trends in the annual mean rainfall, the 1-day annual maximum value and the 20-year return value of the maximum 1-day rainfall for the period 2080–2099 relative to the baseline period 1986–2005; where a 20-year return value is equivalent to a 5 % chance of occurrence within any one year. Comparing the changes in the two extreme indices with those of the annual mean rainfall clearly shows that while the projection for mean rainfall is tending towards a decrease, the extremes are projected to increase. Separated into cool and warm seasons (not shown), the latter being the season where the largest annual daily totals are currently being observed, the increase in 1-day rainfall is larger in the warm season.

Understanding of the physical mechanisms that determine the rate and amount of rainfall suggest that extreme rainfall events are likely to increase in intensity, especially for the most extreme events. Thus, there is *high confidence* that the intensity of daily rainfall extremes will increase. The magnitude of change is less certain as some smaller scale weather systems that generate extreme rainfall are not well resolved by GCMs (Fowler and Ekstroem, 2009). Hence, there is *low confidence* in the magnitude of change, and thus the time when any change may be evident against natural fluctuations.

4.4.2   DROUGHT

In recent history, the Murray Basin cluster has been affected by three prolonged droughts: the Federation drought and the World War II drought in the first half of the 20th century, and the Millennium drought (Figure 4.4.1). The Millennium drought was comparable to the World War II drought across the cluster but was more severe and longer lasting in the south and west (CSIRO, 2012).

To assess the implications of projected climate change for drought occurrence, researchers selected a measure of meteorological drought, the Standardised Precipitation Index (SPI). The amount of time spent in drought and changes to the duration and frequency of droughts of different severities were calculated. Section 7.2.3 of the Technical Report presents details on calculation of the SPI, as well as further information on drought.

FIGURE 4.4.7: SIMULATED CHANGES IN DROUGHT BASED ON THE STANDARDISED PRECIPITATION INDEX (SPI). THE MULTI-MODEL ENSEMBLE RESULTS FOR MURRAY BASIN AVERAGESHOW THE PERCENTAGE OF TIME IN DROUGHT PROPORTION(SPI LESS THAN -1) (TOP), DURATION OF EXTREME DROUGHT DURATION (MIDDLE) AND FREQUENCY OF EXTREME DROUGHT (BOTTOM) FOR EACH 20-YEAR PERIOD CENTRED ON 1995, 2030, 2050, 2070 AND 2090 UNDER RCP2.6 (GREEN), RCP4.5 (BLUE) AND RCP8.5 (PURPLE). NATURAL CLIMATE VARIABILITY IS REPRESENTED BY THE GREY BAR. SEE TECHNICAL REPORT CHAPTER 7.2.3 FOR DEFINITION OF DROUGHT INDICES. BAR PLOTS ARE EXPLAINED IN BOX 4.2.

Projections of time spent in drought (SPI<-1) for Murray Basin
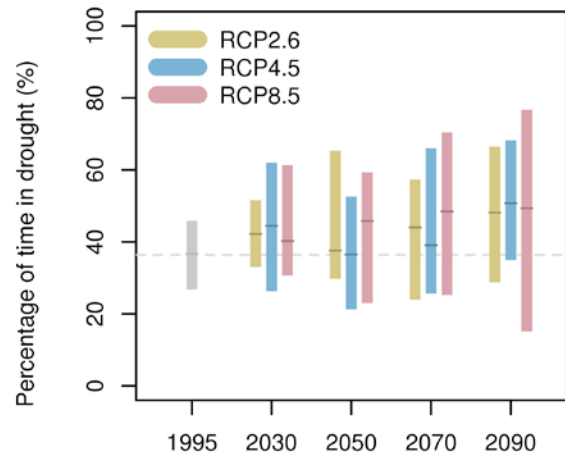
Projections of extreme drought duration for Murray Basin
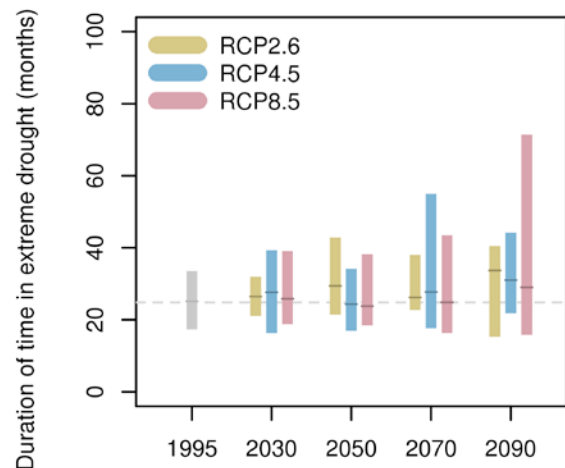
Projections of extreme drought frequency for Murray Basin
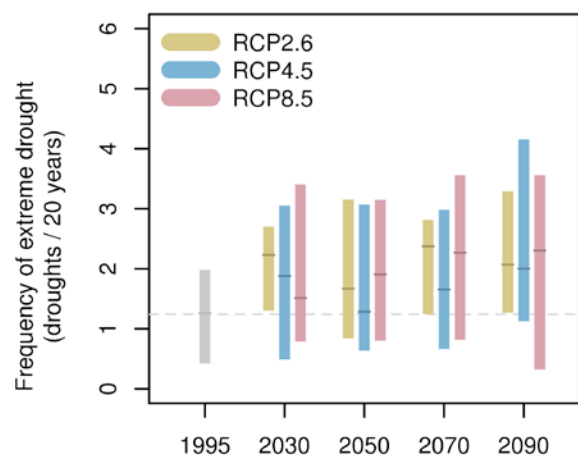
The projected change in the percentage time spent in drought, as well as the projections for duration and frequency for extreme drought are shown in Figure 4.4.7. Increases tend to dominate for time spent in drought and for extreme drought frequency, but not in all cases. This result is associated with the projected decline in annual and cool season rainfall, but changes in rainfall variability could contribute. Changes to extreme drought duration are less clear. For all scenarios, the model ensemble median indicate an increase in the percentage time spent in drought and the frequency of extreme drought for 2090; though some models under RCP8.5 show a clear reduction. These results are of *medium confidence*.

4.4.3   SNOW

A long-term reconstruction of annual maximum snow depth at Cabramurra (Davis, 2013) showed that snow depth has experienced considerable inter-annual and decadal variability (Figure 4.4.8). This is similar to the variability observed for rainfall across the Murray Basin cluster (Figure 4.4.1). There is no significant trend over the entire record (150 years), as natural variability is large. There is however, a significant decline if only the last 100 years of the record are considered, and even more so for the last 60 years. This decline relates to the regional warming trend, rather than rainfall trends. This is consistent with previous work across the snow-covered Australian Alps (see Section 4.2.8 in the Technical Report).

A simple analysis was performed using precipitation on days when the maximum temperature does not exceed 2 °C as a proxy for snowfall from 22 CMIP5 models downscaled using the analogue-based statistical approach for two elevations: 1,419 m (next to the location of the Cabramurra station) and 1,923 m (the highest elevation in the Bureau of Meteorology operational 5 km observation grid). The two elevations provide an insight into future changes in snowfall across the range of elevations spanning the area where the snowpack is currently observed and ski resorts are located. Snowfall is projected to experience a reduction that increases with time, with the magnitude dependent on the emission scenarios and the altitude. Late in the 21st century snow becomes rare under RCP8.5 at 1,400 m (see Section 7.2.4 of the Technical Report for details). More complete projections of snow conditions (snow depth, area covered, length of the snow season) require offline snow modelling. Such a study was completed using CMIP3 climate projections for temperature and rainfall used to drive a snow model (Bhend *et al*., 2012). Results highlight a reduction of the snow area, depth and the length of the snow season (see Technical Report, Section 7.2.4 for details). Taking these two studies into account, we have *high confidence* in substantial reductions in snow particularly under RCP8.5.
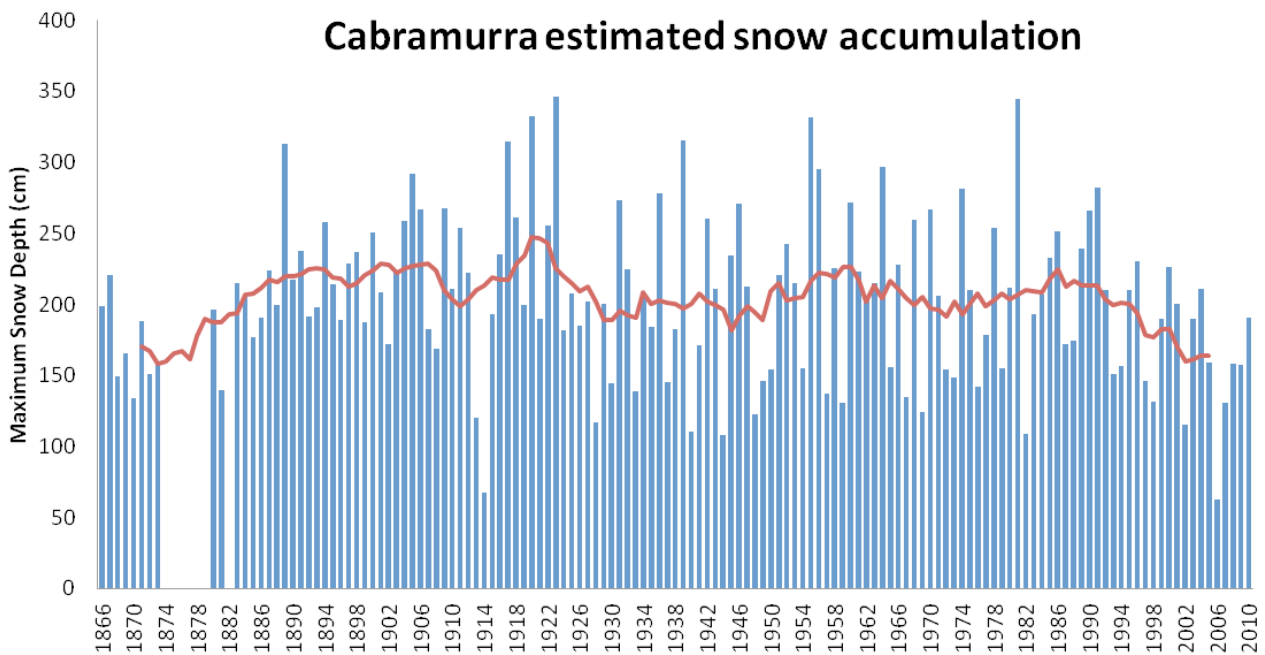
FIGURE 4.4.8: RECONSTRUCTED ANNUAL MAXIMUM SNOW DEPTH AT CABRAMURRA FROM 1866–2010 WITH 11-YEAR RUNNING MEAN (DAVIS, 2013), YEARS WITH NO SNOW ARE MISSING DATA.

4.5   WINDS, STORMS AND WEATHER SYSTEMS

4.5.1   OBSERVED WINDS

Across the Murray Basin cluster, winds are predominantly westerlies. They are stronger during the cool season when the sub-tropical ridge is located equator-ward of the cluster. During this time of the year the 'Roaring Forties' and 'Fifties' blow in a band of strong westerly winds and storms that encircle Antarctica (Sturman and Tapper, 1996), and become very significant for southern Australia climate, when fronts associated with these storms have a major impact. They bring the classic 'cool change' and the associated strong winds, fire danger (Mills, 2005) and dust events (Trewin, 2010). In the region to the north of the sub-tropical ridge, while frontal systems play a role, low pressure systems known as 'cut-off lows' are very important.

Trends in observed winds are difficult to establish due to sparse coverage of wind observations and difficulties with instruments and the changing circumstances of anemometer sites (*e.g.* increased sheltering effects over time due to increases in proximate vegetation or structures, which slow the winds). McVicar *et al.* (2012) and Troccoli *et al.* (2012) have reported weak and conflicting trends across Australia (although they considered winds at different altitudes). Circumventing the surface wind observation issues, Alexander *et al.* (2011) reported, using the gradient in MSLP, that storminess affecting south-eastern Australia has experienced a significant reduction during the 20th century.

4.5.2   FUTURE PROJECTIONS FOR WINDS

For 2030, changes in wind speed are projected with *high confidence* to be small under all RCPs (± 5 %). By 2090 under RCP4.5 and RCP8.5, there is an indication in the model results of decreased wind speed in winter (Figure 4.5.1). This aligns with changes in atmospheric circulation already discussed and is of *medium confidence*. Small or inconsistent changes are present in the other seasons. Overall, no large changes in surface wind are expected across the Murray Basin cluster, except in winter.
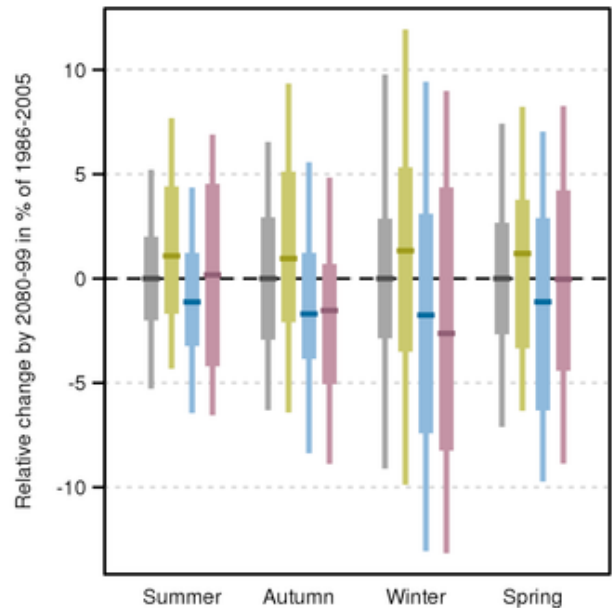
FIGURE 4.5.1: PROJECTED NEAR-SURFACE WIND SPEED CHANGE (%) BETWEEN THE BASELINE PERIOD 1986–2005 AND CHANGES FOR 2090 FOR MURRAY BASIN. ANOMALIES ARE GIVEN IN PERCENT WITH RESPECT TO 1986–2005 MEAN FOR RCP2.6 (GREEN), RCP4.5 (BLUE) AND RCP8.5 (PURPLE), WITH GREY BARS SHOWING THE EXTENT OF NATURAL CLIMATE VARIABILITY. BAR PLOTS ARE EXPLAINED IN BOX 4.2.

4.5.3   EXTREME WINDS

Cool season extreme winds are due to intense lows or associated cold fronts. The fronts and lows were examined in a number of CMIP5 models and there is a decrease in the number of fronts affecting southern Australia by 2090 (Catto *et al.*, 2013). Decreases in the annual maximum daily wind speed and the 20-year return value of the daily maximum are projected by 2090 under RCP4.5 and 8.5 (Figure 4.5.2), where a 20-year return value is equivalent to a 5 % chance of occurrence within any one year. However, there are a range of issues affecting the simulation of extreme winds in GCMs that influence the confidence in these changes (see Technical Report, Chapter 7.3).

Summer extreme winds are primarily due to intense cold fronts. In that season, the interactions between frontal systems and the continent are markedly different than during the cool season due to a stronger thermal contrast between the land and the ocean. For example, using a selection of CMIP3 models, Hasson *et al.* (2009) found that intense frontal systems affecting south-eastern Australia associated with extreme winds and dangerous fire will increase strongly by end of the 21st century, although this increase is strongly affected by the emission scenario.

The projections of extreme wind (1-day annual maximum speed) presented here (Figure 4.5.2) need to be considered in light of several limitations on this variable. These include the limited number of GCMs that provide daily wind data. Furthermore, the intensity of observed extreme wind speeds across land is strongly modified by surrounding terrain (including vegetation and other 'obstacles') that are not resolved at the relevant scale in GCMs, and many meteorological systems generating extreme winds are not resolved either. For these reasons, projected wind changes for the Murray Basin cluster have *low confidence* and their value lies foremost in the direction of change rather than magnitude. See further details in the Technical Report, Chapter 7.3.
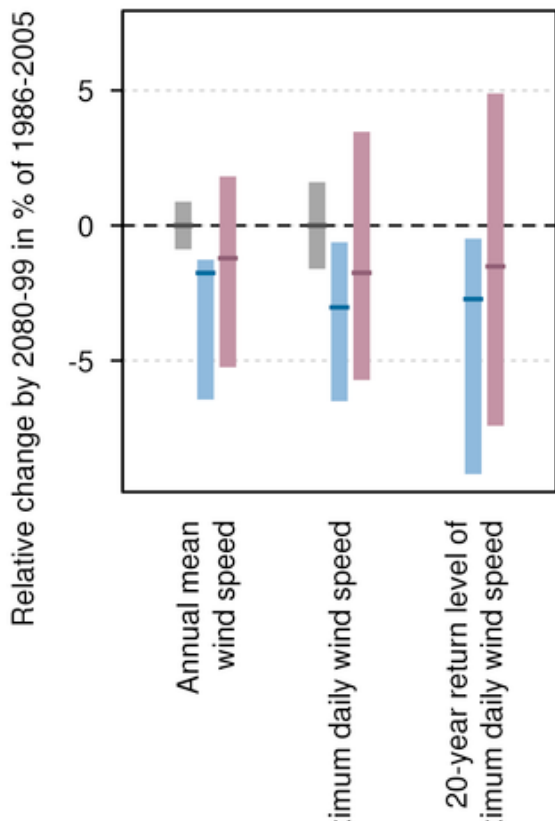
FIGURE 4.5.2: PROJECTED NEAR-SURFACE ANNUAL MEAN WIND SPEED CHANGES (%) BETWEEN THE BASELINE PERIOD OF 1986–2005, ANNUAL MAXIMUM DAILY WIND SPEED AND THE 20-YEAR RETURN VALUE FOR THE ANNUAL MAXIMUM DAILY WIND SPEED FOR 2090 FOR MURRAY BASIN. ANOMALIES ARE GIVEN IN PER CENT WITH RESPECT TO THE 1986–2005 MEAN FOR RCP2.6 (GREEN), RCP4.5 (BLUE) AND RCP8.5 (PURPLE) WITH GREY BARS SHOWING THE EXTENT OF NATURAL CLIMATE VARIABILITY. THE PLOT SHOWS ANNUAL MEAN WIND SPEED, ANNUAL MAXIMUM DAILY WIND SPEED AND 20-YEAR RETURN VALUE OF ANNUAL MAXIMUM DAILY WIND SPEED (SEE TEXT FOR DEFINITION OF VARIABLES). BAR PLOTS ARE EXPLAINED IN BOX 4.2.

4.6   SOLAR RADIATION

By 2030, the CMIP5 models simulate little change in radiation (less that 5 %) for both RCP4.5 and RCP8.5 (Table 1). By 2090, there is high model agreement for a substantial increase of 7 and 15 % respectively for RCP4.5 and RCP8.5 in winter and about half that in spring. Projected changes in summer and autumn are smaller with models showing both increases and decreases (Figure 4.8.1).

The strongest trend is found in the seasons where the largest rainfall decline is projected. It is worth noting that an Australia-wide model evaluation suggested that some models are not able to adequately reproduce the climatology of solar radiation (Watterson *et al.*, 2013). Globally, CMIP3 and CMIP5 models appear to underestimate the observed trends in some regions due to underestimation of aerosol direct radiative forcing and deficient aerosol emission inventories (Allen *et al.*, 2013). Taking this into account, we have *high confidence* in little change for 2030, and *high confidence* in increased winter and spring radiation by 2090.

4.7   RELATIVE HUMIDITY

Relative humidity depends on the absolute amount of moisture in the atmosphere and the ambient temperature and pressure. For example, for the same absolute amount of moisture, an atmosphere with higher temperature will have a lower relative humidity compared to a cooler atmosphere. For this reason, without circulation changes, absolute atmospheric moisture is expected to increase with global warming but relative humidity will decrease.

Across the Murray Basin cluster, the magnitudes of the projected decreases in relative humidity depend on the emission scenario and are modulated by the direction of the rainfall projections (Figure 4.8.1, middle panel and Appendix Table 1). By 2030, decreases are up to 4 %, but by 2090 under RCP8.5 can reach double that, particularly in winter and spring. There are, however, models that simulate increases in relative humidity, as evident by large positive 90th percentile values. Climate models have a reasonable ability to simulate the climatology of global humidity, and we conclude that for summer and autumn there is *medium confidence* in decrease, while for winter and spring there is *high confidence* for substantial decrease.

4.8   POTENTIAL EVAPOTRANSPIRATION

Amongst the various possible measures of evaporation, this report uses Morton's wet-environmental potential evapotranspiration, which is a derived measure of evaporation and transpiration assuming a wet environment (McMahon *et al.*, 2013). This measure combines inputs of air temperature, relative humidity and downward solar radiation at the surface. Overall, the Morton method compares favourably with other methods used to calculate potential evaporation in rainfall-runoff modelling (Chiew and McMahon, 1991) and is strongly correlated to the pan evaporation observations (Kirono *et al.*, 2009).
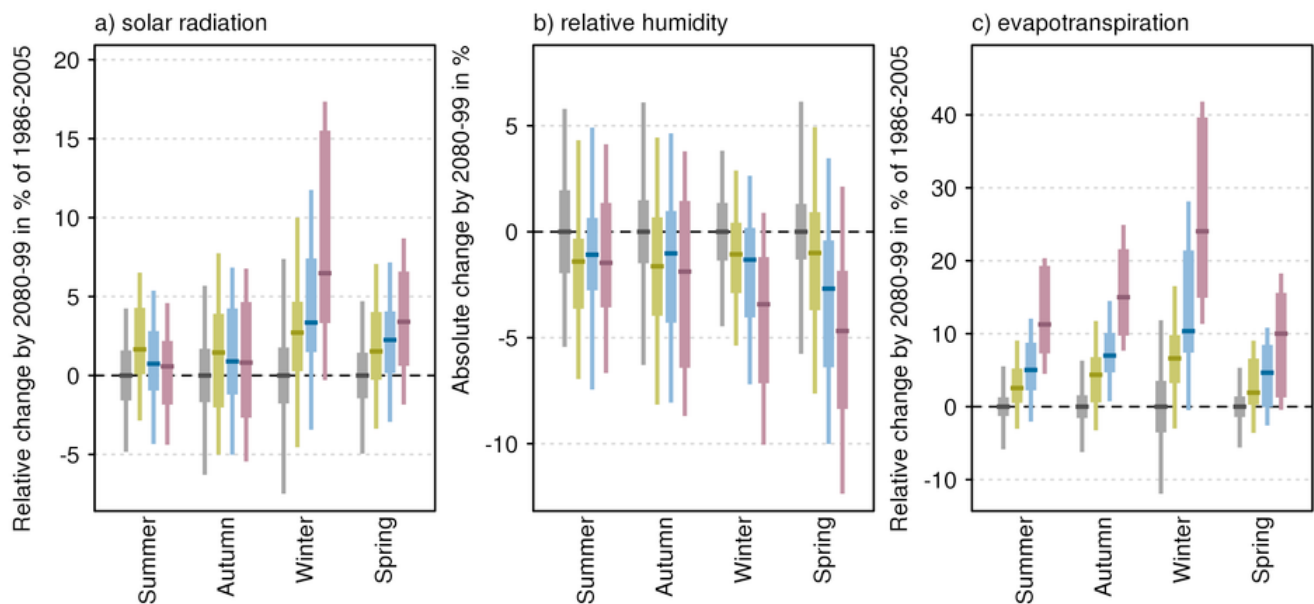
FIGURE 4.8.1: PROJECTED CHANGES IN (A) SOLAR RADIATION (%), (B) RELATIVE HUMIDITY (%, ABSOLUTE CHANGE) AND (C) WET-ENVIRONMENTAL POTENTIAL EVAPOTRANSPIRATION (%) FOR MURRAY BASIN IN 2090. THE BAR PLOTS SHOW SEASONAL PROJECTIONS WITH RESPECT TO THE 1986–2005 MEAN FOR RCP2.6 (GREEN), RCP4.5 (BLUE) AND RCP8.5 (PURPLE), AND THE EXTENT OF NATURAL CLIMATE VARIABILITY IS SHOWN IN GREY. BAR CHARTS ARE EXPLAINED IN BOX 4.2.

With increasing temperatures due to global warming and an intensified hydrological cycle, potential evapotranspiration is generally expected to increase (Huntington, 2006). For the Murray Basin cluster, projected seasonal changes for potential evapotranspiration relative to the 1986–2005 baseline period are shown in Figure 4.8.1 (right panel) and Appendix Table 1. The model results strongly indicate an increase of evaporation in all seasons. Projected increases in 2030 under all RCPS are about 1 to 7 % (3 to 13 % for winter). By 2090, the increases are about 1 to 10 % (about 7 to 20 % for winter) for RCP4.5 and 1 to 20 % (about 15 to 40 % for winter) for RCP8.5 (Appendix Table 1).

In absolute terms, the largest increases in evaporation are found in summer and autumn, with smaller increases in winter and spring. Although there is *high confidence* in an increase, there is only *medium confidence* in the magnitude of this change. The method used is able to reproduce the spatial pattern and the annual cycle of the observed climatology and there is theoretical understanding around increases as a response to increasing temperatures and an intensified hydrological cycle (Huntington, 2006), which adds to confidence. However, there has been no clear increase in observed in Pan Evaporation across Australia in data available since 1970 (see Technical Report, Chapter 4). Also, earlier GCMs were not able to reproduce the historical linear trends found in Morton's potential evapotranspiration (Kirono and Kent 2011).

4.9   SOIL MOISTURE AND RUNOFF

Increases in potential evapotranspiration rates (Figure 4.8.1) combined with a decrease in rainfall during the cool season (Figure 4.4.3) have implications for soil moisture and runoff. However, soil moisture and runoff are difficult to simulate. This is particularly true in GCMs where, due to their relatively coarse resolution, the models cannot simulate much of the rainfall detail that is important to many hydrological processes, such as the intensity of rainfall. For these reasons, and in line with many previous studies, we do not present runoff and soil moisture as directly-simulated by the GCMs. Instead, the results of hydrological models forced by CMIP5 simulated rainfall and potential evapotranspiration are presented. Soil moisture is estimated using a dynamic hydrological model based on an extension of the Budyko framework (Zhang *et al*., 2008), and runoff is estimated by the long-term annual water and energy balance using the Budyko framework (Teng *et al*., 2012). Runoff is presented as change in 20-year averages, derived from output of a water balance model. The latter uses input from CMIP5 models as smoothed time series (30-year running means), the reason being that 30 years is the minimum required for dynamic water balance to attain equilibrium using the Budyko framework. For further details on methods (including limitations) see Section 7.7 of the Technical Report.

The projected seasonal soil moisture changes over the Murray Basin cluster for 2090 are summarised in Figure 4.9.1. Decreases predominate, particularly in winter and spring. The annual-mean changes for the high emission scenario range from around −10 to -1 %. Consistent with the directly simulated surface moisture, the percentage changes in soil moisture are strongly influenced by those in rainfall, but tend to be more negative due to the increase in potential evapotranspiration. Given the potential limitations of each method, there is *medium confidence* that soil moisture will decline.

Projected runoff is inferred from 30-year means of rainfall and potential evapotranspiration for each CMIP5 model for which data are available. The median and ranges for the Murray Basin cluster in the final 30-year period are shown in Figure 4.9.1. The median change for 2090 under RCP8.5 is a decrease of about 20 %, with the majority of models giving a decrease. There is *low confidence* in these projections because the method used is not able to consider changes to rainfall intensity, seasonality and changes in vegetation characteristics, factors that could impact future runoff.

In the Murray Basin cluster, runoff is concentrated in a small part of the cluster: the high elevation catchment of the head of the Murray River. Appropriate projections of future river flow for these catchments are critical to the cluster. Further hydrological modelling with appropriate climate scenarios (*e.g.* Chiew *et al.*, 2009) could provide further insights into impacts on future runoff and soil moisture characteristics that may be needed in detailed climate change impact assessment studies.
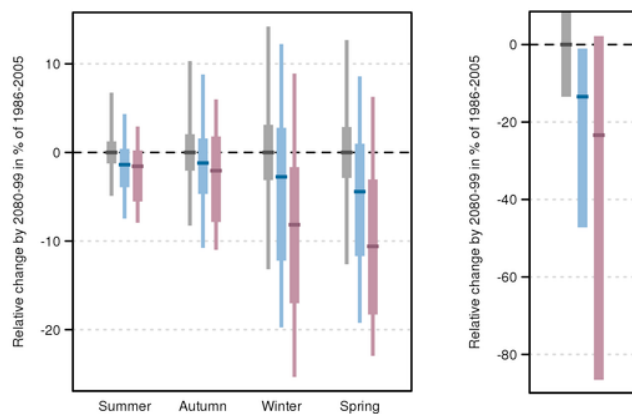
FIGURE 4.9.1: PROJECTED CHANGE IN SEASONAL SOIL MOISTURE (LEFT) AND ANNUAL RUNOFF (RIGHT) (BUDYKO METHOD – SEE TEXT) IN MURRAY BASIN FOR 2080–2099. ANOMALIES ARE GIVEN IN PER CENT WITH RESPECT TO THE 1986–2005 MEAN FOR RCP4.5 (BLUE) AND RCP8.5 (PURPLE) WITH GREY BARS SHOWING THE EXTENT OF NATURAL VARIABILITY. BAR CHARTS ARE EXPLAINED IN BOX 4.2.

4.10   FIRE WEATHER

Bushfire occurrence depends on four 'switches': 1) ignition, either human-caused or from natural sources such as lightning; 2) fuel abundance or load; 3) fuel dryness, where lower moisture contents are required for fire, and; 4) suitable weather conditions for fire spread, generally hot, dry and windy (Bradstock, 2010).

The settings of the switches depend on meteorological conditions across a variety of time scales, particularly the fuel conditions. Given this strong dependency on the weather, climate change will have a significant impact on future fire weather (*e.g.* Hennessy *et al.*, 2005; Lucas *et al.*, 2007; Williams *et al.*, 2009; Clarke *et al.*, 2011; Grose *et al*, 2014). The study of Clarke *et al.*, (2013) indicates strong increasing trends in fire weather from 1973-2010 at Mildura and Wagga in the Murray Basin cluster.

Fire weather is estimated here using the McArthur Forest Fire Danger Index (FFDI; (McArthur, 1967), which captures two of the four switches (note that it excludes ignition). The fuel dryness is summarised by the drought factor (DF) component of FFDI, which depends on both long-term and short-term rainfall. The FFDI also estimates the ability of a fire to spread, as the temperature, relative humidity and wind speed are direct inputs into the calculation. Fuel abundance is not measured by FFDI, but does depend largely on rainfall, with higher rainfall totals generally resulting in a larger fuel load, particularly in regions dominated by grasslands. However, the relationship between fuel abundance and climate change in Australia is complex and only poorly understood. Fire weather is considered 'severe' when FFDI exceeds 50; bushfires have potentially greater human impacts at this level (Blanchi, 2010).

Here, estimates of future fire weather using FFDI are derived from three CMIP5 models (GFDL-ESM2M, MIROC5 and CESM-CAM5), chosen to provide a spread of results across all clusters. Using a method similar to that of Hennessy *et al.* (2005), monthly-mean changes to maximum temperature, rainfall, relative humidity and wind speed from these models are applied to observation-based high-quality historical fire weather records (Lucas, 2010). A period centred on 1995 (*i.e.* 1981–2010) serves as the baseline. These records are modified using the changes from the three models for four 30-year time slices (centred on 2030, 2050, 2070 and 2090) and the RCP4.5 and RCP8.5 emission scenarios. In Southern and Eastern Australia, significant fire activity occurs primarily in areas characterised by forests and woodlands; fuel is abundant and the 'weather switch', well-characterized by FFDI, is key to fire occurrence. Four stations are used in the analysis for this cluster: Mt Gambier, Wagga, Mildura and Canberra.

Focusing on the 2030 and 2090 time slices, the results indicate increased fire weather risk in the future (Table 4.10.1). Increased temperature combined with lower annual-average rainfall results in a higher drought factor (DF).

Across the cluster, the sum of all daily FFDI values over a year (ΣFFDI from July to June) is broadly indicative of general fire weather risk. This index increases by about 10 % by 2030, 15 % under RCP4.5 by 2090, and 35 % under RCP8.5, by 2090. The number of days with a 'severe' fire danger rating increases by about 30 % by 2030, and from 45 % (RCP4.5) to 110 % (RCP8.5) by 2090.

TABLE 4.10.1: CLUSTER-MEAN ANNUAL VALUES OF MAXIMUM TEMPERATURE (T; °C), RAINFALL (R; MM), DROUGHT FACTOR (DF; NO UNITS), THE NUMBER OF SEVERE FIRE DANGER DAYS (SEV; FFDI GREATER THAN 50) AND CUMULATIVE FFDI (ΣFFDI; NO UNITS) FOR THE 1995 BASELINE AND PROJECTIONS FOR 2030 AND 2090 UNDER RCP4.5 AND RCP8.5 SCENARIOS. AVERAGES ARE COMPUTED ACROSS ALL STATIONS AND MODELS IN EACH SCENARIO. FOUR STATIONS ARE USED IN THE AVERAGING: MT GAMBIER, MILDURA, CANBERRA, AND WAGGA.

VARIABLE	1995 BASELINE	2030 RCP4.5	2030 RCP8.5	2090 RCP4.5	2090 RCP8.5
T	21.3	22.6	22.5	23.6	25.4
R	549	472	488	475	460
DF	6.6	6.9	6.8	7.1	7.5
SEV	3.6	4.9	4.6	5.3	7.6
ΣFFDI	3437	3802	3723	3957	4563

If considering indices on individual station and model basis, there is considerable variability from the cluster mean values (Table 2 in the Appendix). The baseline fire climate varies considerably between the stations. Mildura, being warmer and receiving considerably less rainfall than the other stations, has a high fire-weather climate more similar to stations in the Rangelands cluster to the north. Percentage changes are larger at the cooler and wetter stations in the cluster (Canberra and Mt Gambier). This is particularly true for the 2090 RCP8.5 scenario, where the number of severe days is 175-300 % above its baseline value at these two stations.

Considerable variability in the projections is driven by the choice of models for this analysis. While projected temperatures show some variation, rainfall variability is particularly large. On the whole, the wetter models show smaller increases in fire weather. This reflects the interplay between the variables influencing fire danger. Increased temperatures by themselves result in some level of increased fire weather. This temperature effect is modulated by rainfall, as significant reductions in rainfall lead to more severe fire weather (*e.g.* Mt Gambier for 2090 under RCP8.5), even for the smaller temperature changes. The seasonal timing of the rainfall changes in this cluster also matters. In 2030 under RCP8.5, rainfall is lowest in the GFDL model and ΣFFDI is largest. However, the number of 'severe' days is less than in the wetter CESM simulation, as the summer rainfall in GFDL is enhanced in this simulation. The higher summer rainfall acts to moisten the fuel (captured by the lower DF) during the peak fire season, hence reducing the overall fire weather risk. In the mean, changes to relative humidity and wind speed have little influence on future fire-weather climate.

In summary, there is *high confidence* that climate change will result in a harsher fire-weather climate in the future.

This is seen in the mean changes (Table 4.10.1) and when examining individual models and scenarios (Table 2). Rainfall and temperature projections across the models are robust in an annual sense. However, there is *low confidence* in the magnitude of the change to fire weather. This depends on the rainfall projection and its seasonal variation.

4.11   MARINE PROJECTIONS

Changes in sea levels and their extremes, sea surface temperatures and ocean pH (acidity) have the potential to impact both the coastal terrestrial and marine environments. This is discussed at length in Chapter 8 of the Technical Report. Of particular significance for the terrestrial environment of the lower Murray Basin is the impact of sea level rise and changes to the frequency of extreme sea levels. Impacts will be felt through coastal flooding and erosion. For the adjacent marine environment, increases in ocean temperatures and acidity may alter the distribution and composition of marine ecosystems and impact vegetation (*e.g.* sea grass and kelp forests) and coastal fisheries.

4.11.1   SEA LEVEL

Changes in sea level are caused primarily by changes in ocean density (*e.g.* ('thermal expansion') and changes in ocean mass due to the exchange of water with the terrestrial environment, including from glaciers and ice sheets (*e.g.* Church *et al.*, 2014; also see Technical Report, Section 8.1 for details). Over 1966–2009, the average of the relative tide gauge trends around Australia is a rise of 1.4 ± 0.2 mm/yr. After the influence of the El Niño Southern Oscillation (ENSO) on sea level is removed, the average trend is 1.6 ± 0.2 mm/yr. After accounting for and removing the effects of vertical land movements due to glacial

rebound and the effects of natural climate variability and changes in atmospheric pressure, sea levels have risen around the Australian coastline at an average rate of 2.1 mm/yr over 1966–2009 and 3.1 mm/yr over 1993–2009. These observed rates of rise for Australia are consistent with global average values (White *et al.*, 2014).

Projections of future sea level changes are shown for Victor Harbour (Figure 4.11.1), the nearest tide gauge location from the Murray River entrance, with values for this location being indicative of those along the entire Bonney coast. Table 3 in the Appendix provides numbers for the 2030 and 2090 periods relative to the 1986–2005 period for Victor Harbour as well as for the sites of Port Stanvac and Portland that are adjacent to the cluster coastline.
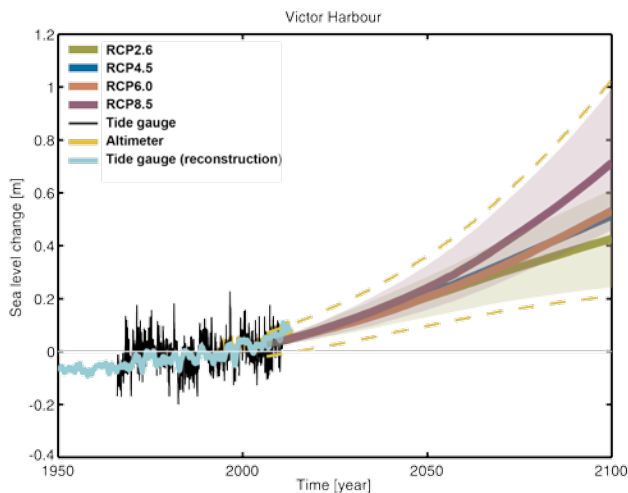
FIGURE 4.11.1: OBSERVED AND PROJECTED RELATIVE SEA LEVEL CHANGE (M) FOR VICTOR HARBOUR (WHICH HAS CONTINUOUS RECORDS AVAILABLE FOR THE PERIOD 1966–2010). THE OBSERVED TIDE GAUGE RELATIVE SEA LEVEL RECORDS ARE INDICATED IN BLACK, WITH THE SATELLITE RECORD (SINCE 1993) IN MUSTARD AND TIDE GAUGE RECONSTRUCTION (WHICH HAS LOWER VARIABILITY) IN CYAN. MULTI-MODEL MEAN PROJECTIONS (THICK PURPLE AND OLIVE LINES) FOR THE RCP8.5 AND RCP2.6 SCENARIOS WITH UNCERTAINTY RANGES ARE SHOWN BY THE PURPLE AND OLIVE SHADED REGIONS FROM 2006–2100. THE MUSTARD AND CYAN DASHED LINES ARE ESTIMATES OF INTER-ANNUAL VARIABILITY IN SEA LEVEL (UNCERTAINTY RANGE ABOUT THE PROJECTIONS) AND INDICATE THAT INDIVIDUAL MONTHLY AVERAGES OF SEA LEVEL CAN BE ABOVE OR BELOW LONGER TERM AVERAGES. NOTE THAT THE RANGES OF SEA LEVEL RISE SHOULD BE CONSIDERED *LIKELY* (AT LEAST 66 % PROBABILITY) AND THAT IF A COLLAPSE IN THE MARINE BASED SECTORS OF THE ANTARCTIC ICE SHEET WERE INITIATED, THESE PROJECTIONS COULD BE SEVERAL TENTHS OF A METRE HIGHER BY LATE IN THE CENTURY.

Continued increase in sea levels for the Murray Basin cluster is projected with *very high confidence*. The rate of sea level rise during the 21st century will be larger than the average rate during the 20th century as greenhouse gas emissions grow (Figure 4.11.1). For the first decades of the 21st century the projections are almost independent of the emission scenario, but they begin to separate significantly from about 2050. For higher greenhouse gas emissions, particularly for RCP8.5, the rate of rise continues to increase through the 21st century and results in sea level rise about 30 % higher than the RCP4.5 level by 2100. Significant inter-annual variability will likely continue through the 21st century. An indication of its magnitude is given by the dashed lines in Figure 4.11.1. Beyond 2100, global mean sea level will continue to increase (see section 8.1 in Technical Report for details). In the near future (2030), the projected range of sea level rise for the Murray Basin cluster coastline is 0.07 to 0.18 m above 1986–2005, with only minor differences between RCPs. For late in the century (2090) it is in the range 0.28 to 0.64 m for RCP4.5 and 0.39 to 0.84 m for RCP8.5. These ranges of sea level rise are considered *likely* (at least 66 % probability), however, if a collapse in the marine based sectors of the Antarctic ice sheet were initiated, these projections could be several tenths of a metre higher by late in the century (Church *et al.*, 2014).

Extreme coastal sea levels are caused by a combination of factors including astronomical tides, storm surges and wind-waves, exacerbated by rising sea levels. Along the south coast, the majority of storm surges occur with the passage of cold fronts during the winter months (McInnes and Hubbert, 2003). Return period curves of extreme sea levels are commonly used to define vertical thresholds for coastal development.

Using the method of Hunter (2012), an allowance has been calculated based on the mean sea level rise, the uncertainty around the rise, and taking into account the nature of extreme sea levels along the Murray Basin coastline (Haigh *et al.*, 2014). The allowance is the minimum distance required to raise an asset to maintain current frequency of breaches under projected sea level rise. When uncertainty in mean sea level rise is high (*e.g.* in 2090), this allowance approaches the upper end of the range of projected mean sea level rise. For the Murray Basin in 2030 the vertical allowances along the cluster coastline are in the range of 0.12 to 0.13 m for all RCPs; and 0.48 to 0.54 for RCP4.5 by 2090; and 0.66 to 0.74 m for RCP8.5 by 2090 (see Table 3 in the Appendix).

4.11.2 SEA SURFACE TEMPERATURE, SALINITY AND ACIDIFICATION

Sea surface temperature (SST) has increased significantly across the globe over recent decades (IPCC, 2013). Increases in SST pose a significant threat to the marine environment through biological changes in marine species, including in local abundance and community structure. For 2030, the range of projected SST increase for Victor Harbour is 0.3 to 0.8 °C under both RCP 2.6 and RCP 8.5 (see Table 3). For 2090, there is a much larger range of warming between the different RCPs. For Victor Harbour the range of increase is projected to be 0.3 to 0.9 °C for RCP 2.6 and 1.6 to 3.4 °C for RCP 8.5. Variations along the Murray Basin coastline are expected to be small (Table 3).

Ocean salinity in coastal waters will be affected by changes to rainfall and evaporation and this in turn can affect stratification and mixing, and potentially nutrient supply. Changes to salinity across the coastal waters of the Murray Basin cluster span a large range that includes possible increase and decrease, particularly over the longer term and higher emission scenarios as indicated in Table 3. Locally, salinity can also be affected by riverine input.

About 30 % of the anthropogenic carbon dioxide emitted into the atmosphere over the past 200 years has been absorbed by the oceans (Ciais *et al.*, 2013) and this has led to a 0.1 unit decrease in the ocean's surface water pH, which represents a 26 % increase in the concentration of hydrogen ions in seawater (Raven *et al.*, 2005). As the carbon dioxide enters the ocean it reacts with the seawater to cause a decrease in pH and carbonate concentration, collectively known as ocean acidification. Carbonate is used in conjunction with calcium as aragonite by many marine organisms such as corals, oysters, clams and some plankton such as foraminifera and pteropods, to form their hard skeletons or shells. A reduction in shell mass has already been detected in foraminifera and pteropods in the Southern Ocean (Moy *et al.,* 2009; Bednaršek *et al.*, 2012). Ocean acidification lowers the temperature at which corals bleach, reducing resilience to natural variability. Ocean acidification can affect fin and shellfish fisheries, aquaculture, tourism and coastal protection. In the cluster by 2030, pH change is projected to be another 0.08 units lower. By 2090 it is projected to be up to 0.15 units lower under RCP4.5 and up to 0.33 units lower for RCP8.5. This represents an additional increase in hydrogen ion concentration of 40 % and 110 % respectively. These changes are also accompanied by reductions in aragonite saturation state (see Table 3) and together with SST changes will affect all levels of the marine food web, and make it harder for calcifying marine organisms to build their hard shells, potentially affecting resilience and viability of marine ecosystems.

In summary, there is *very high confidence* that sea surface temperatures will continue to rise along the Murray Basin coastline, with the magnitude of the warming dependent on emission scenarios. Changes in salinity are related to changes in the hydrological cycle and are of *low confidence*. There is *very high confidence* that around Australia the ocean will become more acidic, showing a net reduction in pH. There is also *high confidence* that the rate of ocean acidification will be proportional to carbon dioxide emissions.

4.12 OTHER PROJECTION MATERIAL FOR THE CLUSTER

Whilst the projections in this report are based solely on CMIP5 outputs, we recognise that readers may want to investigate what impact the new climate projections have on existing impact and adaptation work using earlier projections products and data (see Appendix A in the Technical Report for a discussion on CMIP3 and CMIP5 model-based projections). The most relevant previous projection dataset was the nationwide Climate Change in Australia projections, produced jointly by CSIRO and the Bureau of Meteorology (CSIRO and Bureau of Meteorology, 2007). Additional projections were generated for surface runoff by CSIRO as part of the sustainable yields programme in 2009. Furthermore, a long-standing regional climate research program: the South-Eastern Climate Initiative (SEACI)[3] focused on the lower part of the Murray-Darling basin and the state of Victoria. The key conclusions from this program were summarised in two synthesis reports in 2010 (CSIRO, 2010) and 2012 (CSIRO, 2012). This report is making extensive use of the understanding of the climate system relevant to the Murray Basin cluster developed as part of that program. Currently, state-based initiatives relevant to the cluster exist in NSW and ACT (NSW/ ACT Regional Climate Modelling project, also known as NARCliM)[4], and South Australia (Goyder Institute research program) and Victoria (Victorian Climate Initiative or VicCI)[5].

Some of the projection products that are currently available made use of previous generation models (*e.g.* CMIP3). These projections are still relevant, particularly if placed in the context of the latest modelling results (see Appendix A in the Technical Report for a discussion on CMIP3 and CMIP5 model-based projections).

---

3   http://www.seaci.org

4   http://www.ccrc.unsw.edu.au/NARCliM/

5   http://cawcr.gov.au/projects/vicci/

5   APPLYING THE REGIONAL PROJECTIONS IN ADAPTATION PLANNING

The fundamental role of adaptation is to reduce the adverse impacts of climate change on vulnerable systems, using a wide range of actions directed by the needs of the vulnerable system. Adaptation also identifies and incorporates new opportunities that become feasible under climate change. For adaptation actions to be effective, all stakeholders need to be engaged, resources must be available and planners must have information on 'what to adapt to' and 'how to adapt' (Füssel and Klein, 2006).

This report presents information about 'what to adapt to' by describing how future climates may respond to increasing greenhouse gas concentrations. This Section gives guidance on how climate projections can be framed in the context of climate scenarios (Section 5.1) using tools such as the Climate Futures web tool, available on the Climate Change in Australia website (Box 5.1). The examples of its use presented here are not exhaustive, but rather an illustration of what can be done.

5.1   IDENTIFYING FUTURE CLIMATE SCENARIOS

In Chapter 4 of this report, projected changes are expressed as a range of plausible change for individual variables as simulated by CMIP5 models or derived from their outputs. However, many practitioners are interested in information on how the climate may change, not just changes in one climate variable. To consider how several climate variables may change in the future, data from individual models should be considered because each model simulates changes that are internally consistent across many variables. For example, the projected rainfall from one model with temperature from another, as these would represent the climate responses of unrelated simulations.

The challenge for practitioners lies in selecting which models to look at, since models can vary in their simulated response to increasing greenhouse gas emissions. Climate models can be organised according to their simulated climate response to assist with this selection. For example, sorting according to rainfall and temperature responses would give an immediate feel for how models fall into a set of discrete climate scenarios framed in terms such as: *much drier and slightly warmer, much wetter and slightly warmer, much drier and much hotter,* and *much wetter and much hotter.*

The Climate Futures web tool described in Box 9.1 of the Technical Report presents a scenario approach to investigating the range of climate model simulations for projected future periods. The following Section describes how this tool can be used to facilitate the use of model output in impact and adaptation assessment.

5.2   DEVELOPING CLIMATE SCENARIOS USING THE CLIMATE FUTURES TOOL

The example presented in Figure 5.1 represents the changes in temperature and rainfall in the SSWF for 2060 (years 2050–2069) under the RCP4.5 scenario. The table organises the models into groupings according to their simulated changes in rainfall (rows) and temperatures (columns). Regarding rainfall, models simulate increases and decreases from *much drier* (less than -15 %) to *much wetter* (greater than 15 %), with 18 of 34 models showing drying conditions (less than -5 %) compared to 1 model showing rainfall increases (greater than 5 %) and 5 models showing *little* change (-5 to 5 % change). With regard to temperature, most models show results ranging from *warmer* (0.5 to 1.5 °C warmer) *to hotter* (1.5 to 3 °C warmer), with no models falling into the lowest category *slightly warmer* (0 to 0.5 °C warmer) nor the highest category *much hotter* (greater than 3.0 °C warming). The largest number of models falls into

the 'warmer' category (23 of 34 models). When considering the two variables together, we see that the most commonly simulated climate for the 2060 under RCP4.5 is a *warmer and drier* climate (8 of 34 models), but many model simulations fall in other categories.

In viewing the projection data in this way, the user can gain an overview of what responses are possible when considering the CMIP5 model archive for a given set of constraints. In a risk assessment context, a user may want to consider not only the maximum consensus climate (simulated by most models), but also the best case and worst case scenarios. Their nature will depend on the application. A water-supply manager, for example, is likely to determine from Figure 5.1 that the best case scenario would be a *much wetter and warmer* climate and the worst case the *hotter* and *much drier* scenario.

Assuming that the user has identified what futures are likely to be of most relevance to the system of interest, Climate Futures allows exploration of the numerical values for each of the models that populates the scenarios. Further, it provides a function for choosing a single model that most closely represents the particular future climate of interest, but also taking into account models that have been identified as sub-optimal for particular regions based on model evaluation information (described in Chapter 5

of the Technical Report). Through this approach users can select a small set of models to provide scenarios for their application, taking into consideration model spread and the sensitivity of their application to climate change.

Alternatively, the user may wish to consider a small set of scenarios defined irrespective of emission scenario or date (but with their likelihood of occurrence being time and emission scenario sensitive). This may be in circumstances where the focus is on critical climate change thresholds. This strategy is illustrated for the Murray Basin cluster in Box 5.2, where results are produced in Climate Futures by comparing model simulations from separate time slices and emission scenarios. This box also illustrates each of these scenarios with current climate analogues (comparable climates) for selected sites.

Another user case could be the desire to compare simulations from different climate model ensembles (such as the earlier CMIP3 ensemble, or ensembles of downscaled results such as the NARCliM results for NSW). Comparing model spread simulated by different generations of GCMs in Climate Futures allows assessment of the on-going relevance of existing impact studies based on selected CMIP3 models, as well as to compare scenarios developed using downscaled and GCM results.

CONSENSUS	PROPORTION OF MODELS	June - Aug temperature (°C)			
Not projected — No models; Very low — < 10 %; Low — 10 to 33 %; Moderate — 33 to 66 %; High — 66 - 90 %; Very high — > 90 %		Slightly warmer 0 to +0.5	Warmer +0.5 to 1.5	Hotter +1.5 to +3.0	Much hotter > +3.0
June - Aug rainfall (%)	Much wetter > +15.0		1 of 34 models		
	Wetter +5.0 to +15.0		2 of 34 models	2 of 34 models	
	Little change -5.0 to +5.0		7 of 34 models	4 of 34 models	
	Drier -15.0 to -5.0		8 of 34 models	2 of 34 models	
	Much drier < -15.0		5 of 34 models	3 of 34 models	

FIGURE 5.1: AN EXAMPLE TABLE BASED ON OUTPUT FROM THE CLIMATE FUTURES WEB TOOL SHOWING RESULTS FOR THE MURRAY BASIN CLUSTER WHEN ASSESSING PLAUSIBLE CLIMATE FUTURES FOR 2060 UNDER RCP4.5, AS DEFINED BY GCM SIMULATED CHANGES IN WINTER RAINFALL (% CHANGE) AND TEMPERATURE (°C WARMING).

BOX 5.2: INDICATIVE CLIMATE SCENARIOS FOR THE MURRAY BASIN AND ANALOGUE FUTURE CLIMATES

Users may wish to consider the future climate of their region in terms of a small set of scenarios defined irrespective of emission scenario or date (but with their likelihood of occurrence being time and emission scenario sensitive). An example of using this strategy for the Murray Basin cluster is illustrated here. Combining the results in Climate Futures for 2030, 2050, and 2090, under RCP2.6, RCP4.5, and RCP8.5 gives a set of future climate scenarios (see Figure B5.2). These five highlighted scenarios (below) are considered representative of the spread of results (with other potential scenarios excluded as less likely than the selected cases or lying within the range of climates specified by the selected cases). For each case, when available, the current climate analogue for the future climate of Mildura is given as an example based on matching annual average climate conditions. These were generated using the method described in Chapter 89.3.5 of the Technical Report and are based on matching annual average rainfall (within +/- 5 %) and maximum temperature (within +/- 1 °C). Note that other potentially important aspects of local climate are not matched, such as rainfall seasonality, and thus the analogues should not be used directly in adaptation planning without considering more detailed information.

- *Warmer* (0.5 to 1.5 °C warmer) with *little change in rainfall* (-5 to +5 %). This could occur by 2030 under any emission scenario, but may persist through to late in the 21st century under RCP2.6. In this case, Mildura's future climate would be more like the current climate of Menindee (NSW).

- *Hotter* (greater than 3.0 °C warmer), and *drier* (5 to 15 % reduction). This is possible mid century under an RCP 8.5 emission scenario, or late in the century under RCP4.5. In this case, Mildura's future climate would be more like Mount Magnet (WA).

- *Much hotter* (greater than 3.0 °C warmer) and *much drier* (greater than 15 % reduction). This is possible by late in the 21st century under an RCP 8.5 emission scenario. In this case Mildura's climate would be more like that of Carnarvon (WA).

- *Warmer* (0.5 to 1.5 °C warmer), but *drier* (5 to 15 % reduction). This is also possible by 2030 under any emission scenario, and again may persist through to late in the 21st century under RCP2.6. In this case Mildura's climate would be more like that of Broken Hill (NSW) or Port Augusta (SA).

- *Warmer* (0.5 to 1.5 °C warmer), but *wetter* (5 to 15 % increase). This is also possible by 2030 under higher emission scenarios or by mid-century under any emission scenario, though less likely than other drier futures. In this case Mildura's climate would be more like that of Coolgardie (WA).

Future Realisations for the Murray Basin cluster

Annual Rainfall (%)		RCP	Slightly Warmer 0 to +0.5			Warmer +0.5 to +1.5			Hotter +1.5 to +3.0			Much Hotter > +3.0		
			2030	2050	2090	2030	2050	2090	2030	2050	2090	2030	2050	2090
Much Wetter > +15.0		2.6												
		4.5												
		8.5				1					2			
Wetter +5.0 to +15.0		2.6					2							
		4.5	1			2	1			1				
		8.5				1	2			1	1			
Little Change −5.0 to +5.0		2.6				11	9	6		1	1			
		4.5				12	9	1		5	8			
		8.5				11	1		2	10	1			7
Drier −15.0 to −5.0		2.6				6	1	5		1	1			
		4.5				11	3			5	13			
		8.5				12	1		1	10				8
Much Drier < −15.0		2.6				1	4	3			2			
		4.5				1				3	5			
		8.5				1				4				10

By when and under what greenhouse gas pathway could this occur (colour code=% of models for that period/RCP)?

Not projected	<10%	10-33%	33-66%

RCP2.6-18 models
RCP4.5-27 models
RCP8.5-29 models

FIGURE B5.2: A TABLE BASED OUTPUT FROM CLIMATE FUTURES SHOWING CATEGORIES OF FUTURE CLIMATE PROJECTIONS FOR THE MURRAY BASIN CLUSTER, AS DEFINED BY CHANGE IN ANNUAL TEMPERATURE (COLUMN) AND CHANGE IN RAINFALL (ROWS). WITHIN EACH FUTURE CLIMATE CATEGORY, MODEL SIMULATIONS ARE SORTED ACCORDING TO TIME (2030, 2050, AND 2090) AND CONCENTRATION PATHWAY (RCP2.6, RCP4.5, AND RCP8.5); THE NUMBER INDICATING HOW MANY MODEL SIMULATIONS OF THAT PARTICULAR SUB-CATEGORY FALL INTO THE CLIMATE CATEGORY OF THE TABLE (THE NUMBER OF MODELS USED IN THIS EXAMPLE VARIES FOR DIFFERENT CONCENTRATION PATHWAYS). A COLOUR CODE INDICATES HOW OFTEN A PARTICULAR CLIMATE IS SIMULATED AMONGST THE CONSIDERED MODELS (PER CENT OCCURRENCE). THE SCENARIOS DESCRIBED IN THE TEXT ARE HIGHLIGHTED IN BOLD.

REFERENCES

ALEXANDER, L., WANG, X., WAN, H. & TREWIN, B. 2011. Significant decline in storminess over south-east Australia since the late 19th century. Aust. Meteorol. Oceanogr. Journal, 61, 23-30.

ALLAN, R. & ANSELL, T. 2006. A new globally complete monthly historical gridded mean sea level pressure dataset (HadSLP2): 1850-2004. Journal of Climate, 19, 5816-5842.

ALLEN, R. J., NORRIS, J. R. & WILD, M. 2013. Evaluation of multidecadal variability in CMIP5 surface solar radiation and inferred underestimation of aerosol direct effects over Europe, China, Japan, and India. Journal of Geophysical Research-Atmospheres, 118, 6311-6336.

BEARD, G., CHANDLER, E., WATKINS, A. & JONES, D. 2011. How does the 2010–11 La Niña compare with past La Niña events. Bulletin of the Australian Meteorological and Oceanographic Society, 24, 17-20.

BEDNARŠEK, N., TARLING, G., BAKKER, D., FIELDING, S., JONES, E., VENABLES, H., WARD, P., KUZIRIAN, A., LEZE, B. & FEELY, R. 2012. Extensive dissolution of live pteropods in the Southern Ocean. Nature Geoscience, 5, 881-885.

BHEND, J., BATHOLS, J. & HENNESSY, K. 2012. Climate change impacts on snow in Victoria. Aspendale, Australia: CSIRO report for the Victorian Department of Sustainability and Environment 42.URL: http://www.climatechange.vic.gov.au/__data/assets/pdf_file/0005/200795/cawcr_report_on_climate_change_and_Victorian_snow_final-dec12_web.pdf (Accessed 18/8/2014)

BLANCHI, R., LUCAS, C., LEONARD, J. & FINKELE, K. 2010. Meteorological conditions and wildfire-related house loss in Australia. International Journal of Wildland Fire, 19, 914-926.

BRADSTOCK, R. A. 2010. A biogeographic model of fire regimes in Australia: current and future implications. Global Ecology and Biogeography, 19, 145-158.

BROHAN, P., KENNEDY, J. J., HARRIS, I., TETT, S. F. & JONES, P. D. 2006. Uncertainty estimates in regional and global observed temperature changes: A new data set from 1850. Journal of Geophysical Research: Atmospheres (1984–2012), 111, D12, 1-21.

BUREAU OF METEOROLOGY 2012. Australia's wettest two-year period on record; 2010-11. Special Climate Statement. Melbourne, Australia: National Climate Centre, Bureau of Meteorology. URL: http://www.bom.gov.au/climate/current/statements/scs38.pdf Accessed 19/8/2014

CATTO, J., JAKOB, C. & NICHOLLS, N. 2013. A global evaluation of fronts and precipitation in the ACCESS model. Aust. Meteorol. Ocean. Soc. J, 63, 191-203.

CHIEW, F., KIRONO, D., KENT, D. & VAZE, J. 2009. Assessment of rainfall simulations from global climate models and implications for climate change impact on runoff studies. 18th World Imacs Congress and Modsim09 International Congress on Modelling and Simulation: Interfacing Modelling and Simulation with Mathematical and Computational Sciences. 3907-3913

CHIEW, F. H. & MCMAHON, T. A. 1991. The Applicability of Morton's and Penman's Evapotranspiration Estimates in Rainfall-Runoff Modeling. JAWRA Journal of the American Water Resources Association, 27, 611-620.

CHURCH, J. A., CLARK, P. U., CAZENAVE, A., GREGORY, J. M., JEVREJEVA, S., LEVERMANN, A., MERRIFIELD, M. A., MILNE, G. A., NEREM, R. S., NUNN, P. D., PAYNE, A. J., PFEFFER, W. T., STAMMER, D. & UNNIKRISHNAN, A. S. 2014. Sea Level Change. In: STOCKER, T. F., D. QIN, G.-K. PLATTNER, M. TIGNOR, S. K. ALLEN, J. BOSCHUNG, A. NAUELS, Y. XIA, V. BEX AND P. M. MIDGLEY (ed.) Climate Change 2013: The Physical Science Basis. Contribution of Working Group I to the Fifth Assessment Report of the Intergovernmental Panel on Climate Change.

CIAIS, P., SABINE, C., BALA, G., BOPP, L., BROVKIN, V., CANADELL, J., CHHABRA, A., DEFRIES, R., GALLOWAY, J., HEIMANN, M., JONES, C., LE QUÉRÉ, C., MYNENI, R. B., PIAO, S. & THORNTON, P. 2013. Carbon and Other Biogeochemical Cycles. Contribution of Working Group I to the Fifth Assessment Report of the Intergovernmental Panel on Climate Change. In: STOCKER, T. F., D. QIN, G.-K. PLATTNER, M. TIGNOR, S.K. ALLEN, J. BOSCHUNG, A. NAUELS, Y. XIA, BEX, V. & MIDGLEY, P. M. (eds.) Climate Change 2013: The Physical Science Basis. Cambridge, United Kingdom and New York, NY, USA: Cambridge University Press.

CLARKE, H., LUCAS, C. & SMITH, P. 2013. Changes in Australian fire weather between 1973 and 2010. International Journal of Climatology, 33, 931-944.

CLARKE, H. G., SMITH, P. L. & PITMAN, A. J. 2011. Regional signatures of future fire weather over eastern Australia from global climate models. International Journal of Wildland Fire, 20, 550-562.

CSIRO 2010. Climate variability and change in south-eastern Australia – A synthesis of findings from Phase 1 of the South Eastern Australian Climate Initiative (SEACI). Victoria, Australia: CSIRO 41 pp. URL: http://www.csiro.au/Portals/Publications/Research--Reports/SEACI-report.aspx Accessed 19/8/2014

CSIRO 2012. Climate and water availability in south-eastern Australia – A synthesis of findings from Phase 2 of the South Eastern Australian Climate Initiative (SEACI). Melbourne, Australia: CSIRO 41 pp. URL: http://www.seaci.org/research/phase2.html Accessed 19/8/2014

CSIRO AND BOM 2007. Climate change in Australia: Technical Report. Aspendale, Australia: CSIRO Marine and Atmospheric Research. URL http://www.climatechangeinaustralia.gov.au/technical_report.php Accessed 19/8/2014

DAVIS, C. 2013. Towards the development of long term winter records for the Snowy Mountains. Australian Meteorological Magazine, 63, 303-313.

DROSDOWSKY, W. 2005. The latitude of the subtropical ridge over eastern Australia: The L index revisited. International Journal of Climatology, 25, 1291-1299.

FAWCETT, R., DAY, K. A., TREWIN, B., BRAGANZA, K., SMALLEY, R., JOVANOVIC, B. & JONES, D. 2012. On the sensitivity of Australian temperature trends and variability to analysis methods and observation networks, Centre for Australian Weather and Climate Research Technical Report No.050.

FOWLER, H. & EKSTRÖM, M. 2009. Multi-model ensemble estimates of climate change impacts on UK seasonal precipitation extremes. International Journal of Climatology, 29, 385-416.

FREDERIKSEN, J., FREDERIKSEN, C., OSBROUGH, S. & SISSON, J. Changes in Southern Hemisphere rainfall, circulation and weather systems. 19th International Congress on Modelling and Simulation, 2011 Perth, Australia. Modelling and Simulation Society of Australia and New Zealand, 2712-2718.

FÜSSEL, H.-M. & KLEIN, R. J. 2006. Climate change vulnerability assessments: an evolution of conceptual thinking. Climatic Change, 75, 301-329.

GROSE, M. R., FOX-HUGHES, P., HARRIS, R. M. & BINDOFF, N. L. 2014. Changes to the drivers of fire weather with a warming climate—a case study of southeast Tasmania. Climatic Change, 124, 255-269.

HAIGH, I. D., WIJERATNE, E., MACPHERSON, L. R., PATTIARATCHI, C. B., MASON, M. S., CROMPTON, R. P. & GEORGE, S. 2014. Estimating present day extreme water level exceedance probabilities around the coastline of Australia: tides, extra-tropical storm surges and mean sea level. Climate Dynamics, 42, 121-138.

HASSON, A., MILLS, G., TIMBAL, B. & WALSH, K. 2009. Assessing the impact of climate change on extreme fire weather events over southeastern Australia. Climate Research, 39, 159-172.

HENNESSY, K., LUCAS, C., NICHOLLS, N., BATHOLS, J., SUPPIAH, R. & RICKETTS, J. 2005. Climate change impacts on fire weather in south-east Australia. Melbourne, Australia: Consultancy report for the New South Wales Greenhouse Office, Victorian Department of Sustainability and Environment, Tasmanian Department of Primary Industries, Water and Environment, and the Australian Greenhouse Office. CSIRO Atmospheric Research and Australian Government Bureau of Meteorology 78pp. URL http://laptop.deh.gov.au/soe/2006/publications/drs/pubs/334/lnd/ld_24_climate_change_impacts_on_fire_weather.pdf Accessed 18/8/2014

HUNTER, J. 2012. A simple technique for estimating an allowance for uncertain sea-level rise. Climatic Change, 113, 239-252.

HUNTINGTON, T. G. 2006. Evidence for intensification of the global water cycle: Review and synthesis. Journal of Hydrology, 319, 83-95.

IPCC 2013. Climate Change 2013: The Physical Science Basis. *In:* STOCKER, T. F., D. QIN, G.-K. PLATTNER, M. TIGNOR, S. K. ALLEN, J. BOSCHUNG, A. NAUELS, Y. XIA, V. BEX & P. M. MIDGLEY (eds.) *Contribution of Working Group I to the Fifth Assessment Report of the Intergovernmental Panel on Climate Change.* Cambridge, UK, and New York, NY, USA: Cambridge University Press.

JONES, D. A., WANG, W. & FAWCETT, R. 2009. High-quality spatial climate data-sets for Australia. Australian Meteorological and Oceanographic Journal, 58, 233-248.

KENT, D. M., KIRONO, D. G., TIMBAL, B. & CHIEW, F. H. 2013. Representation of the Australian sub tropical ridge in the CMIP3 models. International Journal of Climatology, 33, 48-57.

KIRONO, D. G. & KENT, D. M. 2011. Assessment of rainfall and potential evaporation from global climate models and its implications for Australian regional drought projection. International Journal of Climatology, 31, 1295-1308.

KIRONO, D. G. C., JONES, R. N. & CLEUGH, H. A. 2009. Pan-evaporation measurements and Morton-point potential evaporation estimates in Australia: are their trends the same? International Journal of Climatology, 29, 711-718.

LEBLANC, M., TWEED, S., VAN DIJK, A. & TIMBAL, B. 2012. A review of historic and future hydrological changes in the Murray-Darling Basin. Global and Planetary Change, 80, 226-246.

LEVITUS, S., ANTONOV, J. I., BOYER, T. P. & STEPHENS, C. 2000. Warming of the world ocean. Science, 287, 2225-2229.

LUCAS, C. 2010. On developing a historical fire weather data-set for Australia. Australian Meteorological Magazine, 60, 1-13.

LUCAS, C., HENNESSY, K., MILLS, G. & BATHOLS, J. 2007. Bushfire Weather in Southeast Australia: Recent Trends and Projected Climate Change Impacts. Consultancy Report prepared for The Climate Institute of Australia. Bushfire CRC and Australian Bureau of Meteorology CSIRO Marine and Atmospheric Research. URL http://www.royalcommission.vic.gov.au/getdoc/c71b6858-c387-41c0-8a89-b351460eba68/TEN.056.001.0001.pdf Accessed 18/8/2014

LUCAS, C., TIMBAL, B. & NGUYEN, H. 2014. The expanding tropics: a critical assessment of the observational and modeling studies. Wiley Interdisciplinary Reviews: Climate Change, 5, 89-112.

−20°   −10°   0°   10°   20°   30°   40°   50°

MASTRANDREA, M. D., FIELD, C. B., STOCKER, T. F., EDENHOFER, O., EBI, K. L., FRAME, D. J., HELD, H., KRIEGLER, E., MACH, K. J. & MATSCHOSS, P. R. 2010. Guidance note for lead authors of the IPCC fifth assessment report on consistent treatment of uncertainties. *Intergovernmental Panel on Climate Change* (IPCC). URL http://www.ipcc.ch/pdf/supporting-material/uncertainty-guidance-note.pdf Accessed 18/8/2014

MCARTHUR, A. G. 1967. Fire behaviour in Eucalypt forests. Leaflet. Forestry Timber Bureau Australia, 35-35.

MCGREGOR, J. & DIX, M. 2008. An updated description of the conformal-cubic atmospheric model. In: HAMILTON, K. & OHFUCHI, W. (eds.) *High Resolution Numerical Modelling of the Atmosphere and Ocean*. Springer New York.

MCINNES, K. L. & HUBBERT, G. D. 2003. A numerical modeling study of storm surges in Bass Strait. Aust. Meterological Magazine, 52, 143-156.

MCMAHON, T. A., PEEL, M. C., LOWE, L., SRIKANTHAN, R. & MCVICAR, T. R. 2013. Estimating actual, potential, reference crop and pan evaporation using standard meteorological data: a pragmatic synthesis. Hydrology and Earth System Sciences, 17, 1331-1363.

MCVICAR, T. R., RODERICK, M. L., DONOHUE, R. J., LI, L. T., VAN NIEL, T. G., THOMAS, A., GRIESER, J., JHAJHARIA, D., HIMRI, Y. & MAHOWALD, N. M. 2012. Global review and synthesis of trends in observed terrestrial near-surface wind speeds: Implications for evaporation. Journal of Hydrology, 416, 182-205.

MILLS, G. A. 2005. A re-examination of the synoptic and mesoscale meteorology of Ash Wednesday 1983. Aust. Meteor. Mag., 54, 35-55.

MOSS, R. H., EDMONDS, J. A., HIBBARD, K. A., MANNING, M. R., ROSE, S. K., VAN VUUREN, D. P., CARTER, T. R., EMORI, S., KAINUMA, M., KRAM, T., MEEHL, G. A., MITCHELL, J. F. B., NAKICENOVIC, N., RIAHI, K., SMITH, S. J., STOUFFER, R. J., THOMSON, A. M., WEYANT, J. P. & WILBANKS, T. J. 2010. The next generation of scenarios for climate change research and assessment. Nature, 463, 747-756.

MOY, A. D., HOWARD, W. R., BRAY, S. G. & TRULL, T. W. 2009. Reduced calcification in modern Southern Ocean planktonic foraminifera. Nature Geoscience, 2, 276-280.

NAKIĆENOVIĆ, N. & SWART, R. (eds.) 2000. *Special Report on Emissions Scenarios. A Special Report of Working Group III of the Intergovernmental Panel on Climate Change*, Cambridge, United Kingdom and New York, NY, USA: Cambridge University Press.

NGUYEN, H., EVANS, A., LUCAS, C., SMITH, I. & TIMBAL, B. 2013. The Hadley Circulation in Reanalyses: Climatology, Variability, and Change. Journal of Climate, 26, 3357-3376.

NGUYEN, H., LUCAS, C., EVANS, A., TIMBAL, B., EVANS, A. & HANSON, L. 2014. Unprecedented expansion of the southern Hemisphere Hadley Cell. Internal review. Melbourne, Australia: Bureau of Meteorology

RAVEN, J., CALDEIRA, K., ELDERFIELD, H., HOEGH-GULDBERG, O., LISS, P., RIEBESELL, U., SHEPHERD, J., TURLEY, C. & WATSON, A. 2005. Ocean acidification due to increasing atmospheric carbon dioxide. The Royal Society 68pp.

SHERWOOD, S. C., ROCA, R., WECKWERTH, T. M. & ANDRONOVA, N. G. 2010. Tropospheric water vapor, convection, and climate. Reviews of Geophysics, 48, RG2001.

STURMAN, A. P. & TAPPER, N. J. 1996. The weather and climate of Australia and New Zealand, Melbourne, Australia, Oxford University Press.

TAYLOR, K. E., STOUFFER, R. J. & MEEHL, G. A. 2012. An overview of CMIP5 and the experiment design. Bulletin of the American Meteorological Society, 93, 485-498.

TENG, J., CHIEW, F., VAZE, J., MARVANEK, S. & KIRONO, D. 2012. Estimation of climate change impact on mean annual runoff across continental Australia using Budyko and Fu equations and hydrological models. Journal of Hydrometeorology, 13, 1094-1106.

TIMBAL, B., ARBLASTER, J., BRAGANZA, K., FERNANDEZ, E., HENDON, H., MURPHY, B., RAUPACH, M., RAKICH, C., SMITH, I. & WHAN, K. 2010. Understanding the anthropogenic nature of the observed rainfall decline across South Eastern Australia. CAWCR Technical Report No. 026. Melbourne, Australia: Centre for Australian Weather and Climate Research. URL: http://www.cawcr.gov.au/publications/technicalreports/CTR_026.pdf Accessed 19/8/2014

TIMBAL, B. & DROSDOWSKY, W. 2013. The relationship between the decline of South Eastern Australia rainfall and the strengthening of the sub-tropical ridge. International Journal of Climatology, 33, 1021-1034.

TIMBAL, B. & MCAVANEY, B. J. 2001. An analogue-based method to downscale surface air temperature: Application for Australia. Climate Dynamics, 17, 947-963.

TREWIN, B. 2010. Exposure, instrumentation, and observing practice effects on land temperature measurements. Wiley Interdisciplinary Reviews: Climate Change, 1, 490-506.

TROCCOLI, A., MULLER, K., COPPIN, P., DAVY, R., RUSSELL, C. & HIRSCH, A. L. 2012. Long-term wind speed trends over Australia. Journal of Climate, 25, 170-183.

VAN VUUREN, D. P., EDMONDS, J., KAINUMA, M., RIAHI, K., THOMSON, A., HIBBARD, K., HURTT, G. C., KRAM, T., KREY, V. & LAMARQUE, J.-F. 2011. The representative concentration pathways: an overview. Climatic Change, 109, 5-31.

WATTERSON, I. G., HIRST, A. C. & ROTSTAYN, L. D. 2013. A skill score based evaluation of simulated Australian climate. Australian Meteorological and Oceanographic Journal, 63, 181-190.

WHETTON, P., HENNESSY, K., CLARKE, J., MCINNES, K. & KENT, D. 2012. Use of Representative Climate Futures in impact and adaptation assessment. Climatic Change, 115, 433-442.

WHITE, N. J., HAIGH, I. D., CHURCH, J. A., KEON, T., WATSON, C. S., PRITCHARD, T., WATSON, P. J., BURGETTE, R. J., ELIOT, M., MCINNES, K. L., YOU, B., ZHANG, X. & TREGONING, P. 2014. Australian Sea Levels - Trends, regional variability and Influencing factors. Earth-Science Reviews, 136, 155-174.

WILLIAMS, R. J., BRADSTOCK, R. A., CARY, G. J., ENRIGHT, N., GILL, A., LIEDLOFF, A., LUCAS, C., WHELAN, R., ANDERSEN, A. & BOWMAN, D. 2009. Interactions between climate change, fire regimes and biodiversity in Australia- A preliminary assessment. Canberra: Department of Climate Change and Department of the Environment, Water, Heritage and the Arts. URL http://climatechange.gov.au/sites/climatechange/files/documents/04_2013/20100630-climate-fire-biodiversity-PDF.pdf Accessed 18/8/2014

ZHANG, L., POTTER, N., HICKEL, K., ZHANG, Y. & SHAO, Q. 2008. Water balance modeling over variable time scales based on the Budyko framework – Model development and testing. Journal of Hydrology 360, 117-131.

−20°   −10°   0°   10°   20°   30°   40°   50°

APPENDIX

TABLE 1: GCM SIMULATED CHANGES IN A RANGE OF CLIMATE VARIABLES FOR THE 2020–2039 (2030) AND 2080–2099 (2090) PERIODS RELATIVE TO THE 1986–2005 PERIOD FOR THE MURRAY BASIN CLUSTER. THE TABLE GIVES THE MEDIAN (50TH PERCENTILE) CHANGE, AS PROJECTED BY THE CMIP5 MODEL ARCHIVE, WITH 10TH TO 90TH PERCENTILE RANGE GIVEN WITHIN BRACKETS. RESULTS ARE GIVEN FOR RCP2.6, RCP4.5, AND RCP8.5 FOR ANNUAL AND SEASONAL AVERAGES. 'DJF' REFERS TO SUMMER (DECEMBER TO FEBRUARY), 'MAM' TO AUTUMN (MARCH TO MAY), 'JJA' TO WINTER (JUNE TO AUGUST) AND 'SON' TO SPRING (SEPTEMBER TO NOVEMBER). THE PROJECTIONS ARE PRESENTED AS EITHER PERCENTAGE OR ABSOLUTE CHANGES. THE COLOURING (SEE LEGEND) INDICATES CMIP5 MODEL AGREEMENT, WITH 'MEDIUM' BEING MORE THAN 60 % OF MODELS, 'HIGH' MORE THAN 75 %, 'VERY HIGH' MORE THAN 90 %, AND 'SUBSTANTIAL' AGREEMENT ON A CHANGE OUTSIDE THE 10TH TO 90TH PERCENTILE RANGE OF MODEL NATURAL VARIABILITY. NOTE THAT 'VERY HIGH AGREEMENT' CATEGORIES ARE RARELY OCCUPIED EXCEPT FOR 'VERY HIGH AGREEMENT ON SUBSTANTIAL INCREASE', AND SO TO REDUCE COMPLEXITY THE OTHER CASES ARE INCLUDED WITHIN THE RELEVANT 'HIGH AGREEMENT' CATEGORY.

VARIABLE	SEASON	2030, RCP2.6	2030, RCP4.5	2030, RCP8.5	2090, RCP2.6	2090, RCP4.5	2090, RCP8.5
Temperature Mean (°C)	Annual	0.8 (0.6 to 1)	0.8 (0.6 to 1.1)	0.9 (0.7 to 1.3)	1 (0.6 to 1.5)	1.8 (1.3 to 2.4)	3.8 (2.7 to 4.5)
	DJF	1 (0.5 to 1.4)	0.9 (0.4 to 1.4)	1.1 (0.6 to 1.5)	1.1 (0.6 to 1.8)	2 (1.2 to 2.9)	3.9 (2.7 to 5.4)
	MAM	0.8 (0.5 to 1.1)	0.8 (0.4 to 1.2)	0.9 (0.5 to 1.4)	1 (0.6 to 1.4)	1.7 (1.3 to 2.3)	3.7 (2.8 to 4.7)
	JJA	0.7 (0.4 to 0.8)	0.7 (0.5 to 0.9)	0.8 (0.6 to 1)	0.8 (0.5 to 1.2)	1.5 (1.1 to 1.9)	3.3 (2.6 to 3.8)
	SON	0.8 (0.4 to 1.2)	0.8 (0.4 to 1.2)	1 (0.7 to 1.4)	1 (0.4 to 1.6)	1.9 (1.4 to 2.6)	3.9 (2.9 to 4.8)
Temperature maximum (°C)	Annual	0.9 (0.6 to 1.1)	0.9 (0.6 to 1.3)	1.1 (0.8 to 1.4)	1.1 (0.7 to 1.7)	2 (1.3 to 2.6)	4.1 (2.9 to 5)
	DJF	1 (0.6 to 1.4)	1 (0.6 to 1.6)	1.1 (0.6 to 1.5)	1.3 (0.8 to 2.1)	2.1 (1.4 to 3.1)	4.1 (2.9 to 5.1)
	MAM	0.9 (0.5 to 1.2)	0.8 (0.2 to 1.4)	0.9 (0.5 to 1.5)	1.1 (0.5 to 1.6)	1.8 (1.2 to 2.5)	3.8 (2.7 to 4.9)
	JJA	0.7 (0.5 to 0.9)	0.8 (0.5 to 1.2)	1 (0.7 to 1.4)	0.9 (0.6 to 1.2)	1.7 (1.3 to 2.4)	3.8 (2.8 to 4.5)
	SON	1 (0.4 to 1.4)	1 (0.6 to 1.4)	1.1 (0.7 to 1.7)	1.3 (0.4 to 1.9)	2.2 (1.5 to 3)	4.5 (3.1 to 5.8)
Temperature minimum (°C)	Annual	0.8 (0.4 to 1)	0.7 (0.5 to 1)	0.9 (0.7 to 1.2)	0.9 (0.4 to 1.4)	1.7 (1.1 to 2.1)	3.5 (2.8 to 4.2)
	DJF	1 (0.3 to 1.3)	0.9 (0.6 to 1.3)	1 (0.7 to 1.5)	1.2 (0.5 to 1.7)	1.9 (1.1 to 2.7)	3.9 (2.8 to 5)
	MAM	0.8 (0.4 to 1)	0.7 (0.4 to 1.2)	1 (0.4 to 1.4)	0.9 (0.5 to 1.3)	1.7 (1.2 to 2.2)	3.8 (2.9 to 4.6)
	JJA	0.6 (0.3 to 0.8)	0.6 (0.4 to 0.8)	0.7 (0.5 to 1)	0.7 (0.3 to 1.2)	1.4 (0.9 to 1.7)	2.9 (2.3 to 3.6)
	SON	0.7 (0.3 to 1.1)	0.7 (0.3 to 1.1)	0.9 (0.6 to 1.3)	0.8 (0.3 to 1.4)	1.7 (1.1 to 2.1)	3.6 (2.7 to 4.2)
Sea level pressure (hPa)	Annual	0.3 (-0.1 to 0.7)	0.2 (-0.1 to 0.7)	0.4 (-0.1 to 0.8)	0.2 (-0.1 to 0.7)	0.5 (-0.1 to 1)	0.9 (0.1 to 1.9)
	DJF	0.1 (-0.3 to 0.6)	0.1 (-0.4 to 0.5)	0.1 (-0.3 to 0.7)	0.1 (-0.5 to 0.6)	0.1 (-0.6 to 0.7)	0.2 (-0.9 to 0.8)
	MAM	0.1 (-0.3 to 0.5)	0.1 (-0.4 to 0.7)	0.3 (-0.4 to 0.7)	0.1 (-0.4 to 0.7)	0.2 (-0.4 to 0.7)	0.4 (-0.6 to 1.2)
	JJA	0.4 (-0.4 to 1.5)	0.5 (-0.5 to 1.4)	0.7 (-0.3 to 1.4)	0.4 (-0.7 to 1.3)	0.8 (-0.2 to 2.3)	1.6 (0.2 to 3.7)
	SON	0.5 (0 to 1.4)	0.4 (-0.2 to 1.2)	0.6 (0 to 1.3)	0.4 (-0.1 to 1.1)	0.7 (0 to 1.6)	1.3 (0.3 to 3.2)
Rainfall (%)	Annual	-1 (-11 to +4)	-2 (-9 to +5)	-1 (-11 to +5)	-4 (-19 to +3)	-6 (-16 to +4)	-5 (-27 to +9)
	DJF	-2 (-15 to +14)	0 (-15 to +13)	+1 (-9 to +16)	-5 (-27 to +6)	-2 (-17 to +10)	+6 (-13 to +27)
	MAM	-3 (-21 to +14)	-1 (-24 to +12)	-1 (-21 to +12)	-4 (-25 to +16)	-3 (-23 to +18)	0 (-29 to +26)
	JJA	-2 (-12 to +7)	-3 (-15 to +8)	-5 (-17 to +7)	-2 (-13 to +6)	-8 (-21 to +7)	-13 (-38 to +4)
	SON	-4 (-17 to +12)	-3 (-16 to +12)	-6 (-17 to +7)	-4 (-31 to +10)	-11 (-28 to +5)	-12 (-48 to +6)
Wind speed (%)	Annual	0.7 (-1.3 to 3.1)	-1 (-2.9 to 1.5)	0.1 (-2.6 to 2.4)	1.3 (-1.7 to 3.7)	-1.3 (-4.6 to 0.8)	-0.6 (-5 to 2.6)
	DJF	0.5 (-1.9 to 3.1)	-0.8 (-2.1 to 1.1)	0.1 (-2 to 2.2)	1.1 (-1.7 to 4.4)	-1.1 (-3.2 to 1.2)	0.2 (-4.2 to 4.5)
	MAM	0.9 (-1.8 to 3.9)	-0.4 (-3.6 to 2.2)	-0.5 (-4 to 3.5)	1 (-2.1 to 5.1)	-1.7 (-3.9 to 1.2)	-1.5 (-5.1 to 0.7)
	JJA	1 (-3.5 to 5)	0.1 (-6 to 3.8)	0.3 (-3 to 3.2)	1.3 (-3.5 to 5.3)	-1.8 (-7.4 to 3.1)	-2.6 (-8.2 to 4.4)
	SON	0.1 (-2.2 to 3.4)	-1.2 (-3.8 to 1.8)	0.1 (-4 to 3.6)	1.2 (-3.3 to 3.8)	-1.1 (-6.3 to 2.9)	0 (-4.4 to 4.2)

−20°   −10°   0°   10°   20°   30°   40°   50°

VARIABLE	SEASON	2030, RCP2.6	2030, RCP4.5	2030, RCP8.5	2090, RCP2.6	2090, RCP4.5	2090, RCP8.5
Soil moisture (Budyko) (%)	Annual	NA	-2.5 (-4.4 to 0.3)	-3.1 (-5.1 to -0.4)	NA	-2.6 (-8.3 to 1.2)	-7 (-10 to -1)
	DJF	NA	-0.7 (-2.8 to 0.6)	-0.7 (-4.7 to 0.1)	NA	-1.4 (-3.9 to 0.4)	-1.6 (-5.5 to 0.2)
	MAM	NA	-1.5 (-3.5 to 2.1)	-0.7 (-4 to 1.2)	NA	-1.2 (-4.7 to 1.6)	-2.1 (-7.9 to 1.8)
	JJA	NA	-3.2 (-5.7 to 2.1)	-3.1 (-8.4 to 1.7)	NA	-2.8 (-12.2 to 2.8)	-8.2 (-17 to -1.6)
	SON	NA	-3.1 (-8.2 to -0.6)	-4.3 (-8.2 to -0.5)	NA	-4.4 (-11.7 to 1)	-10.6 (-18.3 to -3)
Solar radiation (%)	Annual	1.1 (0.4 to 2.9)	0.7 (-0.1 to 1.7)	1 (-0.4 to 2)	1.6 (0.1 to 3.7)	1.5 (0.1 to 3.2)	2.2 (0 to 4.9)
	DJF	1.2 (-0.4 to 2.9)	0.5 (-1.1 to 1.7)	0.2 (-1.2 to 1.7)	1.7 (0.1 to 4.3)	0.7 (-1 to 2.8)	0.6 (-1.9 to 2.2)
	MAM	1 (-1.4 to 4.2)	0.5 (-1.4 to 3)	0.6 (-1.6 to 2.6)	1.5 (-2 to 3.9)	0.9 (-1.2 to 4.2)	0.8 (-2.7 to 4.7)
	JJA	2.4 (0.6 to 4.3)	1.8 (-0.7 to 5.1)	2.6 (0.4 to 6.4)	2.7 (0.3 to 4.7)	3.3 (1.5 to 7.4)	6.5 (3.3 to 15.5)
	SON	1.4 (-0.2 to 3.7)	1.1 (-0.5 to 2.2)	1.4 (-0.7 to 3.3)	1.5 (-0.3 to 4)	2.3 (0.1 to 4.1)	3.4 (0.6 to 6.6)
Relative humidity (%, absolute)	Annual	-0.8 (-3.3 to +0.1)	-0.7 (-1.6 to +0.5)	-0.9 (-2.3 to +0.2)	-1.3 (-2.7 to +0.1)	-1.6 (-4.1 to -0.3)	-2.7 (-5.8 to -0.8)
	DJF	-0.9 (-2.7 to +0.5)	-0.5 (-1.9 to +2)	-0.6 (-2.8 to +0.8)	-1.4 (-3.6 to -0.3)	-1.1 (-2.8 to +0.7)	-1.5 (-3.6 to +1.4)
	MAM	-0.9 (-3.4 to +1.4)	-0.2 (-3.4 to +1.3)	-0.3 (-2.8 to +1.2)	-1.6 (-4 to +0.7)	-1 (-4.3 to +1)	-1.9 (-6.4 to +1.5)
	JJA	-0.5 (-2.2 to +0.6)	-0.8 (-2.4 to +0.6)	-0.7 (-3.5 to +0.2)	-1.1 (-2.9 to +0.4)	-1.3 (-4 to +0.2)	-3.4 (-7.1 to -1.2)
	SON	-0.4 (-3.7 to +0.7)	-1.2 (-2.7 to +0.5)	-1 (-4.1 to +0.5)	-1 (-3.7 to +0.9)	-2.7 (-6.4 to -0.4)	-4.7 (-8.4 to -1.8)
Evapo-transpiration (%)	Annual	3.5 (2.3 to 5)	2.6 (1 to 4.5)	3.1 (1.9 to 5.1)	3 (1.8 to 5.5)	5.4 (2.9 to 8.5)	12 (7.6 to 18.1)
	DJF	3.1 (2.3 to 4.7)	2.6 (0.7 to 4.1)	3.2 (1.2 to 4.6)	2.6 (0.5 to 5.2)	5 (2.2 to 8.8)	11.3 (7.3 to 19.3)
	MAM	3.7 (1.6 to 6.9)	2.5 (0.7 to 5.9)	4.4 (2.3 to 6.3)	4.4 (0.6 to 6.8)	7 (4.7 to 10.1)	15 (9.7 to 21.6)
	JJA	5.4 (2.8 to 8.7)	4.5 (2.2 to 12.8)	6.8 (3.3 to 12.2)	6.6 (3.2 to 9.8)	10.4 (7.4 to 21.4)	24 (14.9 to 39.7)
	SON	2.8 (1.3 to 5.4)	2.6 (0.2 to 5.1)	2.8 (-0.4 to 5.9)	1.9 (0.3 to 6.6)	4.7 (0 to 8.5)	10 (1.3 to 15.6)

LEGEND

	Very high model agreement on substantial increase
	High model agreement on substantial increase
	Medium model agreement on substantial increase
	High model agreement on increase
	Medium model agreement on increase
	High model agreement on little change
	Medium model agreement on little change
	High model agreement on substantial decrease
	Medium model agreement on substantial decrease
	High model agreement on decrease
	Medium model agreement on decrease

TABLE 2: ANNUAL VALUES OF MAXIMUM TEMPERATURE (T; °C), RAINFALL (R; MM), DROUGHT FACTOR (DF; NO UNITS), THE NUMBER OF SEVERE FIRE DANGER DAYS (SEV: FFDI GREATER THAN 50 DAYS PER YEAR) AND CUMULATIVE FFDI (ΣFFDI; NO UNITS) FOR THE 1995 BASELINE AND PROJECTIONS FOR 2030 AND 2090 UNDER RCP4.5 AND RCP8.5. VALUES.

STATION	VARIABLE	1995 BASELINE	2030, RCP4.5			2030, RCP8.5			2090, RCP4.5			2090, RCP8.5		
			CESM	GFDL	MIROC	CESM	GFDL	MIROC	CESM	GFDL	MIROC	CESM	GFDL	MIROC
Mt Gambier	T	19.1	20.2	20.7	20.3	20.5	20.4	20.2	22.0	21.3	21.1	24.2	23.3	22.1
	R	712	671	502	696	674	557	678	654	539	690	613	386	793
	DF	5.7	5.8	6.3	5.8	5.8	6.0	5.9	6.1	6.3	6.0	6.5	7.6	5.8
	SEV	1.6	1.9	2.8	1.9	2.3	1.8	1.8	2.8	2.1	2.6	3.9	4.4	2.4
	ΣFFDI	2026	2105	2613	2134	2208	2281	2157	2412	2423	2301	2898	3475	2161
Mildura	T	23.9	24.9	25.5	25.1	25.2	25.1	24.9	26.8	26.0	25.8	28.9	28.0	26.9
	R	289	257	191	262	258	222	257	248	212	257	237	153	302
	DF	8.6	8.7	9.2	8.6	8.7	9.0	8.7	8.9	9.1	8.7	9.0	9.5	8.5
	SEV	7.2	8.5	12.0	8.2	9.6	9.4	8.6	10.8	10.1	9.8	15.7	17.2	9.1
	ΣFFDI	5488	5605	6617	5658	5820	6157	5687	6220	6346	5926	7089	7775	5717
Wagga	T	22.3	23.3	23.9	23.5	23.6	23.6	23.4	25.2	24.4	24.2	27.3	26.4	25.3
	R	575	540	401	549	539	465	537	522	443	533	499	325	635
	DF	6.4	6.5	7.3	6.4	6.6	6.9	6.4	6.8	7.2	6.6	7.3	8.4	6.4
	SEV	4.3	5.3	7.0	5.1	5.8	5.5	5.1	6.6	6.1	5.9	9.7	10.6	5.5
	ΣFFDI	3599	3742	4523	3758	3896	4063	3770	4214	4302	4012	4948	5668	3828
Canberra	T	19.9	21.0	21.5	21.2	21.3	21.2	21.0	22.8	22.1	21.9	25.0	24.1	23.0
	R	623	583	435	588	583	511	577	561	483	564.3	541	357	685
	DF	5.8	5.9	6.7	5.9	6.0	6.2	5.9	6.3	6.5	6.2	6.9	7.8	5.9
	SEV	1.4	1.9	2.8	1.7	2.1	2.0	1.7	2.6	2.3	2.2	4.9	5.9	2.1
	ΣFFDI	2634	2704	3433	2737	2859	3025	2748	3138	3229	2963	3804	4595	2796

−20°   −10°   0°   10°   20°   30°   40°   50°

TABLE 3: PROJECTED ANNUAL CHANGE IN SIMULATED MARINE CLIMATE VARIABLES FOR 2020–2039 (2030) AND 2080–2099 (2090) PERIODS RELATIVE TO 1986–2005 PERIOD FOR MURRAY BASIN, WHERE SEA ALLOWANCE IS THE MINIMUM DISTANCE REQUIRED TO RAISE AN ASSET TO MAINTAIN CURRENT FREQUENCY OF BREACHES UNDER PROJECTED SEA LEVEL RISE. FOR SEA LEVEL RISE, THE RANGE WITHIN THE BRACKETS REPRESENTS THE 5TH AND 95TH PERCENTILE CHANGE, AS PROJECTED BY THE CMIP5 MODEL ARCHIVE WHEREAS FOR SEA SURFACE TEMPERATURE, SALINITY, OCEAN PH AND ARAGONITE CONCENTRATION THE RANGE REPRESENTS THE 10TH TO 90TH PERCENTILE RANGE. ANNUAL RESULTS ARE GIVEN FOR RCP2.6, RCP4.5, AND RCP8.5. NOTE THAT THE RANGES OF SEA LEVEL RISE SHOULD BE CONSIDERED *LIKELY* (AT LEAST 66 % PROBABILITY), AND THAT IF A COLLAPSE IN THE MARINE BASED SECTORS OF THE ANTARCTIC ICE SHEET WERE INITIATED, THESE PROJECTIONS COULD BE SEVERAL TENTHS OF A METRE HIGHER BY LATE IN THE CENTURY.

VARIABLE	LOCATION (°E, °S)	2030, RCP2.6	2030, RCP4.5	2030, RCP8.5	2090, RCP2.6	2090, RCP4.5	2090, RCP8.5
Sea level rise (m)	Port Stanvac (138.47E, 35.11S)	0.12 (0.07-0.16)	0.12 (0.08-0.16)	0.13 (0.08-0.17)	0.39 (0.23-0.55)	0.46 (0.29-0.63)	0.61 (0.40-0.84)
	Victor Harbour (138.64, -35.56)	0.12 (0.07-0.16)	0.12 (0.08-0.16)	0.13 (0.08-0.17)	0.38 (0.23-0.55)	0.45 (0.28-0.63)	0.60 (0.39-0.83)
	Portland (141.61, -38.34)	0.12 (0.08-0.17)	0.12 (0.08-0.16)	0.13 (0.08-0.18)	0.39 (0.23-0.55)	0.46 (0.29-0.64)	0.61 (0.39-0.84)
Sea allowance (m)	Port Stanvac (138.47E, 35.11S)	0.12	0.12	0.12	0.41	0.48	0.66
	Victor Harbour (138.64, -35.56)	0.12	0.12	0.13	0.43	0.50	0.69
	Portland (141.61, -38.34)	0.12	0.12	0.13	0.46	0.54	0.74
Sea surface temperature (°C)	Port Stanvac (138.47, -35.11)	0.5 (03 to 0.8)	0.5 (0.3 to 0.6)	0.5 (0.3 to 0.9)	0.6 (0.3 to 0.9)	1.2 (0.7 to 1.7)	2.2 (1.5 to 3.4)
	Victor Harbour (138.64, -35.56)	0.5 (0.3 to 0.8)	0.5 (0.3 to 0.6)	0.5 (0.3 to 0.8)	0.6 (0.3 to 0.9)	1.2 (0.8 to 1.7)	2.2 (1.6 to 3.4)
	Portland (141.61, -38.34)	0.5 (0.2 to 0.7)	0.5 (0.3 to 0.7)	0.5 (0.3 to 0.8)	0.6 (0.3 to 0.9)	1.1 (0.7 to 1.6)	2.2 (1.6 to 3.4)
Sea surface salinity	Port Stanvac (138.47, -35.11)	-0.02 (-0.13 to 0.12)	-0.06 (-0.12 to 0.15)	-0.06 (-0.12 to 0.11)	-0.01 (-0.12 to 0.12)	-0.02 (-0.18 to 0.20)	-0.09 (-1.09 to 0.36)
	Victor Harbour (138.64, -35.56)	-0.01 (-0.15 to 0.12)	-0.06 (-0.12 to 0.15)	-0.06 (-0.12 to 0.10)	-0.01 (-0.14 to 0.12)	-0.04 (-0.19 to 0.21)	-0.09 (-1.12 to 0.37)
	Portland (141.61, -38.34)	-0.03 (-0.08 to 0.11)	-0.03 (-0.09 to 0.13)	-0.04 (-0.11 to 0.08)	-0.05 (-0.10 to 0.07)	-0.05 (-0.16 to 0.18)	-0.03 (-0.32 to 0.38)
Ocean pH	Port Stanvac (138.47, -35.11)	-0.07 (-0.07 to -0.06)	-0.07 (-0.07 to -0.07)	-0.08 (-0.08 to -0.08)	-0.07 (-0.07 to -0.06)	-0.15 (-0.16 to -0.15)	-0.33 (-0.33 to -0.32)
	Victor Harbour (138.64, -35.56)	-0.07 (-0.07 to -0.06)	-0.07 (-0.07 to -0.07)	-0.08 (-0.08 to -0.08)	-0.07 (-0.07 to -0.06)	-0.15 (-0.15 to -0.15)	-0.32 (-0.33 to -0.32)
	Portland (141.61, -38.34)	-0.07 (-0.07 to -0.06)	-0.07 (-0.08 to -0.07)	-0.08 (-0.09 to -0.08)	-0.07 (-0.07 to -0.06)	-0.15 (-0.16 to -0.15)	-0.33 (-0.33 to -0.32)
Aragonite saturation	Port Stanvac (138.47, -35.11)	-0.29 (-0.30 to -0.26)	-0.30 (-0.32 to -0.28)	-0.34 (-0.38 to -0.31)	-0.28 (-0.29 to -0.24)	-0.60 (-0.65 to -0.56)	-1.14 (-1.28 to -1.11)
	Victor Harbour (138.64, -35.56)	-0.29 (-0.29 to -0.25)	-0.30 (-0.32 to -0.28)	-0.34 (-0.38 to -0.31)	-0.27 (-0.29 to -0.25)	-0.58 (-0.65 to -0.56)	-1.14 (-1.29 to -1.10)
	Portland (141.61, -38.34)	-0.29 (-0.29 to -0.25)	-0.29 (-0.31 to -0.28)	-0.35 (-0.36 to -0.30)	-0.27 (-0.29 to -0.24)	-0.60 (-0.65 to -0.53)	-1.1 (-1.3 to -1.1)

ABBREVIATIONS

ACORN-SAT	Australian Climate Observations Reference Network – Surface Air Temperature
AWAP	Australian Water Availability Project
BOM	Australian Bureau of Meteorology
CCAM	Conformal Cubic Atmospheric Model
CCIA	Climate Change in Australia
CMIP5	Coupled Model Intercomparison Project (Phase 5)
CO$_2$	Carbon Dioxide
CSIRO	Commonwealth Scientific and Industrial Research Organisation
ENSO	El Niño Southern Oscillation
FFDI	Forest Fire Danger Index
GCMs	General Circulation Models or Global Climate Models
GDR	Great Dividing Range
IOD	Indian Ocean Dipole
IPCC	Intergovernmental Panel on Climate Change
LLS	Local Land Service
MB	Murray Basin cluster
MD	Millennium Drought
MSLP	Mean Sea level Pressure
NARCliM	NSW/ACT Regional Climate Modelling project
NRM	Natural Resource Management
RCP	Representative Concentration Pathway
SAM	Southern Annular Mode
SEACI	South Eastern Australian Climate Initiative
SPI	Standardised Precipitation Index
SRES	Special Report on Emissions Scenarios
SST	Sea Surface Temperature
STR	Sub-tropical Ridge
VicCI	Victorian Climate Initiative

NRM GLOSSARY OF TERMS

Adaptation	The process of adjustment to actual or expected climate and its effects. Adaptation can be autonomous or planned.
	Incremental adaptation
	Adaptation actions where the central aim is to maintain the essence and integrity of a system or process at a given scale.
	Transformational adaptation
	Adaptation that changes the fundamental attributes of a system in response to climate and its effects.
Aerosol	A suspension of very small solid or liquid particles in the air, residing in the atmosphere for at least several hours.
Aragonite saturation state	The saturation state of seawater with respect to aragonite (Ω) is the product of the concentrations of dissolved calcium and carbonate ions in seawater divided by their product at equilibrium: $([Ca^{2+}] \times [CO^3_2]) / [CaCO^3] = \Omega$
Atmosphere	The gaseous envelope surrounding the Earth. The dry atmosphere consists almost entirely of nitrogen and oxygen, together with a number of trace gases (*e.g.* argon, helium) and greenhouse gases (*e.g.* carbon dioxide, methane, nitrous oxide). The atmosphere also contains aerosols and clouds.
Carbon dioxide	A naturally occurring gas, also a by-product of burning fossil fuels from fossil carbon deposits, such as oil, gas and coal, of burning biomass, of land use changes and of industrial processes (*e.g.* cement production). It is the principle anthropogenic greenhouse gas that affects the Earth's radiative balance.
Climate	The average weather experienced at a site or region over a period of many years, ranging from months to many thousands of years. The relevant measured quantities are most often surface variables such as temperature, rainfall and wind.
Climate change	A change in the state of the climate that can be identified (*e.g.* by statistical tests) by changes in the mean and/or variability of its properties, and that persists for an extended period of time, typically decades or longer.
Climate feedback	An interaction in which a perturbation in one climate quantity causes a change in a second, and that change ultimately leads to an additional (positive or negative) change in the first.
Climate projection	A climate projection is the simulated response of the climate system to a scenario of future emission or concentration of greenhouse gases and aerosols, generally derived using climate models. Climate projections are distinguished from climate predictions by their dependence on the emission/concentration/radiative forcing scenario used, which in turn is based on assumptions concerning, for example, future socioeconomic and technological developments that may or may not be realised.
Climate scenario	A plausible and often simplified representation of the future climate, based on an internally consistent set of climatological relationships that has been constructed for explicit use in investigating the potential consequences of anthropogenic climate change, often serving as input to impact models.
Climate sensitivity	The effective climate sensitivity (units; °C) is an estimate of the global mean surface temperature response to doubled carbon dioxide concentration that is evaluated from model output or observations for evolving non-equilibrium conditions.
Climate variability	Climate variability refers to variations in the mean state and other statistics (such as standard deviations, the occurrence of extremes, etc.) of the climate on all spatial and temporal scales beyond that of individual weather events. Variability may be due to natural internal processes within the climate system (internal variability), or to variations in natural or anthropogenic external forcing (external variability).
Cloud condensation nuclei	Airborne particles that serve as an initial site for the condensation of liquid water, which can lead to the formation of cloud droplets. A subset of aerosols that are of a particular size.

CMIP3 and CMIP5	Phases three and five of the Coupled Model Intercomparison Project (CMIP3 and CMIP5), which coordinated and archived climate model simulations based on shared model inputs by modelling groups from around the world. The CMIP3 multi-model dataset includes projections using SRES emission scenarios. The CMIP5 dataset includes projections using the Representative Concentration Pathways (RCPs).
Confidence	The validity of a finding based on the type, amount, quality, and consistency of evidence (e.g. mechanistic understanding, theory, data, models, expert judgment) and on the degree of agreement.
Decadal variability	Fluctuations, or ups-and-downs of a climate feature or variable at the scale of approximately a decade (typically taken as longer than a few years such as ENSO, but shorter than the 20–30 years of the IPO).
Detection and attribution	Detection of change is defined as the process of demonstrating that climate or a system affected by climate has changed in some defined statistical sense, without providing a reason for that change. An identified change is detected in observations if its likelihood of occurrence by chance due to internal variability alone is determined to be small, for example, less than 10 per cent. Attribution is defined as the process of evaluating the relative contributions of multiple causal factors to a change or event with an assignment of statistical confidence.
Downscaling	Downscaling is a method that derives local to regional-scale information from larger-scale models or data analyses. Different methods exist e.g. dynamical, statistical and empirical downscaling.
El Niño Southern Oscillation (ENSO)	A fluctuation in global scale tropical and subtropical surface pressure, wind, sea surface temperature, and rainfall, and an exchange of air between the south-east Pacific subtropical high and the Indonesian equatorial low. Often measured by the surface pressure anomaly difference between Tahiti and Darwin or the sea surface temperatures in the central and eastern equatorial Pacific. There are three phases: neutral, El Niño and La Niña. During an El Niño event the prevailing trade winds weaken, reducing upwelling and altering ocean currents such that the eastern tropical surface temperatures warm, further weakening the trade winds. The opposite occurs during a La Niña event.
Emissions scenario	A plausible representation of the future development of emissions of substances that are potentially radiatively active (e.g. greenhouse gases, aerosols) based on a coherent and internally consistent set of assumptions about driving forces (such as demographic and socioeconomic development, technological change) and their key relationships.
Extreme weather	An extreme weather event is an event that is rare at a particular place and time of year. Definitions of rare vary, but an extreme weather event would normally be as rare as or rarer than the 10th or 90th percentile of a probability density function estimated from observations.
Fire weather	Weather conditions conducive to triggering and sustaining wild fires, usually based on a set of indicators and combinations of indicators including temperature, soil moisture, humidity, and wind. Fire weather does not include the presence or absence of fuel load.
Global Climate Model or General Circulation Model (GCM)	A numerical representation of the climate system that is based on the physical, chemical and biological properties of its components, their interactions and feedback processes. The climate system can be represented by models of varying complexity and differ in such aspects as the spatial resolution (size of grid-cells), the extent to which physical, chemical, or biological processes are explicitly represented, or the level at which empirical parameterisations are involved.
Greenhouse gas	Greenhouse gases are those gaseous constituents of the atmosphere, both natural and anthropogenic, that absorb and emit radiation at specific wavelengths within the spectrum of terrestrial radiation emitted by the Earth's surface, the atmosphere itself, and by clouds. Water vapour (H_2O), carbon dioxide (CO_2), nitrous oxide (N_2O), methane (CH_4) and ozone (O_3) are the primary greenhouse gases in the Earth's atmosphere.
Hadley Cell/Circulation	A direct, thermally driven circulation in the atmosphere consisting of poleward flow in the upper troposphere, descending air into the subtropical high-pressure cells, return flow as part of the trade winds near the surface, and with rising air near the equator in the so-called Inter-Tropical Convergence zone.

−20°   −10°   0°   10°   20°   30°   40°   50°

Indian Ocean Dipole (IOD)	Large-scale mode of interannual variability of sea surface temperature in the Indian Ocean. This pattern manifests through a zonal gradient of tropical sea surface temperature, which in its positive phase in September to November shows cooling off Sumatra and warming off Somalia in the west, combined with anomalous easterlies along the equator.
Inter-decadal Pacific Oscillation	A fluctuation in the sea surface temperature (SST) and mean sea level pressure (MSLP) of both the north and south Pacific Ocean with a cycle of 15–30 years. Unlike ENSO, the IPO may not be a single physical 'mode' of variability, but be the result of a few processes with different origins. The IPO interacts with the ENSO to affect the climate variability over Australia. A related phenomena, the Pacific Decadal Oscillation (PDO), is also an oscillation of SST that primarily affects the northern Pacific.
Jet stream	A narrow and fast-moving westerly air current that circles the globe near the top of the troposphere. The jet streams are related to the global Hadley circulation. In the southern hemisphere the two main jet streams are the polar jet that circles Antarctica at around 60 °S and 7–12 km above sea level, and the subtropical jet that passes through the mid-latitudes at around 30 °S and 10–16 km above sea level.
Madden Julian Oscillation (MJO)	The largest single component of tropical atmospheric intra-seasonal variability (periods from 30 to 90 days). The MJO propagates eastwards at around 5 m s^{-1} in the form of a large-scale coupling between atmospheric circulation and deep convection. As it progresses, it is associated with large regions of both enhanced and suppressed rainfall, mainly over the Indian and western Pacific Oceans.
Monsoon	A monsoon is a tropical and subtropical seasonal reversal in both the surface winds and associated rainfall, caused by differential heating between a continental-scale land mass and the adjacent ocean. Monsoon rains occur mainly over land in summer.
Percentile	A percentile is a value on a scale of one hundred that indicates the percentage of the data set values that is equal to, or below it. The percentile is often used to estimate the extremes of a distribution. For example, the 90th (or 10th) percentile may be used to refer to the threshold for the upper (or lower) extremes.
Radiative forcing	Radiative forcing is the change in the net, downward minus upward, radiative flux (expressed in W m^{-2}) at the tropopause or top of atmosphere due to a change in an external driver of climate change, such as a change in the concentration of carbon dioxide or the output of the Sun.
Representative Concentration Pathways (RCPs)	Representative Concentration Pathways follow a set of greenhouse gas, air pollution (*e.g.* aerosols) and land-use scenarios that are consistent with certain socio-economic assumptions of how the future may evolve over time. The well mixed concentrations of greenhouse gases and aerosols in the atmosphere are affected by emissions as well as absorption through land and ocean sinks. There are four Representative Concentration Pathways (RCPs) that represent the range of plausible futures from the published literature.
Return period	An estimate of the average time interval between occurrences of an event (*e.g.* flood or extreme rainfall) of a defined size or intensity.
Risk	The potential for consequences where something of value is at stake and where the outcome is uncertain. Risk is often represented as a probability of occurrence of hazardous events or trends multiplied by the consequences if these events occur.
Risk assessment	The qualitative and/or quantitative scientific estimation of risks.
Risk management	The plans, actions, or policies implemented to reduce the likelihood and/or consequences of risks or to respond to consequences.
Sub-tropical ridge (STR)	The sub-tropical ridge runs across a belt of high pressure that encircles the globe in the middle latitudes. It is part of the global circulation of the atmosphere. The position of the sub-tropical ridge plays an important part in the way the weather in Australia varies from season to season.

Southern Annular Mode (SAM)	The leading mode of variability of Southern Hemisphere geopotential height, which is associated with shifts in the latitude of the mid-latitude jet.
SAM index	The SAM Index, otherwise known as the Antarctic Oscillation Index (AOI) is a measure of the strength of SAM. The index is based on mean sea level pressure (MSLP) around the whole hemisphere at 40 °S compared to 65 °S. A positive index means a positive or high phase of the SAM, while a negative index means a negative or low SAM. This index shows a relationship to rainfall variability in some parts of Australia in some seasons.
SRES scenarios	SRES scenarios are emissions scenarios developed by Nakićenović and Swart (2000) and used, among others, as a basis for some of the climate projections shown in Chapters 9 to 11 of IPCC (2001) and Chapters 10 and 11 of IPCC (2007).
Uncertainty	A state of incomplete knowledge that can result from a lack of information or from disagreement about what is known or even knowable. It may have many types of sources, from imprecision in the data to ambiguously defined concepts or terminology, or uncertain projections of human behaviour. Uncertainty can therefore be represented by quantitative measures (e.g. a probability density function) or by qualitative statements (e.g. reflecting the judgment of a team of experts).
Walker Circulation	An east-west circulation of the atmosphere above the tropical Pacific, with air rising above warmer ocean regions (normally in the west), and descending over the cooler ocean areas (normally in the east). Its strength fluctuates with that of the Southern Oscillation.

GLOSSARY REFERENCES

AUSTRALIAN BUREAU OF METEOROLOGY - http://www.bom.gov.au/watl/about-weather-and-climate/australian-climate-influences.shtml (cited August 2014)

INTERGOVERNMENTAL PANEL ON CLIMATE CHANGE - http://www.ipcc.ch/pdf/glossary/ar4-wg1.pdf (cited August 2014)

INTERGOVERNMENTAL PANEL ON CLIMATE CHANGE - http://ipcc-wg2.gov/AR5/images/uploads/WGIIAR5-Glossary_FGD.pdf (cited August 2014)

MUCCI, A. 1983. The solubility of calcite and aragonite in seawater at various salinities, temperatures, and one atmosphere total pressure *American Journal of Science*, 283 (7), 780-799.

NAKIĆENOVIĆ, N. & SWART, R. (eds.) 2000. *Special Report on Emissions Scenarios. A Special Report of Working Group III of the Intergovernmental Panel on Climate Change*, Cambridge, United Kingdom and New York, NY, USA: Cambridge University Press.

STURMAN, A.P. & TAPPER, N.J. 2006. *The Weather and Climate of Australia and New Zealand*, 2nd ed., Melbourne, Oxford University Press.

FLOOD LEVEL
1956

-20°   -10°   0°   10°   20°   30°   40°   50°